UNIVERSITÀ DI SIENA 1240

Dipartimento di Medicina Molecolare e dello sviluppo

Dottorato in Medicina Molecolare

XXXVI° Ciclo

Coordinatore Prof. Vincenzo Sorrentino

Titolo della tesi

Biotechnological methods for the study of cardiomyopathies and the evaluation of new pharmacological therapies based on patient-specific in vitro models

Settore scientifico disciplinare: BIO/09

Candidata
Lucrezia Giammarino
Dipartimento Neurofarba

Firma digitale del/della candidato/a

Firmato digitalmente da
LUCREZIA GIAMMARINO
13/05/2024 17:25:10 +0200
powered by cheFirma!

Supervisore
Prof.ssa Elisabetta Cerbai
Dipartimento Neurofarba/LENS

Co-supervisore
Dott. Raffaele Coppini
Dipartimento Neurofarba

Anno accademico di conseguimento del titolo di Dottore di ricerca
2022/23

Università degli Studi di Siena

Dottorato in Medicina Molecolare

XXXVI° Ciclo

Data dell'esame finale
30/05/2024

Commissione giudicatrice

Prof.ssa Rossi Daniela

Prof.ssa Vitiello Marianna

Prof.ssa Sticchi Elena

Supplenti

Prof. Amato Rosario

Index

Chapter 4

RESULTS..... 72

Summary

Inherited cardiomyopathies are a heterogeneous group of cardiac disease characterized by functional and structural alteration of myocardium, representing the major cause of morbidity and mortality over the past two decades. Recently, extensive genetic screenings have highlighted the importance to expand our knowledge regarding the effects that specific mutations cardiomyopathies-associated have on contractile functionality of the heart. Therefore, focused and specific pharmacological treatments for cardiomyopathies are missing, considering all the different clinical manifestations observed in the various forms of cardiomyopathies, including hypertrophic cardiomyopathy (HCM) and dilated cardiomyopathy (DCM), the two most widely represented forms of these cardiac diseases. In this context, human pluripotent stem cells-derived cardiomyocytes (hiPSC-CMs) are a powerful model of study to investigate the pathological mechanisms underlying these diseases, allowing to preserve the genetic heritage of patient and then model satisfactorily inherited cardiomyopathies. Moreover, hiPSC-CMs enable pharmacological in vitro testing and functional investigations, identifying specific drug interventions to address the pathological alterations caused from specific associated mutations. Despite this potentiality, electrophysiological and mechanical immaturity of hiPSC-CMs represent a limitation on their use. In recent years, new methods to induce their maturation were developed, including micropatterned substrates and engineered heart tissues (EHTs), to promote cellular elongation and maturation. In particular, up of 60% of HCM cases are caused from mutation occurring in β-myosin heavy chain (β-MHC) and myosin-binding protein C (MYBPC3). Then, in this work we used hiPSC-CMs to model HCM end DCM, by using different hiPSC lines derived from patients carrying β-MHC and MYBPC3 mutations, to investigate the main pathological characteristic associated to this disease. Also, we used four different hiPSCs line derived from patients affected from dilated cardiomyopathy associated to Duchenne Muscular Dystrophy (DMD), resulting in total absence of dystrophin. In the first part of this work, we elucidated that specific micropatterned substrates with different stiffness could strongly affect calcium handling and electrophysiological features of DMD cardiomyocytes in comparison to control. In fact, the absence of full-length dystrophin in DMD patients induce pathological modifications due the lack of interaction between intracellular environment and extracellular matrix (ECM), resulting in calcium handling abnormalities and alterations in sarcoplasmic reticulum (SR) re-uptake. Moreover, a deficit of diastolic calcium mobilization occurs in dystrophin-deficient cardiomyocytes. Based on this evidence, EHTs were derived from HCM and DMD lines, as previously described, to more closely mimic the physiological myocardium. More in detail, we performed contractile force recording and action potential evaluation by using a confocal microscope using HCM lines carrying c.772G>A variant in MYBPC3 gene, highlighting an effect of this mutation on cross bridge cycling end contractile properties of HCM-EHTs. In addition, we performed chronic treatment with Mavacamten, an allosteric myosin inhibitor, on HCM-EHTs showing a significant decrease of contractile force development in HCM-EHTs treated compared to basal. Moreover, we performed mechanical evaluation, via calcium transient measurements and In Vitro Motility Assay (IVMA) on myosin isolated from hiPSC-CMs carrying R403Q mutation, resulting in a particularly severe form of HCM, showing calcium handling modification and impaired contractility in mutated

cardiomyocytes compared to control. Therefore, in the second part of this work, we evaluated DMD-EHTs derived from four patients, carrying mutation that result in total absence of full-length dystrophin (Δexon 46-48, Δexon 50, Δexon 51, Δexon 49). Also, contractile force measurements were performed on DMD-EHTs, demonstrated a reduction of active tension exerted from DMD tissues in association to kinetics preserved. Finally, Dapagliflozin, a novel type 2 sodium glucose cotransporter inhibitor, that act "off-label" bringing various beneficial effects at cardiovascular level through effects still unknow. For these reasons, we performed acute treatment with Dapagliflozin (1 and 5 μM) on DMD-EHTs and cardiomyocytes isolated from human surgical samples, highlighting an increase of active tension in DMD-tissues treated compared to untreated. Moreover, a reduction in action potential duration (APD) occur in HCM cardiomyocytes compared to basal conditions. Overall, these results provide evidence that, although there is different phenotypical manifestation in different inherited cardiomyopathies, specific pathological mechanisms could be in common, including calcium handling and electrophysiological alterations. These mechanisms can be exploited to performed specialized patient-specific medicine, to improve the knowledge on these genetic disorders, establishing the basis for ever more innovative pharmacological treatments.

Chapter 1

INTRODUCTION

1.1 Inherited cardiomyopathies

Cardiomyopathies are a class of heterogeneous cardiac disorder characterized by marked structural and functional myocardium alterations. Cardiomyopathies remain currently the main causes of morbidity and mortality in young people around the world, representing an emerging health epidemic of the 21st century (Hariharan et al., 2011). The term "cardiomyopathy" was first used in 1957 by Brigden, who described a group of uncommon, non-coronary myocardial diseases (Brigden W. et al. 1957). Usually, cardiomyopathies have been described as associated with heart failure, arrythmia and sudden cardiac death (SCD). Recently, the detection of cardiomyopathies in patients has increased due the advances in imaging techniques and clinical practice, although the majority of patients are still likely to be undiagnosed or misdiagnosed. The American Heart Association introduced a classification in two major categories: (I) primary cardiomyopathies, which can be genetic, acquired, or mixed in aetiology, and are caused by cardiac disorders; (II) secondary cardiomyopathies, developed as a result of various conditions, such as ischemia, infection, inflammation, stress or abuse of toxic substances. Genetic cardiomyopathies may derive from specific chromosomal anomalies resulting in cardiac dysfunction and are genetically heterogeneous, characterized by mutations that may occur in multiple genes, including β-myosin heavy chain, cardiac myosin binding protein C, troponin I and many others. Instead, the acquired forms involve non-genetic causes that can affect myocardium, such as hypertension, coronary heart disease, heart valve disorders, diabetes, alcohol and drug abuse or chemotherapy drugs. Finally, mixed cardiomyopathies may derive from a combination of genetic and non-genetic alteration. However, despite the efforts made to classify all the various cardiomyopathies, this classification system is imperfect and overlaps often occur (Maron BJ et al., 2006).

Recently, based to functional and morphological features, a new classification for cardiomyopathies was developed. According to this subdivision, cardiomyopathies are classified in hypertrophic cardiomyopathy (HCM), the most common inherited cardiomyopathy, dilated cardiomyopathy (DCM), one of the main causes of heart failure in the young (Richardson P. et al., 1996), and restrictive cardiomyopathy (RCM), a rare heart-muscle disease characterized by stiffness of ventricular wall that led diastolic dysfunction (Maron BJ et al., 2006). Finally, arrhythmogenic ventricular cardiomyopathy (ARVC) is characterized by

the substitution of cardiac tissue with fibrofatty tissue, resulting in the development of arrhythmia, especially in young patients (Maron BJ et al., 2006).

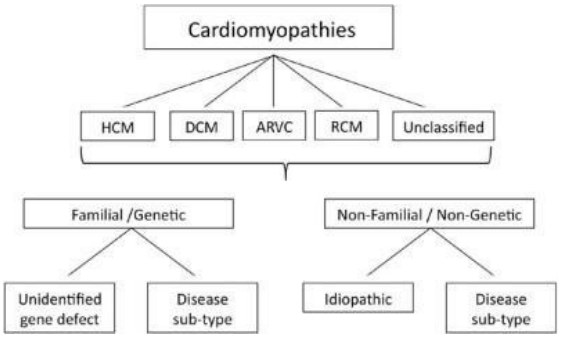

Figure 1. *Classification of cardiomyopathies. European Society of Cardiology. Cecchi F, Tomberli B, Olivotto I. Clinical and molecular classification of cardiomyopathies, Global Cardiology Science and Practice 2012:4* http://dx.doi.org/10.5339/gcsp.2012.4

Table 1. Hypertrophic cardiomyopathy.

FAMILIAL	Unknown gene
	Sarcomeric protein disease ß myosin heavy chain, Cardiac myosin binding protein C Cardiac troponin I, T and C, a-tropomyosin, Essential myosin light chain, Regulatory myosin light chain, Cardiac actin, a- myosin heavy chain, Titin
	Glycogen storage diseases (e.g. GSD II (Pompe's disease); GSD III (Forbes' disease), AMP kinase (WPW, HCM, conduction disease)
	Lysosomal storage diseases (e.g. Anderson-Fabry disease, Hurler's syndrome)
	Disorders of Fatty Acid Metabolism Carnitine, Phosphorylase B kinase deficiency
	Mitochondrial cytopathies (e.g. MELAS, MERFF, LHON)
	Syndromic HCM Noonan's syndrome, LEOPARD syndrome, Friedreich's ataxia, Beckwith-Wiedermann syndrome; Swyer's syndrome (pure gonadal dysgenesis)
	Other: Muscle LIM protein Phospholamban promoter Familial Amyloid
NON-FAMILIAL	
	Obesity; Infants of diabetic mothers; Athletic training; Amyloid (AL / prealbumin)

Table 2. Dilated cardiomyopathy.

FAMILIAL, unknown gene	
	Sarcomeric protein mutations (see HCM)
	Z band : Cypher/Zasp, Muscle LIM protein, TCAP
	Cytoskeletal genes: Dystrophin, Desmin, Metavinculin, Sarcoglycan complex, CRYAB, Epicardin
	Nuclear membrane: Lamin A/C, Emerin
	Mildly dilated CM
	Intercalated disc protein mutations (see ARVC)
	Mitochondrial cytopathy
NON FAMILIAL	
	Myocarditis (infective/toxic/immune)
	Kawasaki disease
	Eosinophilic (Churg Strauss syndrome)
	Viral persistence
	Drugs, Pregnancy, Endocrine
	Nutritional: thiamine, carnitine, selenium, hypophosphataemia, hypocalcemia.
	Alcohol
	Tachycardiomyopathy

Table 3. Restrictive cardiomyopathy.

FAMILIAL, unknown gene
Sarcomeric protein mutations: Troponin I (RCM +/− HCM), Essential myosin light chain
Familial Amyloidosis Transthyretin (RCM + neuropathy)
Apolipoprotein (RCM + nephropathy)
Desminopathy
Pseuxanthoma elasticum
Haemochromatosis
Anderson-Fabry disease
Glycogen storage disease
Endomyocardial fibrosis (Familial) (Fusion FIP1-like-1 / PDGFRA genes)
NON FAMILIAL
Amyloid (AL/prealbumin)
Scleroderma
Endomyocardial fibrosis
Hypereosinophilic syndrome, Idiopathic chromosomal cause
Drugs: serotonin, methysergide, ergotamine, mercurial agents, busulfan, anthracyclines
Carcinoid heart disease, Metastatic cancers, Radiation

Table 4. Arrhythmogenic right ventricular cardiomyopathy.

FAMILIAL, unknown gene
Intercalated disc protein mutations: Plakoglobin,
Desmoplakin
Plakophilin 2
Desmoglein 2
Desmocollin 2
Cardiac ryanodine receptor (RyR2)
Transforming growth factor-β_3 (TGFβ_3)
NON FAMILIAL
Inflammation?

Table 5. Unclassified cardiomyopathies.

FAMILIAL unknown gene
Left ventricular non-compaction:
Barth Syndrome
Lamin A/C
ZASP
a-dystrobrevin
NON FAMILIAL
Takotsubo cardiomyopathy

Figure 2. *Mutations associated to inherited cardiomyopathies. Cecchi, Tomberli & Olivotto. Global Cardiology Science and Practice, 2012.*

1.1.1 Hypertrophic Cardiomyopathy

Hypertrophic cardiomyopathy (HCM) is the most common inherited global heart disease, with a prevalence of 1:200-1:500 in the general population. However, the prevalence of HCM has been underestimated for years. In fact, the classic diagnostic techniques, such as the echocardiogram, have a lower sensitivity than magnetic resonance imaging (MRI) (Maron B.J. et al., 2012), and MRI has only recently been introduced in the standard medical practice for the diagnostic workup of such patients. Moreover, HCM can remain asymptomatic or

paucisymptomatic for a long time before to being diagnosed, thus delaying the diagnosis, especially in young patients.

HCM is characterized by a very variable genetic expression and phenotypes and affects both genders and many ethnic groups around the world (Maron BJ at al., 2022). The main evidence of HCM is the abnormal thickening of the ventricular walls of myocardium, resulting in the reduction of the internal cavities and impairing the contractile capacity of the heart. In particular, HCM is defined by the presence of increased left ventricular (LV) wall thickness; for adults, >15 mm in one or more LV myocardial segments, that is not solely explained by abnormal loading conditions (e.g. valve diseases or severe hypertension). This ventricular thickening can further be classified as mild (13-15 mm) or extreme (> or = 30 mm) (Nistri S. et al. 2006) (Iacopo Olivotto et al. 2003). Usually, this condition affects mainly the left ventricle and only in rare cases also involves the right ventricle (Polakit Teekakirikul et al, 2019), with a distribution of hypertrophy that is largely variable, affecting interventricular septum, apex or mid-cavity of myocardium. The diagnosis of hypertrophic cardiomyopathy is based on echocardiography (ECHO) or cardiac magnetic resonance (CMR). Classically, QRS complexes with ST depression and severe T wave inversion occurs in HCM patients, although alteration in the electrocardiographic exams may not be present at the debut of the disease (Hariharan R. et al., 2011).

Moreover, HCM leads to specific cellular alteration and histological features, including cardiomyocyte hypertrophy and disarray, triggering the onset of cardiac arrhythmias and myocardial fibrosis, ultimately resulting in significant cardiac complications. The hypertrophy is also frequently associated with left ventricular diastolic dysfunction. Patients affected by HCM can present highly variable clinical manifestation that include exertional chest pain and breathlessness, palpitations, dyspnea, asymptomatic murmur, syncope, culminating in sudden cardiac death (SCD) (Hensley N. et al, 2015).

In addition, hypertrophic cardiomyopathy can be divided into two main subtypes:

- *Obstructive hypertrophic cardiomyopathy*, that involves a severe impediment to blood leakage from the left ventricle;
- *Non-obstructive hypertrophic cardiomyopathy*, where blood flow from the left ventricle is only moderately reduced.

Depending on the severity of the hypertrophy, HCM patients may also develop diastolic dysfunction, myocardial ischaemia, or mitral regurgitation. Approximately, about two thirds of patients (70-75%) affected by HCM will develop left ventricular (LV) outflow tract obstruction (LVOTO). The development of the obstructive or non-obstructive form of hypertrophic cardiomyopathy is determined from the presence of an important thickening extended also to the interventricular septum. This condition is characterized by a partial obstruction in the left ventricular blood outflow, causing hemodynamic adverse events, associated with acute heart failure symptoms exacerbated by physical exertion (Ommen S.R. et al., 2020).

HCM has been defined primarily as a "disease of the sarcomere" (B. J. Maron, 2012, Semsarian 2012), counting more than 1500 mutations in 11 genes encoding fundamental proteins involved in the function of the thin and thick filaments of the cardiac sarcomere. During the past two decades, several genetic studies were performed to assess the pathogenesis of HCM, providing new perspectives for the diagnosis, treatment and management of patients. In this contest, the importance of gene defects in the aetiology of primary cardiomyopathies has been recognized. To date, several genes were discovered as genetic causes for HCM, the majority of which affecting the sarcomere, including the beta-myosin heavy chain, the myosin-binding protein C, troponin I and T. In other cases, HCM is caused from different genetic disorders, such as neuromuscular diseases (Friedreich ataxia), inherited metabolic disorders (Barth syndrome) or genetic disease (Noonan syndrome). Moreover, non-sarcomere mutations occur in genes encoding proteins of the Z-disk and calcium modulators have also been identified.

Typically, mutations that occur in sarcomere genes are single nucleotide substitutions, that impact the sarcomere functionality exerting a dominant negative effect. The only exception is represented by MYBPC3 mutations, which are mainly deletions or insertions that may result into a truncated protein with an altered function, leading to absolute deficiency of MyBPC protein, the so called "haploinsufficiency" (Marston et al., 2009).

Most HCM-related mutations (~80%) are identified in the MYH7 gene, located in locus 11p11.2, and in the MYBPC3 gene, located in locus 14q11.2, providing instructions for the beta (β)-myosin heavy chain and for cardiac myosin binding protein C (cardiac MyBP-C), respectively (Maron BJ et al., 2013).

Moreover, TNNT2 gene mutations, encoding for cardiac muscle troponin T of thin filament, represent 5-10% of cases encountered in association with HCM, and mutation in TNNT3 gene, coding for troponin I represent 4-8% of cases. In addition, rare mutation in genes encoding for regulatory myosin light chain (MYL2), essential myosin light chain (MYL3), α-tropomyosin (TPM1) and α-cardiac actin (ACTC1) have also been described. Unfortunately, in 40-55% of

HCM patients, the genes involved in the pathogenesis of this disease remain unidentified (Marian AJ et al., 2017).

Several studies on patients subjected to sudden cardiac death (SCD) have shown that sarcomere mutations associated with HCM favoured the presence of a myocardial structural remodelling, leading a severe alteration of the microcirculation. This functional alteration may promote the occurrence of ischemia and the onset of interstitial fibrosis in HCM myocardium (Maron MS et al., 2009).

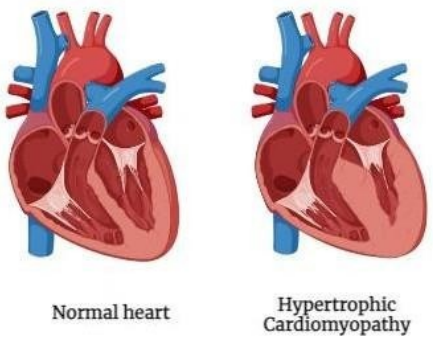

Figure 3. *Morphological alteration of myocardium in hypertrophic cardiomyopathy (HCM).*

At the molecular level, the excessive formation of actin-myosin cross-bridge in the sarcomere during the systolic phase can drive an excessive cardiomyocyte energy consumption, leading to the onset of hypertrophy and myocardial dysfunction (Edelberg JM et al., 2022).

Among the possible consequences of the energy depletion in HCM, one of the major issues is the impairment of Ca^{2+} reuptake to the sarcoplasmic reticulum, due to the extreme energy requirements of the cardiac SERCA pump (He et al. 2007; Spindler et al. 1998). In addition, elevated diastolic intracellular [Ca^{2+}] and impaired function of other ion transporters could make the myocardium vulnerable to arrhythmias. In fact, previous studies on patch clamp and intracellular Ca^{2+}, performed on cardiomyocytes isolated from human surgical sample of HCM patients, highlight an impairment of electromechanical profile of cardiomyocytes (Coppini et al. 2013). In particular, HCM cardiomyocyte were more vulnerable compared with controls, showing a prolongation of action potential (AP) in association with an increase of late Na^{+} (INaL) and Ca^{2+} currents. Also, changes in potassium repolarizing currents were identified, in particular the "Transient Outward" (I_{to}) and the "Inward rectifier" (I_{k1}) currents, determined by a reduced expression of the genes encoding the respective channels (Coppini et al. 2013). These pathological modifications increase the probability of occurrence of "early after depolarizations" (EADs), spontaneous depolarizations occurring during the plateau phase of the

AP, associated with a reopening of Na^+ and Ca^{2+} channels before the completion of repolarization (Maron et al. 2006): EADs are considered among the main responsible for ventricular arrhythmias in HCM (Yan et al., 2001). In addition, HCM cardiomyocytes showed alterations in diastolic calcium concentration, with slowed down calcium transient kinetics and increased intracellular ion concentrations. These observations suggest that HCM may lead to marked changes in the excitation-contraction coupling mechanisms (Coppini et al. 2013).

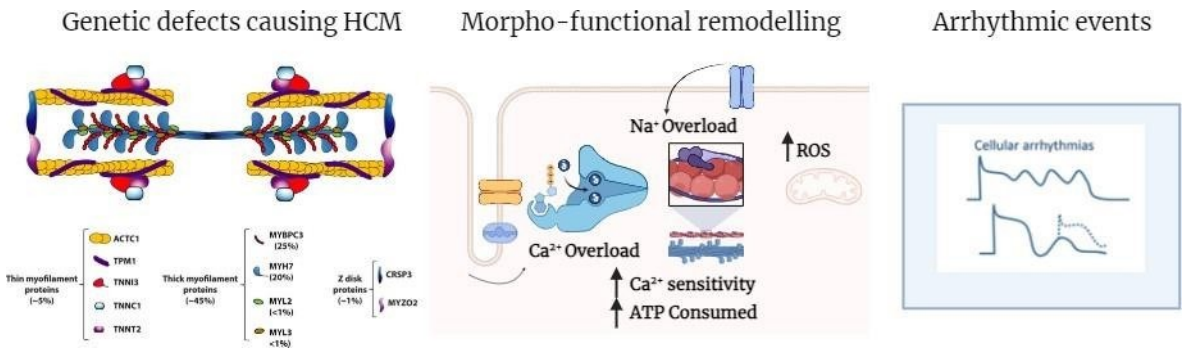

Figure 4. *Electromechanical remodelling in hypertrophic cardiomyopathy (HCM) cardiomyocytes. Sarcomere mutations cause an increase in intracellular Ca^{2+} that lead an increase of reactive oxygen species production, resulting in the activation of Ca^{2+}/calmodulin kinase II (CaMKII); increased phosphorylation of its downstream targets (Ca^{2+} channel, ryanodine receptor, phospholamban, Na^+ channel) is responsible for the abnormalities observed in HCM cardiomyocytes, including increased I_{NaL}.*

1.1.2 Cardiomyocytes cellular physiology

Cardiac muscle fibres are comprised of distinct cellular units connected with each other through specialized areas of interdigitating cellular membrane called “intercalated discs”, involving adherent junctions, desmosomes and gap junctions, that allow the transmission of mechanical force in a synchronous mode. Cardiomyocytes are surrounded by the sarcolemma and the intracellular environment contains bundles of longitudinally arranged myofibrils with characteristic striated appearance, formed by repeating sarcomeres. The sarcomere is the fundamental structural and functional unit of cardiac muscle consisting of thick and thin filaments (Figure 5), composed by myosin, myosin binding protein C, H and X and cardiac actin, -tropomyosin, and troponins C, I, and T, respectively. Each sarcomere is constituted of an A-band, localized where thick and thin filaments overlap, with a central M-line, comprising thick filaments only. Moreover, I bands are localized at each side of the A band. Sarcomere

scaffold is provided by the giant protein titin, spanning between the Z and the M lines, representing the major determinant of the elastic properties of cardiac myofibrils.

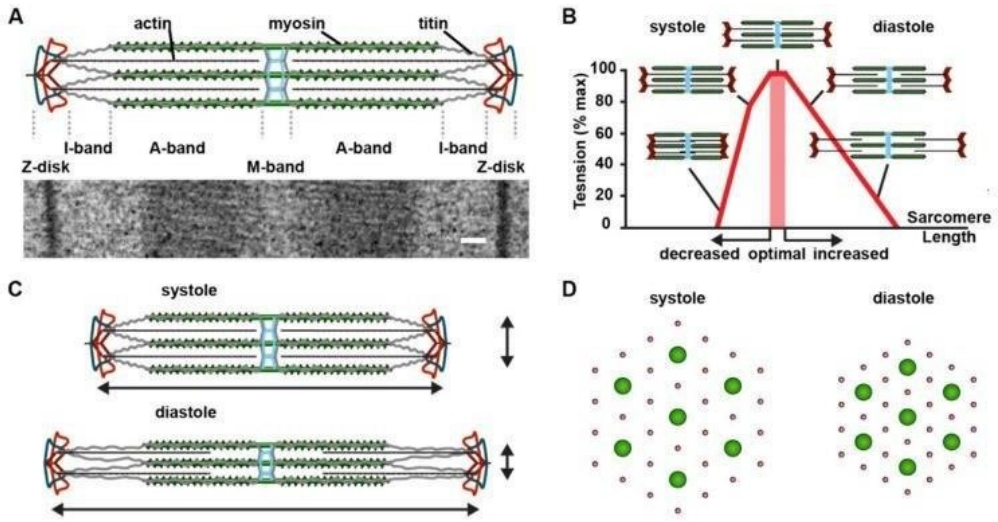

Figure 5. *Sarcomere structure during muscle contraction.*

In the myocardium, the force exerted by sarcomere is regulated by modification in beat frequency, sarcomere length, intracellular calcium and phosphorylation of sarcomere protein, such as troponin I, titin and myosin-binding protein C (Toepfer CN et al., 2016). When a cardiomyocyte is required to exert a greater contraction force, there is an increase in the number of myosin heads available for cross-bridge formation with actin, leading to increased ATP consumption (Toepfer CN et al., 2016). An efficient myocardial performance depends on two myosin conformations, super relaxed state (SRX), in which both ATP-binding domains are sterically inhibited and unable to bind actin, and a disordered state (DRX), where only one myosin head is available to hydrolyse ATP and interact with actin (Alamo L. et al., 2017). In addition to these two main conformations, researchers have discovered a folded-back structural state of myosin, which is termed "interacting-heads motif" (IHM), where the two-myosin sub fragment 1 (S1) heads of myosin asymmetrically interact with one another and fold back onto its sub fragment 2 (S2) tail (Woodhead et al., 2005; Zoghbi et al., 2008; Wendt et al., 1999) (Fig. 6).

Hypertrophic cardiomyopathy mutations may disrupt the balance between the two-myosin conformation, resulting in an alteration of cardiomyocyte contraction and metabolism, increasing the risks of cause heart failure and atrial fibrillation. In fact, previous finding provide

evidence that HCM mutations, such as MYH7 and MYBPC3, may alter the distribution of myosin states in the myocardium (Alamo L. et al., 2017).

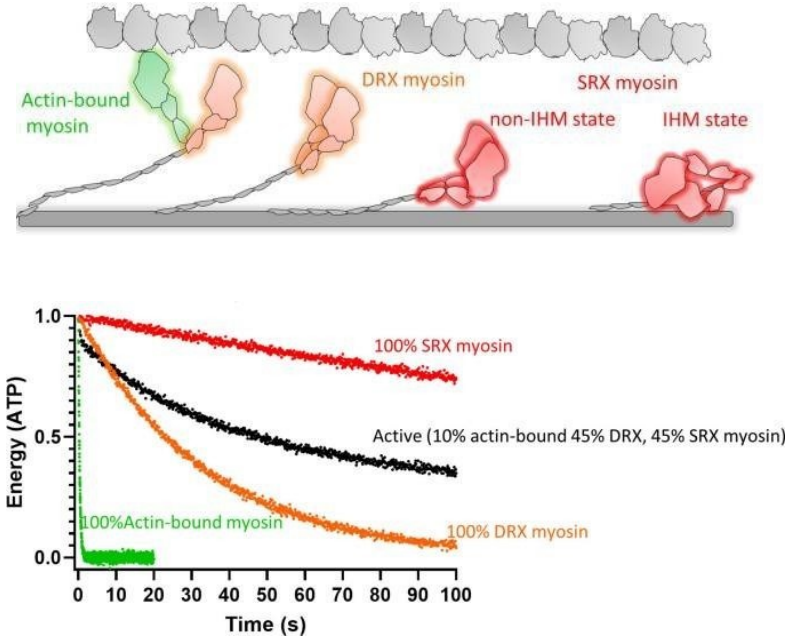

***Figure 6**. Schematic representation of the possible different functional states of myosin: actin-bound myosin, in green, DRX state of myosin, in orange, and SRX state, in red. The SRX state of myosin could be due to either a traditional IHM state or a non-IHM state (To lie or not to lie: super-relaxing with myosins, Nag S. et al., 2021)*

1.1.3 The role of HCM mutations on myocardium function

In addition to the main components of thick and thin filaments, several other structural and regulatory proteins are involved in the maintenance of sarcomere structure and function. The most common mutations associated with HCM occurs in the myosin-binding protein C (cMyBP-C) and β-myosin heavy chain (β-MHC), encoded by MYBP3 and MYH7 genes, respectively.

In this thesis, we will focus on cMyBP3 and MYH7 mutations, to investigate the effect of these alteration on the HCM pathogenesis.

Identified from Starr and Offer over 30 years ago, myosin-binding protein C (MyBP-C) is a sarcomeric thick filament protein consisting of 1274 amino acid residues (149 kDa), interacting with titin, myosin, and actin to regulate sarcomeric assembly (Barefield D. et al., 2009). Encoding by distinct genes, three isoforms of MyBP-C exist: fast-skeletal, slow-skeletal and

cardiac muscle-specific (Yamamoto K. at al., 1983), with the cardiac isoform being exclusively expressed in the heart (Fougerousse F. et al., 1998).

MyBP-C is localized at level of sarcomere, transversally, in the C-zones of A bands and forms transverse strips of ~ 43 nm, consisting of immunoglobulin (IgC2-like) and fibronectin (FN3) domains (Schlossarek S. et al., 2011). This protein interacts with multiple sarcomere components through specific domains. The interaction with the S2 fragment of myosin is mediated by the MyBP-C motif (Gruen M. et al., 1999); the interaction with the light meromyosin (LMM) via the C10 domain (Gilbert R. et al., 1999) and the link with titin is mediated by the C8–C10 domains (Freiburg A. et al., 1996). The precise organization of cMyBP-C within the sarcomere is still not completely understood, although the most accredited model is represented by the "trimeric collar" model (Winegrad S. et al., 1999). In this model, the C5–C10 domains, localized in three staggered parallel cMyBP-C molecules, surround the myosin filament. In fact, previous finding on isolated thick filaments suggests a role of cMyBP-C in myosin filament assembly and stability (Koretz JF. Et al., 1979).

In myocardium contractility, the functional role of cMyBP-C is the maintenance of myosin heads close to the thick filament backbone, acting as physical impediment and reducing the probability of the acto-myosin cycle during diastole. In fact, the absence of cMyBP-C results in left ventricular hypertrophy, cardiomyocytes disarray and diastolic function (Harris S.P. et al., 2022). The cMyBP-C binding to the other sarcomere proteins is regulated by the phosphorylation that occur on the M domain, containing three serine residues (S275, S284, and S304), targeted by cAMP-dependent protein kinase (PKA) or other protein kinases (Hartzell and Glass 1984); (Gautel et al. 1995). The main function of cMyBP-C is the regulation of cross-bridge formation, alternating the phosphorylated to the dephosphorylated state: when cMyBP-C is phosphorylated, induces a reduction of the interaction with thick filament heads, promoting cross-bridge formation; instead, the de-phosphorylated state promotes the bind to myosin S2 and limit cross-bridge formation.

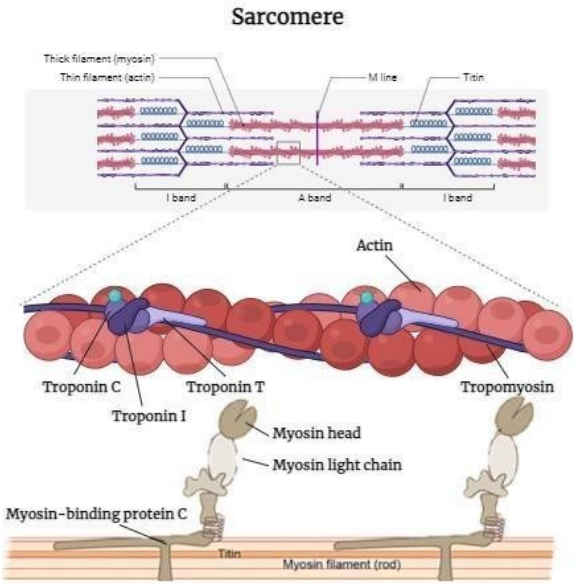

Figure 7. *Role of cMyBP-C in sarcomere structure.*

Therefore, considering its important function in cardiac contractility, mutations of cMyBP-C can greatly affect the functionality of the myocardium. In fact, hundreds of mutations in the MyBPC3 gene are the leading causes of hypertrophic cardiomyopathy (Wang H. et al., 2010). One of these pathogenic mutations, the c.772G>A has been reported as a pathological mutation in HCM patients. This mutation is caused by a missense substitution of the ammino acid lysin with a glutamic acid at position 258 (p. Glu258Lys, E258K), resulting in an exon skipping mechanism that impair spicing process (Singer et al. 2019). E258K mutation occurs in the last residue of the C1 IgC2 domain (L. Carrier et al. 1997), resulting in the weakening of the interaction between the C1 domain of cMyBPC and the S2 segment of myosin (Govada et al. 2008). The c.772G>A: MYBPC3 mutation acts to a mechanism of protein haploindufficiency as many MYBPC3 mutations in HCM. This results in a reduced regulation of myosin due to the reduced interaction between cMyBPCs and myosins. Several studies highlighted that this process may cause an acceleration of the contractile kinetics, increasing contraction force and an increased probability of cross-bridge formation (De Lange et al. 2013). For these reasons, HCM patient carrying E258K mutation show an important systolic dysfunction and a severe disease progression (Gajendrarao et al. 2015).

More recently, our group found that the c.772G>A: MYBPC3 mutation, very frequent in the cohort of the Careggi University-Hospital is founder-effect mutation in the Tuscany region as releaved by patient haplotype analysis. In the cohort of 1098 HCM patients about 98 carriers of the mutation showed a reduction of the occurrence of systolic dysfunction after the fifth-sixth

decade of life. Four of these patients, all in the fifth decade of life showed preserved ejection fraction but underwent myectomies to reduce obstructive symptoms. Left ventricular septal tissue analysis showed a reduction of about 30% of the total cMyBPC suggesting that the mutation acts through a mechanism of haploinsufficiency (Pioner et al., Circ res, 2023). Of note, other MYBPC3 mutation were associated to protein haploinsufficiency. This result was also confirmed in human induced pluripotent stem cell-derived cardiomyocytes (hiPSC-CMs) generated from the same patients (Streczina et al., 2024). The functional consequences of the mutation at sarcomere level were faster crossbridge cycling kinetics and impaired sarcomere energetics (increase tension cost). However, the mutation leads to secondary remodelling related to slower action potential and calcium transient duration likely counterbalancing the primary effect at sarcomere level, which cause an apparent preserved twitch duration and similar force but increasing the risk of arrhythmias (Pioner et al., Circ Res 2023).

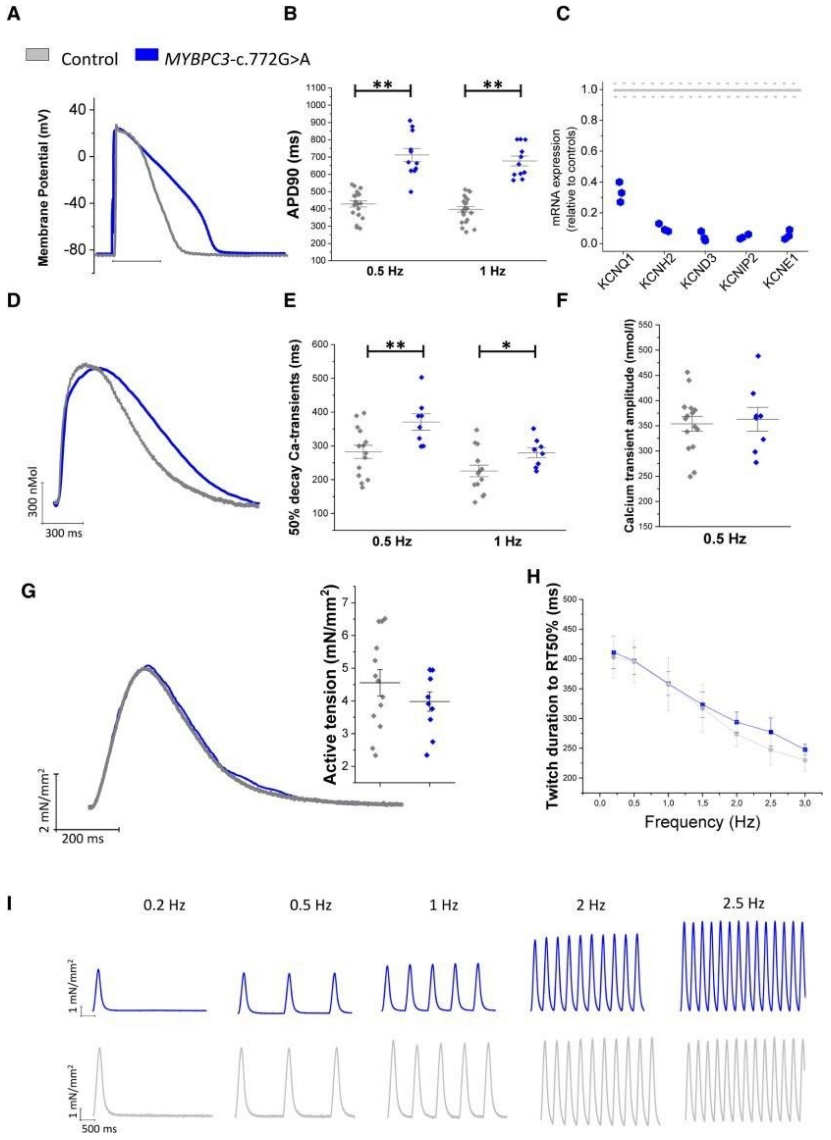

Figure 8. *Functional data from isolated cardiomyocytes and intact trabeculae. A) Representative trace of action potential and B) action potential duration at 90% of repolarization (APD90%) from control cardiomyocytes N=7, n=21) and c.772G>A cardiomyocytes (N=3, n=11), during stimulation at 0.5 and 1 Hz. C) RNA expression of potassium current genes in hypertrophic cardiomyopathy (HCM) samples (N=3) relative to the 18S ribosomal RNA), expressed as a fraction of control values (N=1, indicated with a grey line with confidence intervals in dotted lines). D, Representative superimposed calcium transients from control and c.772G>A cardiomyocytes during stimulation at 1Hz. E and F, Ca2+ transient decay duration (time from peak to 50% decay) and amplitude from control cardiomyocytes (N=6, n=14) and c.772G>A cardiomyocytes (N=2, n=8), during stimulation at 0.5 and 1 Hz. G, Representative superimposed force twitches from control and c.772G>A intact trabeculae during stimulation at 0.5 and 1 Hz (inset: twitch amplitude at 0.5 Hz) and (H and I) twitch duration from stimulus to 50% of relaxation by increasing of stimulation frequency (0.2, 0.5, 1, 2, and 2.5 Hz). Controls: N=9; n=1320; c.772G>A: n=7, N=3. E–H, *P.*

In addition to cMyBP-C mutation, other alterations are involved in the pathogenesis of HCM, with the onset of severe symptoms, involving myocardium hypercontractility (Sarkar et al., 2020), impaired relaxation (Toepfer et al., 2020), elevated cardiac energy consumption, diastolic dysfunction, arrhythmogenesis, and heart failure (Sarkar et al., 2020).

More than two decades ago, the R403Q mutation of cardiac myosin heavy-chain (MYH7) was the first cardiomyopathy-causing mutation ever discovered. This mutation results in conversion of a highly conserved arginine residue to a glutamine at position 403, located in the globular head of myosin (subfragment 1, S1) (Geisterfer-Lowrance et al. 1990). R403Q -MYH7 is associated with a particularly malignant form of inherited hypertrophic cardiomyopathy. This point mutation is localized in the S1 domain of the β-myosin heavy chain, the globular head of myosin, responsible for the interaction with actin. Moreover, since S1 domain is localized at the surface loop that directly interacts with actin, R403Q mutation can interfere with motor and sarcomere function (Rayment et al. 1995; Volkmann et al. 2007). A model for the effect of the R403Q mutation in β-cardiac myosin proposes that arginine 403 interacts with a tyrosine residue on the β-strand, and a mutation at this site weakens the interaction of the CM-loop with actin. In addition, several studies showed that this mutation is associated with an acceleration of cross-bridge relaxation kinetics that can lead to an increase in the energetic cost of sarcomere tension generation compared to healthy individuals (Belus et al. 2008).

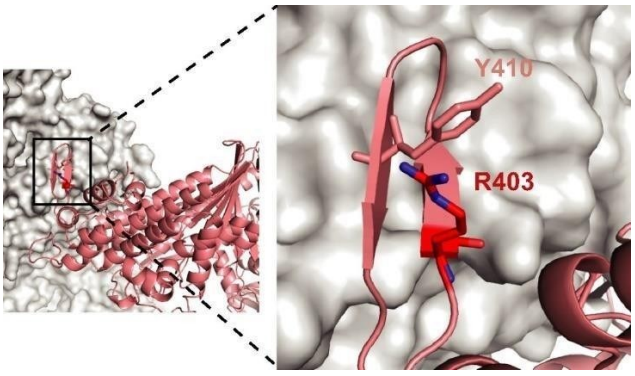

***Figure 9**. Cryoelectronic microscopy of cardiomyopathy loop at the actin-myosin interface. R403Q mutation is located on the sub-fragment S1 of β-cardiac myosin gene, MYH7, encoding for β-myosin heavy chain (β-MyHC). The CM-loop (in red) form an antiparallel β-strand that interact with actin (in gray).*
Hypertrophic cardiomyopathy R403Q mutation in rabbit β-myosin reduces contractile function at the molecular and myofibrillar levels, Lowey S. et al, 2018.

1.2 Dilated cardiomyopathy

Dilated cardiomyopathy (DCM) is a wide-range cardiac disorder characterized by an abnormal enlargement of ventricular cavity, often associated with the onset of cardiac fibrosis and myocardial dysfunction, in the absence of hypertensive or congenital cardiac disease. Moreover, the thickness of left ventricular wall appears in normal range. DCM is defined as the most common cause of heart failure, having an estimated prevalences of 1:2500 in the general population with 5-7 cases per 100.000 individuals per year (Hershberger R.E. et al.,2013).
In DCM, the typical ventricular dilatation can promote systolic heart failure symptoms, including arrhythmias, thromboembolic events, or cardiogenic shock. In addition, in DCM patients, usually a lower ejection fraction occurs (D. Reichart et al., 2019). The left ventricular remodelling caused from the dilation leads to pathophysiological modifications, including impaired ventricular filling and an increased end-diastolic pressure. These changes may promote higher venous pressure and an increase of circulating blood volume, resulting in elevated ventricular wall stress (Alter P. et al., 2012). In addition, a dysfunction of ventricular relaxation occurs, reducing the ventricular filling velocity and promoting arrhythmic events, with the increase of myocardial oxygen demand and cardiotoxicity (Lewis J.F. et al., 1993). These adaptations promote cardiomyocyte damage and a dramatic reduction of cardiac performance (Weintraub R.G. et al, 2017).

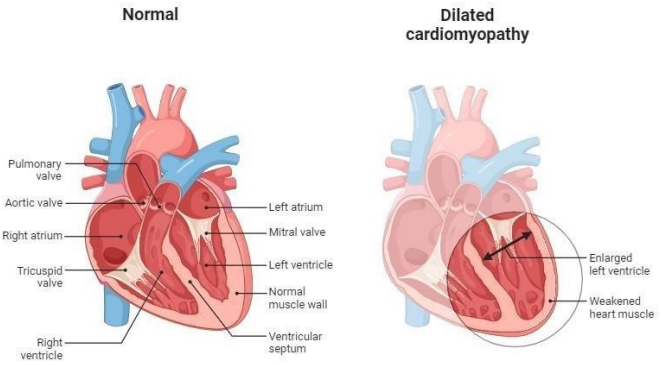

***Figure 10**. Dilated Cardiomyopathy induces a severe enlargement of left ventricular cavity, resulting in cardiac impairment and heart failure.*

To date, multiple DCM studies have reported alterations of the mechanical features of the myocardium, including disruption of energy production, abnormal nuclear integrity, alteration in force generation/transmission and ion channels modifications, pathological calcium homoeostasis and calcium handling abnormalities (Towbin J.A. et al., 2002).

The symptoms associated with DCM are very heterogeneous and may appear at any age: most patients receive diagnosis between 20 and 60 years of age, but affected children are not uncommon (Weintraub RG et al., 2017). However, patients can remain asymptomatic for a long time before receiving a diagnosis, especially in familial and idiopathic DCM.

The leading causes of dilated cardiomyopathy are heterogeneous and can be classified in genetic and nongenetic. In particular, infectious and inflammatory diseases (myocarditis), endocrine diseases, abuse of toxic substances have been described as leading nongenetic causes of DCM. In fact, alcohol or drugs like cocaine or methamphetamine can trigger the occurrence of this disease (Laonigro I. et al., 2019). Also, therapeutic drugs like anthracyclines may lead to oxidative stress, altering cardiac mitochondria and ultimately causing DCM (Lipshultz S.E. et al., 2013).

In about 35% of DCM patients, genetic mutations with autosomal dominant trait can be identified. In the last decades, many advances have been made in the understanding of the genetic basis of DCM. Starting from 1970s, several mutations have been identified in different genes associated with DCM. Mainly, the mutations occur in genes associated with cytoskeleton, sarcomere, as well as nuclear envelope proteins associated with the biomechanical coupling of contractile elements (Reaichart D. et al., 2019). These specific alterations can lead to an important impairment of cardiac contractility and a reduction of the wall elasticity during

diastolic filling (Weintraub RG et al., 2017). Another symptom is represented by a dysbalanced distribution of oxygen and nutrients, that may lead to cardiomyocyte death through necrosis, the onset of cardiac fibrosis associated with scarring and a reduction of contractile performance (Blechman I. et al., 2014; Cirulli E.T. et al., 2010).

Up to 25% of DCM mutations occur in the TTN gene (Gerull B. et al., 2002), encoding for the giant sarcomere protein titin; mutations in the LMNA gene, coding for the nuclear proteins lamins A and C, are present in about 5% of cases of genetic DCM (Taylor MR et al., 2003). Also, Phospholamban (PLN) and filamin C (FLNC) gene mutation and has been described with a high prevalence and a variable phenotype (Haghighi K. Et al., 2006). Finally, Furthermore, loss-of-function mutations associated with DCM have been described in the genes encoding for desmin (DES), dystrophin (DMD), cardiac actin (ACTC), beta-myosin-heavy chain (MYH7), troponin T (TNNT2) and delta-sarcoglycan (SGCD).

TABLE 1 | Principal pathogenic gene mutations described in genetic DCM along with their clinical and cellular phenotype.

Gene	Prevalence	Clinical phenotype	#hiPSC studies (References)	Functional output
Titin (*TTN*)	19–25% of familial forms 11–18% of sporadic forms	Usually milder forms of DCM, with LV reverse remodeling described after OMT. Can be associated with tibial muscle dystrophy and HCM (McNally and Mestroni, 2017). Truncating variants are related to alterations in mitochondrial function, increased interstitial fibrosis and reduced hypertrophy, along with increased ventricular arrhythmias at long-term follow-up, with a similar survival and overall cardiac function with respect to idiopathic DCM (Verdonschot et al., 2018).	5 (Hinson et al., 2015; Streckfuss-Bomeke et al., 2017; Chopra et al., 2018; Schick et al., 2018; Zaunbrecher et al., 2019)	Contractile deficit
Lamin A/C (*LMNA*)	5–6% of genetic DCM	Malignant DCM characterized by young onset, high penetrance, dysrhythmias (sinus node dysfunction, AF, atrioventricular node dysfunction, VT, VF, SCD), LV dysfunction and HF with reduced survival and frequent need for HT. Cardiac conduction system disease usually precedes the development of LV dilation and dysfunction (Hasselberg et al., 2018).	6 (Siu et al., 2012; Wyles et al., 2016a; Lee et al., 2017; Bertero et al., 2019; Salvarani et al., 2019; Shah et al., 2019)	LMNA haploinsufficieny; conduction defects; contractile defects
β-Myosin heavy chain (*MYH7*)	3–4% of DCM	Sarcomeric rare variant carriers show a more rapid progression toward death or HT compared to non-carriers, particularly after 50 years of age (Merlo et al., 2013).	?	
Cardiac troponin T (*TNNT2*)	3% of DCM	Clinical and prognostic profiles depend on type of mutation: carriers of Arg92Gln mutation have a worse prognosis than those with other mutations in *TNNT2* or other sarcomeric genes (Ripoll-Vera et al., 2016).	6 (Sun et al., 2012; Wu et al., 2015; Broughton et al., 2016; Burridge et al., 2016; Wang L. et al., 2018; Shafaattalab et al., 2019)	Calcium handling abnormalities; contractile defects
Type V voltage-gated cardiac Na channel (*SCN5A*)	2–3% of DCM	Arrhythmias (commonly AF) and myocyte dysfunction leading to progressive deterioration of LV systolic function (Bondue et al., 2018). Overlapping phenotypes: LQT, Brugada.	1 (Moreau et al., 2018)	Electrophysiological defects; Arrhythmias
RNA-binding protein 20 (*RBM20*)	1–5% of DCM	Malignant arrhythmic phenotype with high frequency of AF and progressive HF (Ripoll-Vera et al., 2016).	3 (Wyles et al., 2016a,b; Streckfuss-Bomeke et al., 2017)	Calcium handling abnormalities; contractile defects

Desmoplakin (*DSP*)	2% of DCM	Associated with Carvajal syndrome (autosomal recessive genetic disorder characterized by woolly hair, striate palmoplantar keratoderma and DCM). Additional phenotypic signs: dental abnormalities and leukonychia. LV dilatation usually asymptomatic at an early age. DCM progresses rapidly, leading to HF or SCD in adolescence (Yermakovich et al., 2018).	1 (Ng et al., 2019)	ACM
Dystrophin (*DMD*, Xp21.1 locus 16)	<2% of genetic DCM	Associated with Duchenne and Becker muscular dystrophy. Severe cardiac involvement in Duchenne (milder and later onset in Becker muscular dystrophy) with supraventricular arrhythmias, atrio-ventricular blocks and right bundle branch block, progressive LV dysfunction and HF (Mestroni et al., 2014).	20 (Dick et al., 2013; Guan et al., 2014; Zatti et al., 2014; Lin et al., 2015; Macadangdang et al., 2015; Japp et al., 2016; Nanni et al., 2016; Young et al., 2016; Kyrychenko et al., 2017; Zhang et al., 2017; Long et al., 2018; Caluori et al., 2019; Eisen et al., 2019; Farini et al., 2019; Jelinkova et al., 2019; Min et al., 2019; Pioner et al., 2019a; Sato et al., 2019; Tsurumi et al., 2019; Moretti et al., 2020)	Calcium handling abnormalities; contractile defects
α-Tropomyosin (*TPM1*)	1–2% of DCM	Overlapping phenotypes: LVNC, HCM (McNally and Mestroni, 2017)	1 (Takasaki et al., 2018)	Sarcomere defects
Desmin (*DES*)	1–2% of DCM (Taylor et al., 2007)	Malignant phenotype associated with desminopathies and myofibrillar myopathy. Can cause a spectrum of phenotypes from skeletal myopathy, mixed skeletal–cardiac disease ("desmin-related myopathy"), and cardiomyopathy (DCM as well as HCM or RCM). DCM is typically preceded by skeletal myopathy and can be associated with conduction defects (Mestroni et al., 2014).	1 (Tse et al., 2013)	DES protein aggregates
Filamin C (*FLNC*)	1% of DCM	Cardiomyopathy associated with myofibrillar myopathy and LVNC; high rate of ventricular arrhythmias and SCD (particularly in truncating variants) (Ader et al., 2019).	?	
Metavinculin (*VCL*)	1% of DCM	Can cause either DCM or HCM phenotype (Vasile et al., 2006)	?	
Phospholamban (PLN)	Rare (except for Netherlands where prevalence reaches 15% of DCM due to R14del mutation with founder effect) (van der Zwaag et al., 2012)	Early onset DCM with lethal ventricular arrhythmias. Low QRS complex potentials and decreased R wave amplitude, negative T waves in left precordial leads (Hof et al., 2019). PLN R14del mutation associated with high risk for malignant arrhythmias and end-stage HF from late adolescence, can cause either a DCM phenotype or ARVC (Mestroni et al., 2014). A milder phenotype is also reported (DeWitt et al., 2006).	4 (Karakikes et al., 2015; Stillitano et al., 2016; Ceholski et al., 2018; Stroik et al., 2019)	Electrophysiological defects
α-/β-/δ-Sarcoglycan (SGCA, SGCB, SGCD)	Rare	Recessive mutations in δ-sarcoglycan linked to limb girdle muscular dystrophy 2F, dominant mutations in δ-sarcoglycan linked to DCM (Campbell et al., 2016).	?	Ca handling abnormalities; Contractile defects
α-cardiac actin (*ACTC1*)	Rare	Familial atrial septal defect combined with a late-onset DCM (Frank et al., 2019). Can be associated with HCM and LVNC	?	
Cardiac troponin I (*TNNI3*)	Rare	Overlapping phenotype: HCM (McNally and Mestroni, 2017).	1 (Chang et al., 2018)	Telomere shortening
Cardiac troponin C (*TNNC1*)	Rare	Overlapping phenotypes: LVNC, HCM (McNally and Mestroni, 2017).	?	
Troponin I–interacting kinase (*TNNI3K*)	Rare	Conduction defect, AF (McNally and Mestroni, 2017).	?	
α-actinin 2 (ACTN2)	Rare	Overlapping phenotype: LVNC (McNally and Mestroni, 2017).	?	
BCL2-associated athanogene 3 (*BAG3*)	Rare	Associated with myofibrillar myopathy (McNally and Mestroni, 2017).	1 (Judge et al., 2017)	Disrupted myofibril; Contractile deficit
α-B-crystallin (*CRYAB*)	Rare	Associated with protein aggregation myopathy (McNally and Mestroni, 2017).	1 (Mitzelfelt et al., 2016)	Protein Aggregates; cellular stress
Titin-cap/telethonin (*TCAP*)	Rare	Associated with limb-girdle muscular dystrophy (McNally and Mestroni, 2017).	?	
Muscle LIM protein (*CSRP3*)	Rare	Overlapping phenotype: HCM (McNally and Mestroni, 2017).	1 (Li et al., 2019)	Calcium handling abnormalities
Cardiac ankyrin repeat protein (*ANKRD1*)	Rare	Associated with congenital heart disease (McNally and Mestroni, 2017).	?	
Cipher/ZASP (*LDB3*)	Rare	Overlapping phenotype: LVNC (McNally and Mestroni, 2017).	?	
Nebulette (*NEBL*)	Rare	Overlapping phenotypes: LVNC, HCM (McNally and Mestroni, 2017).	?	
Emerin (*EMD*)	Rare	Associated with Emery–Dreifuss muscular dystrophy (McNally and Mestroni, 2017).	1 (Shimojima et al., 2017)	Calcium handling abnormalities

Gene	Prevalence	Clinical phenotype	#hiPSC studies (References)	Functional output
Sulfonylurea receptor 2A, component of ATP-sensitive potassium channel (*ABCC9*)	Rare	Associated with AF, Osteochondrodysplasia (McNally and Mestroni, 2017).	?	
Potassium channel (*KCNQ1*)	Rare	Associated with AF, LQT1, short QT1, Jervell and Lange-Nielsen syndrome (McNally and Mestroni, 2017).	?	
HSP40 homolog, C19 (*DNAJC19*)	Rare	Associated with 3-methylglutaconic aciduria, type V (McNally and Mestroni, 2017).	1 (Rohani et al., 2020)	Mitochondrial abnormalities
Tafazzin (*TAZ/G4.5*)	Rare	Associated with LVNC, Barth syndrome, endocardial fibroelastosis 2 (McNally and Mestroni, 2017).	1 (Wang et al., 2014)	Mitochondrial defects; contractile defects

Figure 11. *Principal pathogenic gene mutations described in genetic DCM along with their clinical and cellular phenotype (Advances in stem cell modelling of dystrophin-associated disease: implications for the wider world of dilated cardiomyopathy, Pioner et al., 2020, frontiers in physiology).*

Cardiac magnetic resonance imaging (CMR) provides accurate assessment of ventricular chamber size and wall thickness. Especially in patients with unclear echocardiographic phenotypes, CMR can represent a valuable tool to provide a non-invasive tissue characterization.

To date, pharmacological treatments of DCM involve the administration of ACE-inhibitors, angiotensin receptor blockers (ARB), β-adrenoreceptor blockers (BB), aldosterone antagonists and vasodilators, with an improvement in associated symptomatology and an increased patient survival (Lakdawala et al, 2013).

1.2.1 Duchenne Muscular Dystrophy (DMD)

Duchenne Muscular Dystrophy (DMD) is a X-linked neuromuscular disease that causes a progressive degeneration of skeletal and cardiac muscle. It is characterized by a gradual muscular weakness and cardiovascular and respiratory complications. DMD is the most prevalent neuromuscular disorder, affecting up to 1/3600 male births around the world (Chung J. et al., 2015) and it is caused by a mutation in the Dystrophin gene (DMD gene), the largest gene described in human, localized in the X chromosome and encoding for the protein dystrophin, an “adsorber” protein involved in the protection of muscle fibres integrity during contraction. Dystrophin is localized through the plasma membrane of myocytes and represent one of the components of a large glycoprotein complex called dystrophin-associated glycoprotein complex (DAGC), including other components like dystroglycan, sarcoglycan, and neuronal nitric oxide synthase. DAGC is involved in several pathways, regulating excitation-contraction coupling, mitochondrial function, Ca^{2+} homeostasis and gene expression. Within the DAGC, dystrophin acts as a connection between the cytoskeleton and the

extracellular matrix, reducing the mechanical stress exerted on the cellular membrane during contraction.

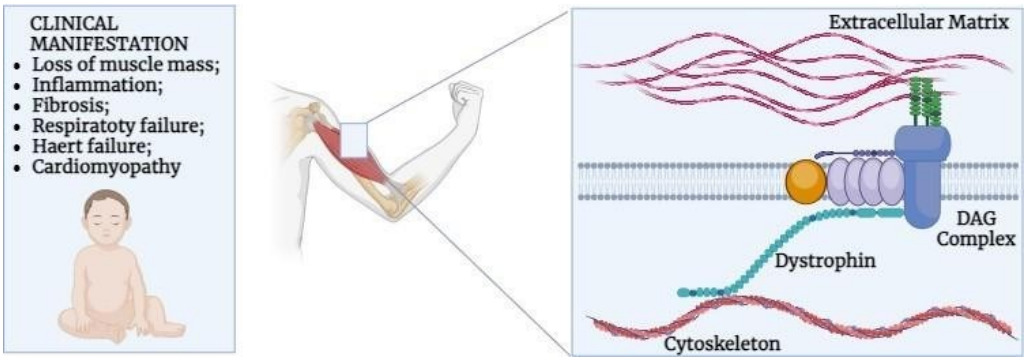

***Figure 12**. Clinical manifestation of Duchenne Muscular Dystrophy and role of dystrophin in the maintenance of cardiomyocytes integrity*

The DMD gene produces three full-length isoforms of dystrophin, starting from three independent promoters, in brain, muscle, and Purkinje cerebellar neurons, but other isoforms are generated by alternative splicing events. Moreover, dystrophin is a 427 kD protein folded into specific distinct domains: an amino terminus domain, that contains the binding domain for actin, a large rod-like domain composed of several "spectrin-like" repeats, a cysteine-rich domain and the C-terminus, which binds the dystrophin-associated glycoprotein complex (DAGC) (Ferlini et al., 2013).

Up of 65% of mutations associated with DMD are deletions, but in about 6%-10% of the cases duplications may occur, interrupting the open reading frame of RNA (Ferlini A. et al., 2012). All these mutations result in the total absence of dystrophin expression, that promote membrane instability, myocyte damage and cardiac failure, causing an increase of cellular susceptibility to injury and cardiomyocytes death. In addition, in DMD patients, the regenerative capability of myofibers result impaired due to the persistent damages which satellite cells are subjected to (Ogura I. et al., 2014).

The clinical manifestations occur early in the childhood, with progressive loss of walking capacity, culminating in a complete loss of ambulation at age between 8 and 14 years. Cardiac complications are present in up to 25% of DMD patients and involve the onset of arrhythmias and a severe form of dilated cardiomyopathy (DCM), that strongly impair the cardiac function

of these patients. Chronic respiratory insufficiency appears within the third decade of life and represent the main causes of death for these patients (You E.M. et al., 2015).
The diagnosis of DMD usually is based on high levels of muscle protein creatine kinase (CK), caused by progressive muscle damage to which they are subject, exceeding 10 times or even 100 times normal serum levels (Konagaya M. et al., 1986). The confirmation can be made with a muscle biopsy or using appropriate genetic tests for the analysis of mutations in the DMD gene.

1.2.2 Limitation for modelling Duchenne Muscular Dystrophy

To date, the knowledge of the main mechanisms of human diseases is crucial to provide new and effective pharmacological treatments, but the lack of suitable experimental models and the scarce availability of human surgical samples has strongly limited scientific and pharmacological research. To date, the understanding of the genetic causes of heart disease is significantly increase, but the development of models to study the pathogenetic mechanisms remains poorly investigated. Functional studies were mainly limited to the use of animal models which, however, present important limitations related species differences, electrophysiological and mechanical behaviour. Several studies have been conducted to assess the suitability of a variety of cell sources, including embryonic stem cells (ESCs) (Clements and Thomas, 2014) and induced pluripotent stem cells (iPSCs) (Mathur et al., 2015). In this context, the study of Duchenne Muscular Dystrophy (DMD) is limited by the absence of a valuable model of study showing mechanical and electrophysiological parameters that can represent the features of adult myocardium. Patient-derived induced pluripotent stem cells (hiPSCs) allow personalized medicine, drug testing and in vitro modelling of several inherited disorders, maintaining the genetic heritage of patient. Cardiomyocytes obtained from hiPSCs lines represent a unique tool to investigate the main pathophysiological mechanisms related to early-stage alterations underlying the progression of DMD cardiomyopathy. This represents a unique opportunity to study dilated cardiomyopathy (DCM) associated to DMD, a disease that rarely require surgical interventions, making it difficult to use human surgical samples. In fact, recent evidence show that these cellular models may reflect characteristics that are getting closer to those of adult myocardium, also in association to an increase of level of maturation, including the use of long-term cultures combined with nanostructured surfaces (Pioner et al., 2019). Moreover, patient-derived tissues may represent the final stage of disease, thus other model of study that may lead the investigation of primary pathological mechanisms, induced by the absence of full-length

dystrophin are required. These “early” mechanisms should be distinguished from secondary process, resulting from the effect of neurohormonal stimulation, adverse cardiac remodelling, or drugs intervention. For these reasons, since the first report of Yamanaka and Takahashi in 2006 (Takahashi and Yamanaka, 2006), cardiomyocytes obtained from hiPSCs, via CRISPR7Cas9 or TALEN technique are the most relevant model for modelling human heart in vitro.

1.3 Human induced pluripotent stem cells (hiPSCs)

The knowledge of the main mechanisms of human diseases is crucial for the development of new and better pharmacological treatments, but the lack of suitable experimental models and the scarce availability of human surgical samples has strongly limited scientific research, in particular in the pharmacological field. To date, the understanding of the genetic causes of heart disease is significantly increased, but the availability of models to study the underlying pathogenetic mechanisms remains limited. In the cardiology field, functional studies are limited by the use of animal models (in particular small rodents), which have important limitations related with inter-species variability in the electrical and mechanical behaviour of cardiac muscle. Several studies have been conducted to assess the suitability of a variety of cell sources, including embryonic stem cells (ESCs) (Clements and Thomas, 2014) and induced pluripotent stem cells (iPSCs) (Mathur et al., 2015). Human induced pluripotent stem cells (hiPSCs) can overcome the limitations of human surgical samples and animal models, representing a valuable tool to study several acquired and genetic cardiac diseases, including hypertrophic and dilated cardiomyopathies. In fact, the possibility to induce the differentiation of hiPSCs into several desired cell type, maintaining the genetic profile of patient, allows researchers to perform patient-specific studies, heart regeneration and drug testing.

Induced pluripotent cell lines are obtained from terminally differentiated cell lines using specific genetic editing techniques that allow the expression of specific transcription factors to induce reprogramming of the differentiated cells into hiPSCs. From this “immature” stage it is possible to generate the three different primary germ layers and, therefore, potentially all cell types present in the human body (Mourad A. M. et al., 2021). The obtained cells present typical self-renewal characteristics of stem cells, avoiding ethical problems related to the use of human embryonic cells (ESCs). The generation of iPSCs began with the work of Dr. Yamanaka's group (Takahashi and Yamanaka 2006) with the discovery of four reprogramming factor (Oct4, Sox2, c-Myc, Klf4) for the induction of an embryonic pluripotent state in somatic cells. Recently, the

most commonly used method to induce the reprogramming into hiPSCs is the integration of the four "Yamanaka" factors into the genome by lentiviral or retroviral transduction (Novak et al., 2019), but new and innovative techniques, including the CRISPR/Cas9 system, can be used (Borestrom C. et al., 2018). However, to induce hiPSCs differentiation into a specific cell type and exploit their full potential, reproducible and effective differentiation protocols are fundamental. In most cases, in vitro differentiation summarizes the gradual stages of embryonic development towards the cell type of interest.

Reprogramming of somatic cells into iPSCs can be performed using cells from different tissue sources, including dermal fibroblasts, squamous urethral cells, monocytes, and keratinocytes (Takahashi et al., 2007).

- *Fibroblasts*. Because of their ease of growth, propagation and storage, this cell type has been widely used for the derivation of pluripotent stem cells in vitro. Fibroblasts can be obtained from skin biopsies or from other organs and are characterised by high stability. However, the main problem related to their use is represented by the low percentage of reprogramming efficiency (0.01-0.5%), from the long period of time that elapses from the induction of the reprogramming factors to the obtaining of the pluripotent-cell colonies, and from the invasiveness of the intervention (biopsy), if compared to the procedures needed to collect other cellular types (Raab and al., 2014);
- *Squamous cells of the urethra*. HiPSCs can also be derived from cells present in the tubular system or lower urinary tract, including ureter, urethra, and bladder epithelium, that spontaneously detach from the urothelium and can easily be found in the urine. Starting from urine samples, following some washing and centrifugation steps, these epithelial squamous cells can be easily cultured (Inoue et al., 2003). Their derivation involves the use of a much less invasive process, and they are characterized by a good efficiency of reprogramming, which is around 0,1-4% (Zhou et al., 2011). As a result, these cells represent a good source of hiPSCs and can be used for in vitro studies (Inoue et al., 2003). They can also be frozen without affecting their reprogramming efficiency, which however may decrease after 5 freezing/thawing steps (Xue et al., 2013);
- *Keratinocytes*. More recently, numerous studies have reported the use of keratinocytes as a starting material for the production of hiPSCs (Raab et al., 2014), having a higher rate of growth in culture (1-2 weeks) compared to fibroblasts (3-4 weeks). In this case, several skin attachments can be used as sources, such as hair, beard hair and eyebrows. The advantage of this procedure is to obtain iPSCs through a non-invasive and easy

method. Moreover, keratinocytes have a significant reprogramming efficiency, (about 1-2%). However, the technique of isolation of keratinocytes is relatively laborious;

- *Blood cells (monocytes).* In this case, a distinction should be made between the use of peripheral blood or blood from umbilical cord. In the first case, the isolation procedure has two distinct modalities: it is possible to obtain iPSCs starting from the mobilization of CD34+ cells (Loh et al., 2009), but it is an expensive and time-consuming procedure, as well as painful for the patient. In this case, the isolation of hematopoietic stem cells, which can then be cultured and reprogrammed into iPSCs, leads to the development of cells that have very similar characteristics to those of other iPSCs lines obtained from embryonic stem cells (Loh et al., 2009). Instead, a less invasive method to obtain iPSCs from peripheral blood is represented by the isolation of specific mononucleate cells from standard venous blood through a technique that exploits the gradient of density and centrifugation (Ficoll density gradient technique), with an acceptable efficiency of obtainment (Staerk et al., 2010). Several studies highlighted that the volume of a single blood drop (10 ml) is sufficient to obtain the proper number of cells to simultaneously carry out the reprogramming and serotyping procedures (Tan et al., 2014).

In the recent years, researchers have worked on the protocols to obtain cell cultures of cardiomyocytes and to assess their ability to fully reproduce the characteristics of adult cardiomyocytes, becoming valid study models for cardiomyopathies (Paul W. Burridge et al, 2014). Starting from hiPSCs, the procedure of obtaining functional cardiomyocytes involves the activation and inhibition of particular molecular pathways, at specific stages of cardiomyocyte development, in order to induce the genetic commitment of these cell lines, inducing their differentiation towards cardiomyocytes. This process resembles the embryonic stages of cardiac development, with the modulation of signaling pathways, such as BMP, NODAL, FGF, and Wnt, inducing the commitment into mesoderm, cardiac precursors and finally differentiated cardiomyocytes (Filipczyk et al. 2007).

The protocols recently used to induce cardiac differentiation exploit two main approaches: a cardiac differentiation protocol on monolayers, where cells adhere to a culture substrate consisting of ECM proteins (Laflamme et al., 2007; Palpant et al., 2015); an aggregation-based method, where undifferentiated cells are aggregated to form 3D globular structures, such as embryoid bodies (Zhang J, 2012) or engineered trabecula-like tissues.

1.3.1 hiPSCs derived cardiomyocytes (hiPSCs-CMs) to model cardiomyopathies

hiPSCs obtained from somatic cells have the capability to maintain the specific genetic heritage of the donor patients, representing a valuable tool to investigate cardiac diseases in vitro. In particular, hiPSCs can be generated from patients carrying a specific mutation, generating an in vitro model that recapitulates the background of the subject from which they are derived. In this contest, hiPSC-CMs are an excellent resource for modelling inherited cardiomyopathies, allowing researchers to explore early disease defects before the onset of clinical manifestations. Several techniques can be used to induce specific mutations in hiPSC lines, including CRISPR/Cas9, allowing the generation of patient-specific and isogenic cell lines, that resemble the genetic background of donor patients with the exception of the mutation that caused the disease.

Various research works involved the use of iPSC-based models to study inherited cardiomyopathies, in particular HCM. Studies conducted on hiPSC-CMs derived from HCM patients showed a higher rate of arrhythmogenic delayed after depolarizations in HCM cardiomyocytes compared to controls, paralleled by abnormal Ca^{2+} handling (Lan et al. 2013). Other studies performed on hiPSC-CMs carrying MYH7 mutations shown of a prolongation of action potential (AP) and up-regulation of Na+ and Ca2+ currents, the same alterations that were observed in human cardiomyocytes obtained from HCM patients (Han et al. 2014; Coppini et al. 2013). Instead, in hiPSC-CMs with mutations in MYBPC3 authors have highlighted calcium handling alterations, associated with prolonged transient decay kinetics and elevated diastolic calcium levels in the absence of structural abnormalities in HCM iPSC-CMs compared with isogenic controls (Seeger et al. 2019). Moreover, altered force production was observed in HCM hiPSCs-CMs, showing potential defect in sarcomerogenesis, leading an increase of calcium sensitivity, disrupted crossbridge cycling and diastolic dysfunction (Birket et al. 2015). Also, hiPSC-CMs were used to perform mechanical evaluations. Several studies have used hiPSC-CMs to investigate dilated cardiomyopathy (DCM), showing an important decrease of force production connected to the absence of full-length dystrophin (Bremner et al. 2022). Moreover, it was also observed that DMD hiPSC-CMs showed no enhancement of Ca^{2+} release during maturation in culture, while calcium release tended to gradually increase in control cells (Pioner J.M. et al. 2022); this was associated with a reduction of force generation in DMD cells (Chang et al. 2021), high resting Ca^{2+} levels, mitochondrial damage and cell death.

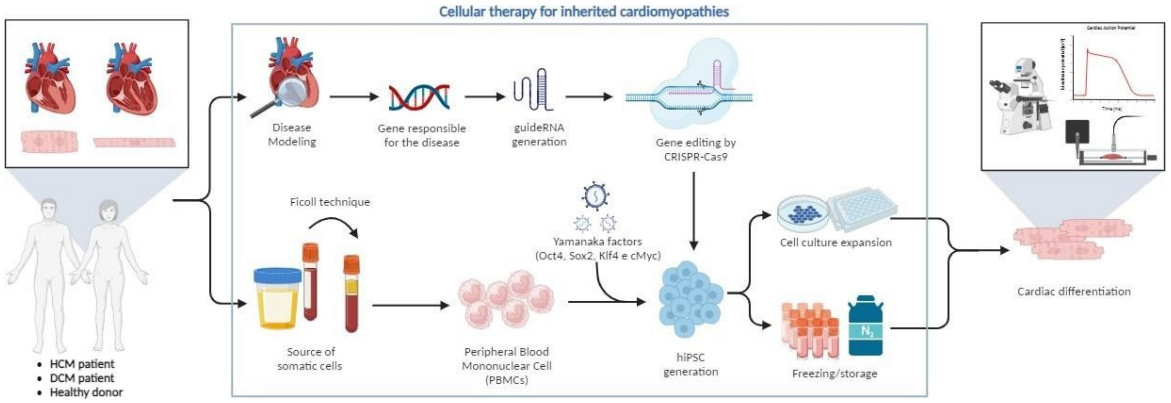

Figure 13. *Generation of induced pluripotent stem cells lines. Somatic cells were obtained from HCM, DCM patients and healthy donor and reprogrammed into hiPSCs through Crispr/Cas9 technique. Viable cardiomyocytes were differentiated from hiPSCs by using a specific differentiation protocol on monolayer and tested to perform mechanical and electrophysiological evaluations.*

1.3.2 Maturation strategies and limitations of induced pluripotent stem cell-derived cardiomyocytes

Despite many advances made in the development of hiPSCs, several problems related to their use remain unresolved. The main limitation is the evidence that different somatic cells used for the hiPSCs derivation have different levels of reprogramming efficiency, variable culture conditions and phenotypic instability. In addition, variability among different clones derived from the same patient is also present, making it difficult to obtaining homogeneous cell populations. In addition, the main limitation to the use of hiPSC-CMs as a model of cardiac disease is the obtainment of a satisfying level of cardiomyocyte maturation, i.e. cells that resemble the features of adult cardiomyocytes. In fact, hiPSC-CMs still have immature structural and functional characteristics, in that they resemble fetal cardiomyocytes, including the persistence of automatisms, the immature electrophysiological responses (Davis et al., 2011), the fetal-like gene expression patterns (van den Berg et al., 2015) and the different size and morphology.

Morphology

Since the sarcomere is the contractile machinery of cardiomyocytes and contains the essential contractile components (actin and myosin), its assembly is fundamental for a correct function of CMs (Willis M. S. et al, 2009). In comparison with adult human cardiomyocytes, hiPSC-

CMs show disorganized sarcomeres stripes, they are mononucleate, exhibit a rounded or mildly elongated shape, and show a total absence of T-tubules (Zhang et al, 2013). In contrast, adult CMs are characterized by a significantly elongated rod-like shape, well-organized contractile components, with evident T-tubules and a high density of Z-band and I-band stripes (Denning C. et al., 2016, Ivashchenko C. Y. et al., 2013). Moreover, hiPSC-CMs contain partially arranged myofibrils and have a short sarcomere lenght (1.6 μm on average) (Wu P. et al., 2021). In adult CMs, after cardiac troponin T staining (cTnT) and cTnI, a highly organized sarcomere structure is appreciable, comprising α-actin and β-myosin heavy chain (β-MHC, MYH7 gene)), with a higher expression of β-MHC as compared with α-MHC (MYH6 gene) (Yang X. et al., 2014). In addition, adult CMs express important structural and functional proteins, such as cardiac titin (N2B), cTnI and sarcoplasmic reticulum ATPase (SERCA2); in contrast, hiPSC-CMs show high levels of MYH6 and express a different N2A titin-subtype rather than N2B (Denning C. et al., 2016).

Metabolism

In the first few months after human birth, cardiomyocytes continue to multiply and grow. As a consequence of this process, an increase of ATP production is required, with the induction of mitochondrial biogenesis and a metabolic conversion from the consumption of glucose and lactic acid into β-oxidation of fatty acids, to induce the production of more energy (Goffart S. et al., 2004). In adult cardiomyocytes, mitochondria account for 20-40% of the cell volume and show oval and lamellar cristae to provide ATP for contraction and other important functions (Scuderi G. J. Et al., 2017). However, in hiPSC-CMs, mitochondria are small and show the absence of mitochondrial cristae, reflecting a deficit in the production of energy necessary for the proper mechanical performance of cardiomyocytes.

Calcium Handling

In adult cardiomyocytes, intracellular Ca^{2+} plays a fundamental role in several processes, including metabolism, signalling, contraction and transcriptional regulation and represent one of the trigger components of excitation-contraction coupling (E-C coupling). In this process, depolarization propagating through the surface sarcolemma and T-tubules causes the opening of voltage-gated L-type calcium channels (LTCCs) and the consequent entry of calcium into the cell. As a result of the increase in the calcium cytosolic concentration, further calcium is released from the sarcoplasmic reticulum (SR) through the ryanodine receptors (RyRs) expressed on its membrane, via a process known as calcium-induced calcium-release (CIRC).

At this point, Ca^{2+} binds to troponin C, leading to myofilaments sliding and activating cardiomyocyte contraction. To stop contraction, calcium is brought inside the SR through the activity of the SERCA2a pump (SR Ca-ATPase) and simultaneously extruded from the cell by the Na^{+}-Ca^{2+} exchanger of the sarcolemma. This whole process is hastened by the presence of T-tubules, that comprise specialized structures connecting the LTCCs on the sarcolemma with the RyRs of SR ("dyads") (Bers D.M. et al., 2002). However, T-tubules are totally absent in hiPSC-CMs, with a low expression of SERCA2a and a scarcely developed SR, resulting in a complete dependence on sarcolemmal LTCCs to promote the increase of calcium concentration that triggers contraction, with a very low E-C coupling gain (Veerman C. et al., 2017).

Electrophysiology

Action potential (AP) is the result of the well-timed opening and closing of multiple ion channels on the cardiomyocytes membrane. During the phase 0, a rapid sodium influx (I_{Na}) occurs depolarizing the cell and promote the beginning of AP. Then, in initial repolarization phase 1, the transient outward potassium current (I_{to1}) is activated causing K^{+} outflow; during phase 2, Ca^{2+} ($I_{Ca,\,L}$) enters inside the cell, counterbalanced by the slow K^{+} currents (I_{Kr} and I_{Ks}), thus inducing the plateau phase of AP, Finally, the inactivation of $I_{Ca,\,L}$ and the prominent activation of K+ channels (I_{Kr} and I_{Ks}) repolarize the membrane in phase 3 and Inward rectification of the background K^{+} channel (I_{K1}) helps to maintain the resting membrane potential in Phase 4 (Drouin E. et al, 1998). In comparison with adult CMs, hiPSC-CMs are characterized by a less negative maximum diastolic potential (MDP), slower kinetics of AP and spontaneous beating, due to the reduced density of I_{K1} and the expression of the pacemaker current If (Lieu D. K. Et al., 2013).

Therefore, this evidence suggests the need to develop more efficient hiPSC-CMs maturation protocols, stimulating maturation through specific methods, including nanostructured surfaces, co-cultures with other cell types, electrical stimulation in vitro and generation of 3D structure, that more closely can mimic the extracellular matrix features (Ribeiro et al., 2015).

1.3.3 Methods to increase hiPSC-CMs maturation in vitro

In recent years, several points of evidence in the literature highlighted successful protocols for the differentiation of hiPSCs into cardiomyocytes (Burridge et al 2012). These hiPSC-CMs show morphological and functional characteristics typical of human adult cardiomyocytes, such as expression of sarcomeric proteins and ion channels, respond efficiently to the hormonal

signalling, display mature-like action potentiasl and calcium transients (Zhu et al., 2009). However, despite these promising initial results, there is much experimental evidence that emphasizes the immaturity of cardiomyocytes derived from induced pluripotent stem cells, compared to adult cardiomyocytes. Recent studies reported the possibility of inducing a more efficient maturation of hiPSC-CMs, using a variety of methods (Lundy et al., 2013).

Long-term culture. In vivo cardiomyocytes require extremely long time to grow and reach a phenotype that replicates that of adult human cardiomyocytes. Therefore, it has proved necessary to develop more efficient in vitro differentiation techniques. For this purpose, an effective in vitro hiPSC-CMs differentiation protocol of 120 days duration was developed (Lundy et al., 2003). Such long-term cultures show slowed contraction kinetics, increased calcium release and reuptake, associated with increased amplitude of action potentials, indicating a progressive time-dependent increase in the maturation of hiPSC-CMs.

Patterning. In vivo cardiomyocytes are subjected to several physical stimuli, allowing their elongation and the acquisition of their characteristic morphology, that may change the alignment of sarcomeres (Bray et al., 2008). For these reasons, reproducing in vitro these physical and mechanical stimuli can favour the maturation of cardiomyocytes; in fact, several evidence highlighted that the plating of hiPSC-CMs on specific nanostructured substrates can increases the organization and the cellular alignment (Wang et al., 2011; Heidi et al., 2009). In addition, the pattern stiffness can modify the cellular maturation. In fact, the cardiomyocytes organization changes greatly during development: collagen accumulation, for example, begins during embryonic development and continues for several weeks after birth. This causes a change in the rigidity of the heart extracellular matrix and affects different functions of the myocardium. Therefore, it has been hypothesized that the growth of hiPSC-CMs on substrates with different rigidity may affect cardiomyocyte maturation, leading to more mature myofibrillary structure and increased intracellular calcium levels.

3D tissues. More recently, new advances in bioengineering allowed researchers to generate specific three-dimensional (3D) constructs based on cardiomyocytes derived from hiPSCs. These innovative systems can produce biochemical and physical stimuli that lead to mature structural and functional properties of cardiomyocytes (Sacchetto C. et al., 2020). In fact, several studies reported an increase of cardiomyocyte physiological and electrical function in comparison with 2D cultures (Karbassi E. et al., 2020). To date, 3D tissues with different shape

were developed, from spheroids and microtissues (for drug screening) to cardiac strips or rings (to investigate mechanical properties).

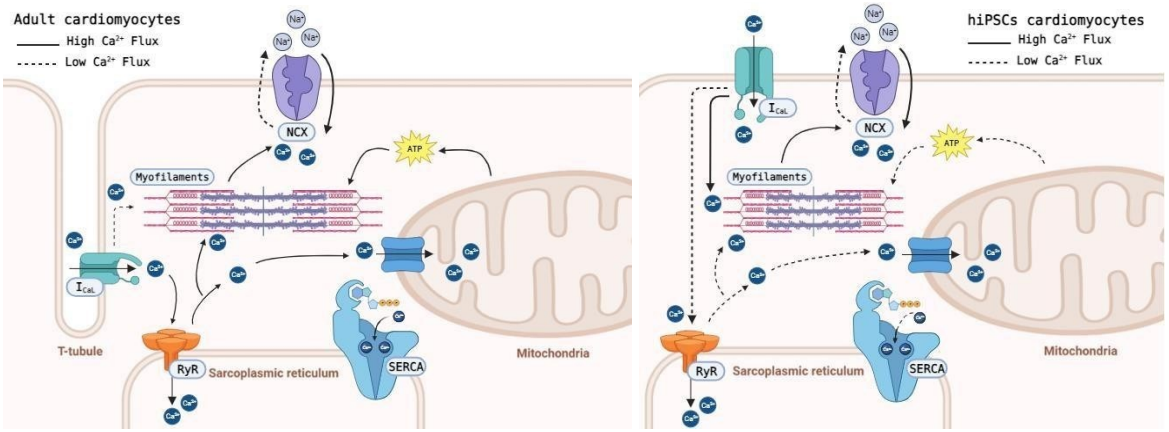

Figure 14. *Excitation-contraction coupling (EC-coupling) in adult cardiomyocytes compared to induced pluripotent stem cells derived cardiomyocytes.*

1.3.4 Cellular patterning

Several studies suggested that abnormalities that occur in cardiomyocytes maturation may lead to structural and functional cardiac alterations in inherited cardiomyopathies (Girolami et al., 2022). In fact, cardiomyopathy-related mutations alter the function of cardiac cells, resulting in pathological modifications that lead to cardiac impairment and heart failure in the adult heart (Olivotto et al., 2009).

Cardiac differentiation from hiPSCs summarizes the changes occurring in myocardium during the embryonic stage. However, since hiPSC-CMs show immature electrophysiological features, in the early stage of differentiation, calcium diffusion in cardiomyocytes cytosol is slower compared to the later stages of cardiac development (Lundy et al., 2013). Moreover, calcium increase before the development of contractile apparatus and calcium handling alterations may influence the electrical and mechanical function of mature cardiomyocytes (Pioner et al., 2020).

Another important aspect of cardiomyocyte maturation is their capacity to increase contraction force in response to increased stiffness (Rodriguez et al., 2011; Ribeiro et al., 2015). In fact, culture surfaces with a specific patterning may lead to an increase of cardiomyocytes maturation, improving a rapid elongation, myofibril alignment and sarcomere length (Carson et al., 2016). Previous findings highlighted that cardiomyocyte regulation of calcium

homeostasis and cellular electrophysiology are improved on micropatterned surfaces (Pioner et al., 2019). Moreover, changes of extracellular stiffness may occur in inherited cardiomyopathies, mainly associated with the onset of myocardial fibrosis, resulting in alteration on cardiomyocyte function.

1.4 Electrophysiological evaluation during cardiomyocyte maturation

1.4.1 Calcium handling measurements

In a previous study, to evaluate the possible implications of cardiac fibrosis, we compared hiPSC-CMs from a Duchenne Muscular Dystrophy (DMD) patient carrying a deletion of exon 50 in DMD gene (Guan et al., 2014) with a control line and an isogenic positive control line created using CRISPR-Cas9 knocking out one exon of the DMD gene (c.263delG) (Pioner et al., 2019). Moreover, we tested the possible implications of different stiffness levels of the extracellular matrix on cardiomyocyte development, by growing hiPSC-CMs on specific micropatterned surfaces with different mechanical features and rigidity. In fact, the absence of full-length dystrophin may directly affect the interaction of cardiomyocytes with the extracellular environment and thus may influence cardiomyocytes maturation.

DMD and control-hiPSC-CMs were plated onto custom-made photopolymerized polyethylene glycol-diacrylate (PEG-DA 100%) surfaces featuring an array of parallel micro-grooves 0.6 µm wide and 1.5 µm deep, with 1.4 µm of space between adjacent lines (Pioner et al., 2019). Cardiomyocyte calcium handling was compared at different stages of maturation (day 60, 75 and 90 p.d.) (Figure 15A).

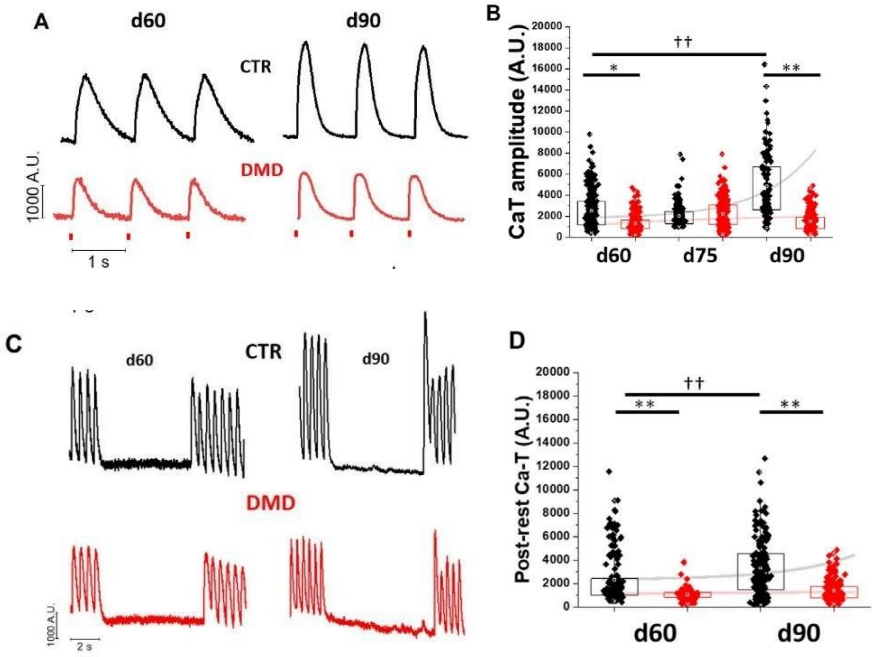

Figure 15. *Changes of calcium transient amplitude during hiPSC-CM maturation. Calcium transients were estimated at day 60, 75 and 90 post differentiation at 37°C, 1.8 mM [Ca2+]. (A) Representative CaT profiles at day 60 and 90 and average CaT amplitude (Fluorescence Arbitrary Units, A.U.) of DMD-versus control-CMs at day 60,75 and 90. (B) Sarcoplasmic reticulum (SR) contribution in calcium handling maturation was tested by a*

*post rest potentiation protocol at multiple maturation time-points. (C) The post-rest potentiation of CaT amplitude was estimated after a resting pause of 5 s, inserted in a regular train of stimulation at 2 Hz. (D) The potentiation is expressed as the % of increase of the first post-rest CaT with respect of CaT pacing train before the pause (%). Post rest potentiation of DMD-versus control-CMs is estimated at day 60 and day 90. Exponential curves with Stirling's approximation were used to show the variation of maturation in both groups. Control d60 N = 3, n = 336; d75 N = 5, n = 251; d90 N = 3, n = 165; DMD d60 N = 3, n = 193, d75 N = 4, n = 292; d90 N = 4, n = 169. Supporting information given in Supplementary Table S2. Oneway analysis of variance (ANOVA) with a Tukey post-hoc test with statistical significance set at ††p < 0.01 versus time point; *p < 0.05 and **p 0.01 versus control-CMs.*

In control hiPSC-CMs, calcium transient (Ca-T) amplitude normally increases during maturation, from day 60 to day 90 (Figure 15B). However, in DMD-hiPSC-CMs, Ca-T amplitude was smaller compared to controls at day 60, with no further increase at later stage of maturation (day 90).

In addition, to investigate the calcium storage in sarcoplasmic reticulum (SR), we performed a post-rest potentiation protocol. In particular, cardiomyocytes were stimulated at high frequency (2Hz) and, after a pause of 10 sec, an additional stimulus was imposed. The amplitude of post-rest potentiation peak was compared to regular contraction during regular pacing (Figure.15C). Control line shows a larger post-rest potentiation at d90 compared to the earlier stage of maturation (d60), highlighting an increase in SR calcium storage. However, Ca-T amplitude of post-rest peak was lower in DMD compared to control-hiPSC-CMs, with no significant differences between d60 and d90 (figure 15D).

1.4.2 Evaluation of action potential and calcium transient kinetics during cardiomyocyte maturation

The kinetics of action potential and calcium transient can greatly affect cardiomyocyte's function, leading to changes in the contractile and electrophysiological properties of the myocardium. To evaluate this aspect, cardiomyocytes were loaded with a voltage-sensitive dye combined with a calcium-sensitive fluorescent dye (Fluovolt and Cal630, respectively).

In control and DMD-hiPSC-CMs, action potential duration (APD) significantly increases during maturation (Figure 16B); instead, at day 75, APD in DMD cardiomyocytes was shorter compared to control line, but not significant differences occurred at d90 in both lines (Figure 14B). Moreover, in both lines, APD at d75 did not show rate adaptation (2 Hz vs. 1 Hz stimulation), albeit with a partial recovery at d90.

In addition, calcium kinetics was evaluated at different time points of maturation. In control-hiPSC-CMs, calcium transient kinetics became more rapid during maturation; similarly, DMD cardiomyocytes showed time-dependent acceleration of calcium kinetics, in term of both calcium rise kinetics (time to peak, TTP) and decay (time from peak 50%, RT50) (Figure 16.D). However, in the DMD line, kinetics of calcium transient were significantly faster than control line at all maturation time-points (Figure D)

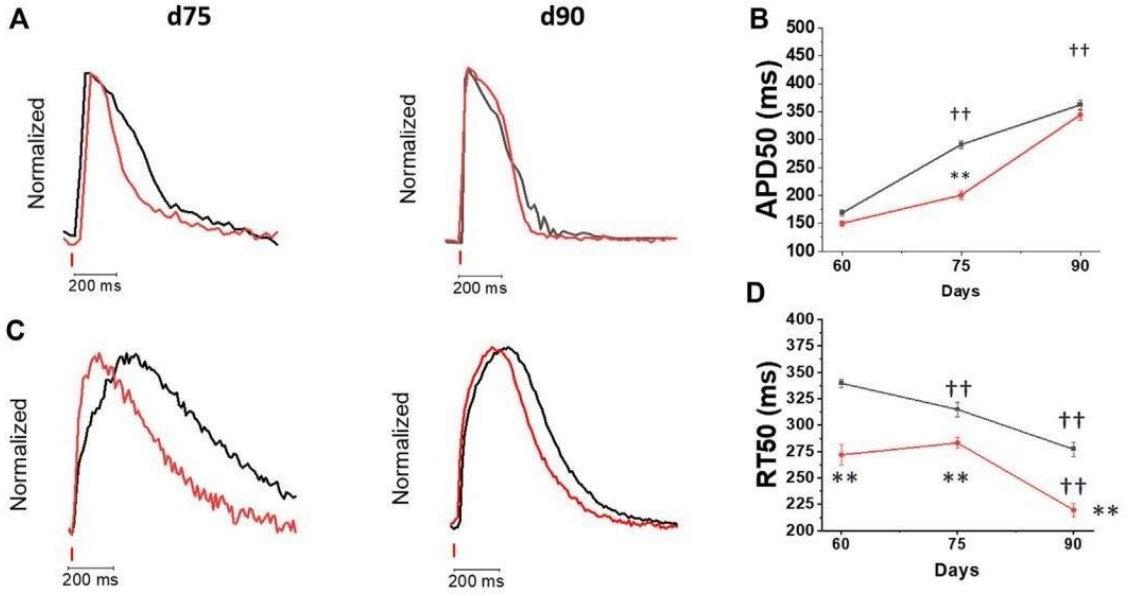

Figure 16*. Changes of action potential and calcium transient kinetics during hiPSC-Cm maturation. Dual recording of action potential and calcium transients was performed at day 60, 75 and 90 post differentiation at 37°C and external [Ca2+] = 1.8 mM on the softer substrate (PEG). (A) Superimposed action potential (AP) traces of day 75 (Control d75 N = 2; n = 186; DMD d75 N = 2; n = 91) vs day 90 (Control N = 2; n = 119; DMD: d90 N = 2; n = 44) recorded by FluoVolt (B) 50% of action potential durations (APD50, ms) at 1 Hz are reported as Mean ± SEM. (C) Superimposed traces of calcium transients recorded by Cal630 at day 60, 75 and 90 (D) average calcium transient (CaT) (difference of 50% of CaT decay and TTP, RT50, ms) are reported, during pacing at 1 Hz. Control d60 N = 3, n = 336; d75 N = 5, n = 251; d90 N = 3, n = 165; DMD d60 N = 3, n = 193, d75 N = 4, n = 292; d90 N = 4, n = 169. One-way analysis of variance (ANOVA) with a Tukey post-hoc test with statistical significance set at †† p < 0.01 versus time point; *p < 0.05 and **p 0.01 versus control-CMs.*

1.4.3 Evaluation of β-adrenergic pathway activation with forskolin exposure

Normally, mature cardiomyocytes show a rapid and efficient response to the β-adrenergic pathway activation. Indeed, in healthy mammals, heart rate and contractile force adapt as a result of inotropic stimulation.

Forskolin is a positive inotropic agent, that acts as activator of adenylate cyclase (AC) and leads to a rise of the intracellular levels of cAMP, resulting in an increase of calcium transients and contraction force.

To investigate the adaptation of hiPSC-CMs to the β-adrenergic response, we performed an acute treatment with forskolin (FSK) on DMD and control cardiomyocytes. In both lines tested, Ca-T amplitude increased by 30% after FSK incubation, compared to basal condition (Figure 17 C, D), suggesting a preserved positive inotropic response to catecholaminergic stimuli. Moreover, after FSK treatment, RT50 hastened in both lines, highlight a positive lusitropic response of these cardiomyocytes.

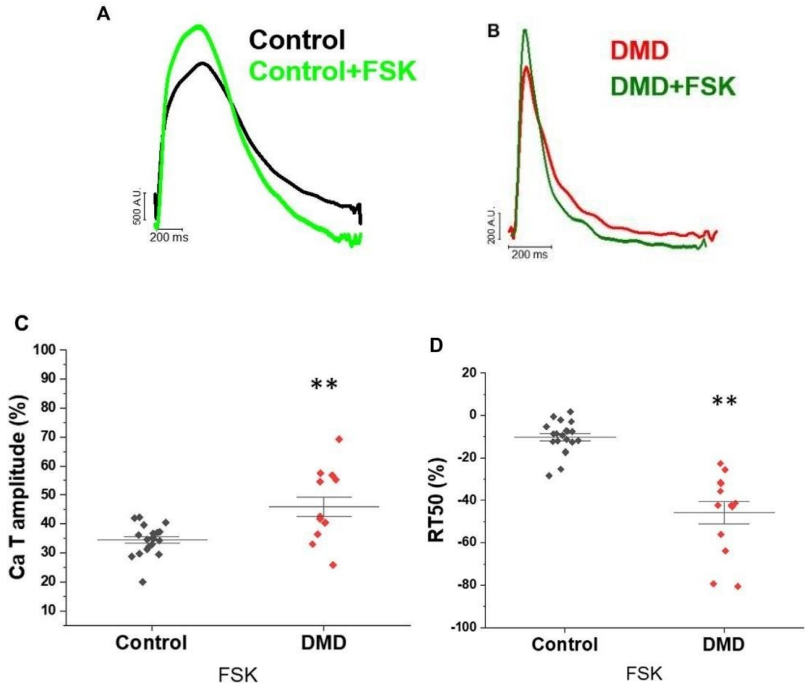

Figure 17. *Effects of forskolin on calcium transients. Calcium transients of the before and after forskolin addition in day 60 control- and DMD-hiPSC-CMs. (A,B) Superimposed normalized traces of calcium transients recorded in the control hiPSC-CMs line, before and after treatment with forskolin (FSK, light green controls, dark green DMD), reported as the variation (%) compared with the basal condition. (C) Calcium transient amplitude is reported, during pacing at 1 Hz, as the % variation related to the basal condition compared to the treatment with FSK in DMD. (D) CaT decay (difference of 50% of CaT decay and TTP, RT50, ms) is reported, during pacing at 1 Hz, as the % variation related to the basal condition compared to the treatment with FSK in controls and DMD.*

1.4.4 CaMKII and RyR2 phosphorylation

Calcium-calmodulin dependent protein kinase (CaMKII) is a key regulator of cardiac electrophysiology, calcium balance, contraction, and transcription.

To assess the presence of phosphorylation (p-) at specific sites of the ryanodine receptors (RyR2), we used antibodies against p-RyR S2814 and p-RyR S2808, that are target sites of CaMKII and PKA, respectively.

At the latest stage of cardiomyocyte maturation (d90), DMD-CMs showed a higher level of phosphorylated CaMKII in comparison with control (Figure 18 A, B). In particular, in DMD-CMs, CaMKII phosphorylation at site S2814 was significantly increased compared to control line. Instead, RyR phosphorylation at the PKA site (S2808) showed no changes (Figure 18.C, D). Since an increase in RyR2 phosphorylation is associated with an increase in the open probability of the channel, this feature is often associated with SR calcium leakage during diastole.

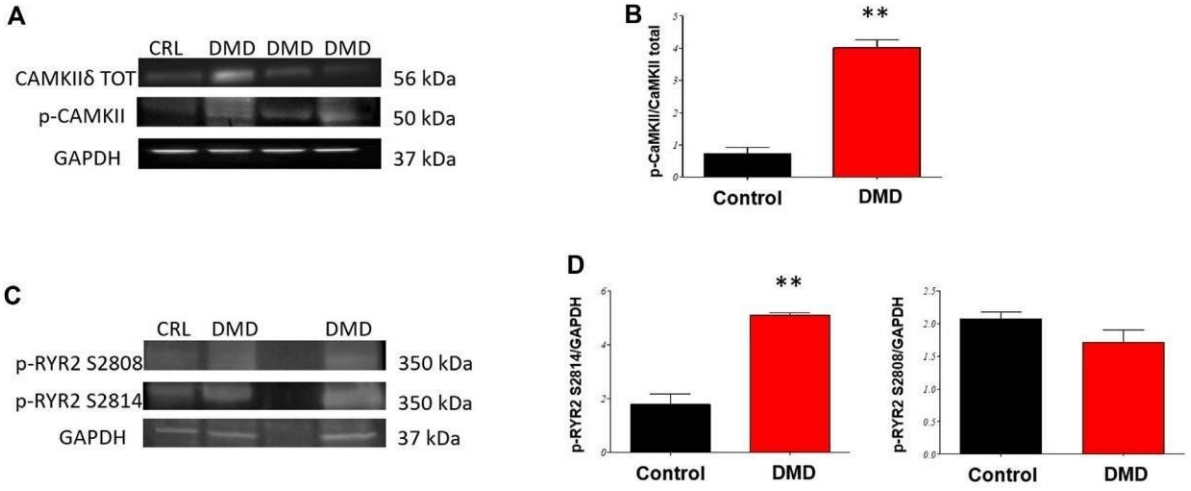

Figure 18. *Phosphorylation of RyR2 and CaMKIIδ in hiPSC-CMs. Western blot (WBs) analysis of Ryanodine receptors (RyR2) phosphorylation status and verification of CaMKII activity in day 90 DMD-vs Control-hiPSC monolayers. (A) Representative WB of CaMKIIδ (B) and analysis normalized for total CaMKII. (C) Representative WB analysis of (D) RyR2 sites of phosphorylation (phospho-specific anti Ser 2814 target of CaMKII and Ser 2808 target of PKA) normalized for GAPDH, *p < 0.05 in ANOVA DMD vs Controls N = 3 (differentiation runs) and n = 2–5 (gel repetitions).*

1.4.5 Evaluation of stiffness substrates on cardiomyocytes calcium handling

Changes in extracellular matrix (ECM) stiffness can greatly impact on cardiomyocyte contractility. In fact, mechanical properties of ECM cause an adaptative response of cardiomyocytes, leading to changes in cell specification and function (Nakayama et al., 2014) During the pathogenesis of DCM associated to DMD, myocardial fibrosis causes an increase in the rigidity of ECM, resulting in cardiomyocyte damage caused by the absence of dystrophin.

For this reason, DMD-hiPSC-CMs grown on stiffer diethyleneglycol (100% DEG) were compared with cardiomyocytes cultivated on a softer substrate of polyethyleneglycol (100% PEG) (Figure 19 A, B).

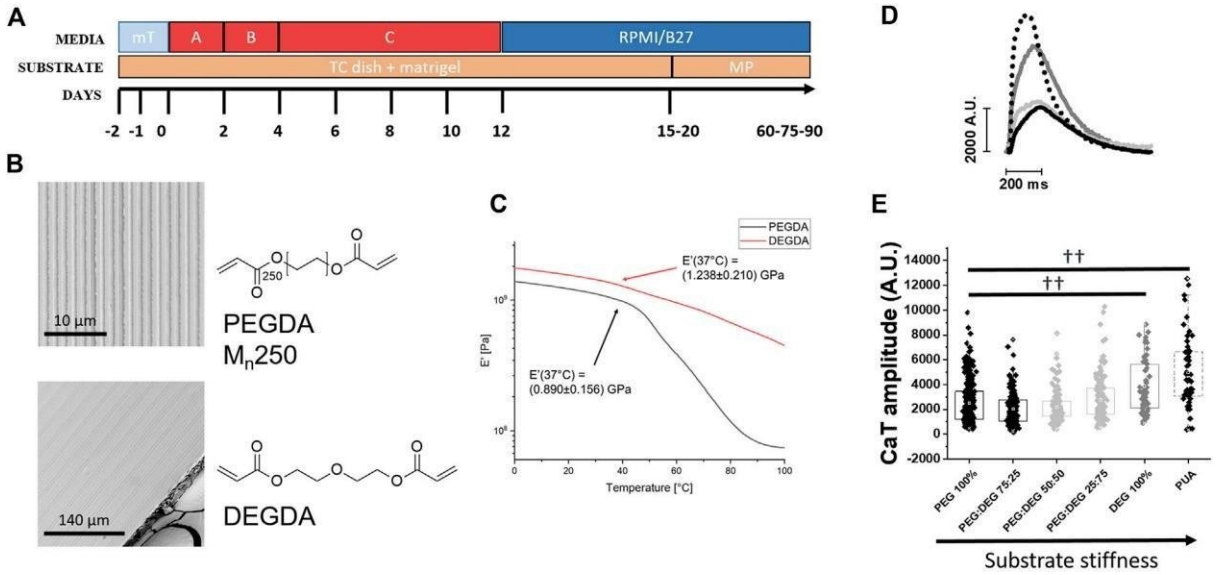

Figure 19. *Ca-transients in DMD-hiPSC-CMs grown on PEG vs DEG patterned substrates. (A) Time course of media (mT mTeSR + suppl.; A + B + C cardiac differentiation kit) and substrates (TC tissue plate; MP micropatterned substrates). (B) S.E.M. image of Poly (ethylene glycol) diacrylate (PEG-DA)- and Di(ethylene glycol) diacrylate (DEG-DA)-based substrates with micropatterned grooves. Scale bars 10 µm. (C) Samples of PEGDA and DEGDA for dynamical mechanical analysis (DMA) with 1% wt. The samples were clamped in tension mode in a DMA800 analyzer (Perkin Elmer). Samples were analyzed in strain-control mode, imposing a 0.020 mm strain with 1 Hz frequency, in the -20°C-120°C temperature range. The mechanical characterization was repeated three times for PEGDA100 and DEGDA100 samples. The value of the storage modulus at E' was obtained by calculating the integral mean of the E'-T curve between 36°C and 38°C. Values are expressed as mean ± SEM. (D) The impact of substrate stiffness in normal control-CMs was tested for CaT amplitude on microgrooved surfaces with increasing ratio of polyethyleneglycole (PEG) and dyethylenglycole (DEG) concentration and polyurethane-based nanopatterned surfaces (PUA) at 37 °C at and external [Ca2+] = 1.8 mM. Representative CaT profiles at day 60 and of CaT amplitude (Fluorescence Arbitrary Units, A.U.) of control-CMs under PEG (N = 3; n = 336), PEG:DEG 75:25 (N = 2; n = 150), 50:50 (N = 2; n = 147), 25:75 (N = 2; n = 150), DEG (N = 2; n = 50) and PUA (N = 2; n = 59). (E) Data were represented as a box (median [interquartile range]) and whisker plots. †p < 0.05, ††p < 0.01 versus control condition (PEG).*

DMD-hiPSC-CMs showed a reduction in Ca-T amplitude on both substrates. Instead, in control line, kinetics of Ca-T decay was significantly accelerated in cardiomyocytes cultivated on 100%

DEG substrates compared with those grown on the softer pattern, and Ca-T amplitude increased (Fig. 17E). Moreover, DMD-hiPSC-CMs exhibited no significant changes in Ca-T kinetics while varying the rigidity of substrates (Figures 20. A, B).

Finally, to investigate SR calcium content, cardiomyocytes were subjected to caffeine-evoked Ca-Ts (Figures 20. C, D). In fact, caffeine can open RyR channel located on SR, spilling SR content in the cytosol, leading a direct measure of calcium SR content of cardiomyocytes.

In control-hiPSC-CMs, caffeine Ca-T amplitude was similar independently of stiffness substrates (Figure 20.D). Moreover, caffeine Ca-T decay kinetics (tau, s^{-1}) was faster in control cardiomyocytes grown on stiffer pattern, highlighting an increase of capability of intracellular calcium removal via sodium-calcium exchanger. Instead, caffeine-calcium transient amplitude was significantly increased in DMD-CMs grown on DEG substrates compared to PEG pattern. Also, the decay kinetics (tau, s^{-1}) of caffeine transients was slower in DMD compared to controls.

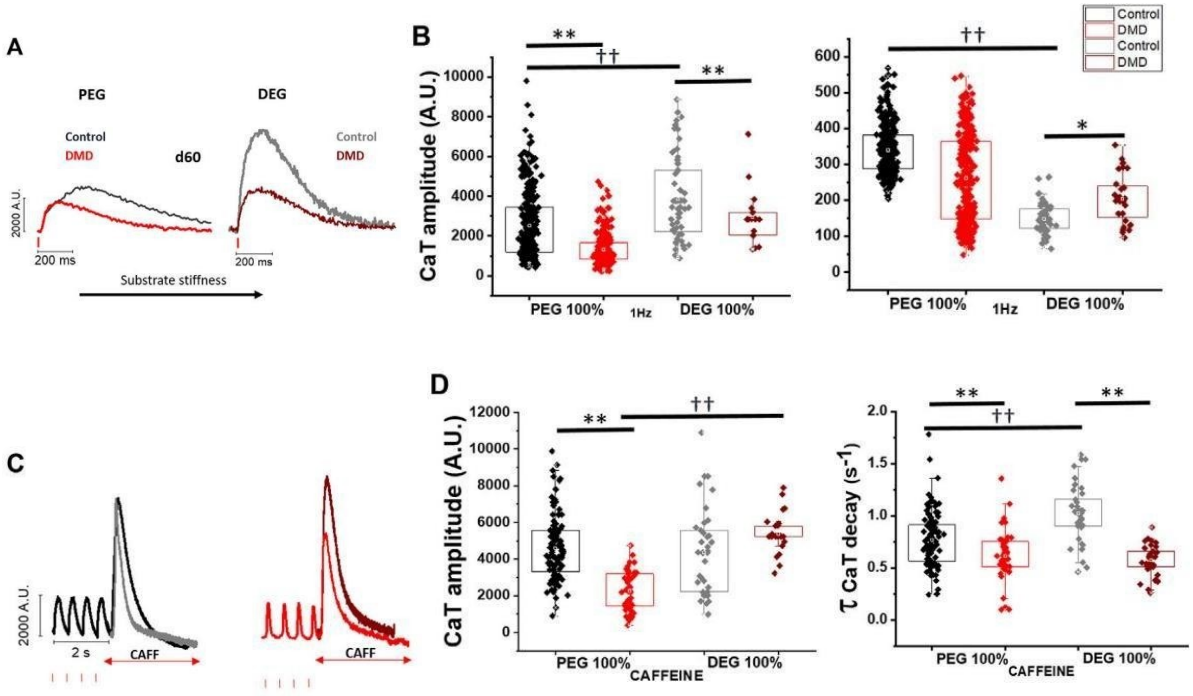

Figure 20. *Impact of substrate stiffness on calcium transient amplitude and duration. To evaluate the impact of substrate stiffness on loss of full-length dystrophin, DMD- and control-CMs were compared for CaT amplitude and caffeine-evoked CaT on softer (PEG)- versus stiffer (DEG)-microgrooved surfaces (MPs) at 37°C at and external [Ca2+] = 1.8 mM.(A) Representative CaT profiles at day 60 and of CaT amplitude (Fluorescence Arbitrary Units, A.U.) and RT50 of CaT decay (ms) of DMD-versus control-CMs under softer or stiffer MPs. (B) Data are reported in box plots report controlversus DMD-CaT amplitude and RT50 (ms) on both softer or stiffer*

*substrates (PEG: Control N = 3, n = 336; DMD N = 5, n = 251; DEG: Control N = 2, n = 50; DMD N = 3, n = 67). (C) Caffeine-induced CaTs (quick exposure to 10 mM Caffeine) after a series of 2 Hz paced CaTs. (D) Average of caffeineinduced CaT amplitude (Fluorescence Arbitrary Units, A.U.) was measured by localized caffeine exposure after steady-state calcium transients at 2 Hz prior. Caffeine transient CaT amplitude (CaTA CAFF/CaTA 2 Hz ratio) and decay (τ, s−1) of DMD- and control-hiPSC-CMs were compared on both PEG (softer) and DEG (stiffer) substrates. (PEG: Control N = 2, n = 83; DMD N = 2, n = 46; DEG: Control N = 2, n = 23; DMD N = 2, n = 21). Data were represented as a box (median [interquartile range]) and whisker plots.. One-way analysis of variance (ANOVA) with a Tukey post-hoc test with statistical significance set at *p < 0.05 and **p < 0.01 versus control and ††p < 0.01 versus internal substrate condition.*

These results reveal a possible reduction in the capability of intracellular calcium extrusion in cardiomyocytes affected by dystrophin deficiency, associated with diastolic calcium anomalies. In fact, several mechanisms can lead to the onset of ventricular arrhythmias in patients affected by DMD, including conduction abnormalities, myocardial fibrosis and fatty replacement of cardiac tissue (Frankel and Rosser, 1976; Fayssoil et al., 2017; Pioner et al., 2020). Although patients usually develop cardiac symptoms in association with overt cardiomyopathy, it is important to investigate the cardiac muscle alterations occurring during the early stages of disease progression. For this reason, our results highlight the occurrence of electrophysiological changes that can presumably be identified during cardiac differentiation, in association with pathological processes that lead to disease progression, including the increase of myocardial fibrosis.

1.4.6 Engineered heart tissue (EHTs)

In vivo cardiomyocytes are continuously subject to a mechanical stress that is cyclically induced by the physiological cell contraction. Therefore, the use of specific 3D scaffolds is useful to reproduce this process, allowing a higher degree of maturation in vitro and the possibility to perform mechanical and functional measurements. A three-dimensional model was first described by Eschenhagen and colleagues and was obtained using neonatal or embryonic rat and chicken cardiomyocytes (Eschenhagen et al. 1997; Zimmermann et al. 2000). These innovative models, known as engineered heart tissues (EHTs), represent a new approach to reproduce the morphological and functional features of the myocardium, by using a 3D scaffold in which cardiomyocytes can be incorporated. More specifically, this method uses a 3D scaffold generated through an enzymatic reaction mediated by thrombin, that create a

hydrogel of fibrin from monomeric fibrinogen, fibrin forms an elongated trabecual-like tissue between two flexible silicon pillars. The cardiomyocytes differentiated from induced pluripotent stem cells are then incorporated inside the forming tissue, giving it the capability to beat after few days in culture. Moreover, the tissue is formed between two flexible silicon pillars, that exert a continuous mechanical stress on the growing beating tissue, promoting cell distribution, maturation and orientation along the major axis. In addition, during maturation, EHTs were maintained in culture for a long period (60 days p.d.) with a medium (RPMI) supplemented with aprotinin to prevent proteolytic degradation of fibrin.

Due to their intrinsic characteristics, EHTs represent a good model to investigate inherited cardiomyopathies, allowing researchers to measure the contraction force changes that occur, such as active tension, relaxation kinetics and pacemaker activity. In fact, contractile tension can be calculated by optically tracking the deflection of the flexible post (Schaaf et al. 2011) (Ruan et al. 2016). The advantage of this method is the possibility to obtain a 3D model with an advanced stage of maturity to study several diseases, performing drug tests and functional measurements. In this field, growing evidence is present in the literature on the use of EHTs to investigate different cardiac diseases, including channelopathies, hypertrophic cardiomyopathy and dilated cardiomyopathy (Streckfuss-Bömeke et al. 2017) (John T. Hinson et al. 2015). Moreover, several studies highlighted that EHTs treated with physiological and pharmacological compounds acting on the electrophysiological features of cardiomyocytes, exhibit a very similar response as compared with native human cardiac tissue (Mannhardt et al. 2016). Moreover, other authors showed an increment of in vitro maturation of EHTs subject to electrical and mechanical stimulation, leading an organized cellular disposition, physiological sarcomere length and increase of electrophysiological functionality (Ronaldson-Bouchard et al. 2018). Then, despite the level of maturation achieved is not yet at the same level of the adult heart, this model remains a powerful tool to explore the mechanisms underlying cardiomyopathies, to perform pharmacological tests and lay the basis for personalized therapies.

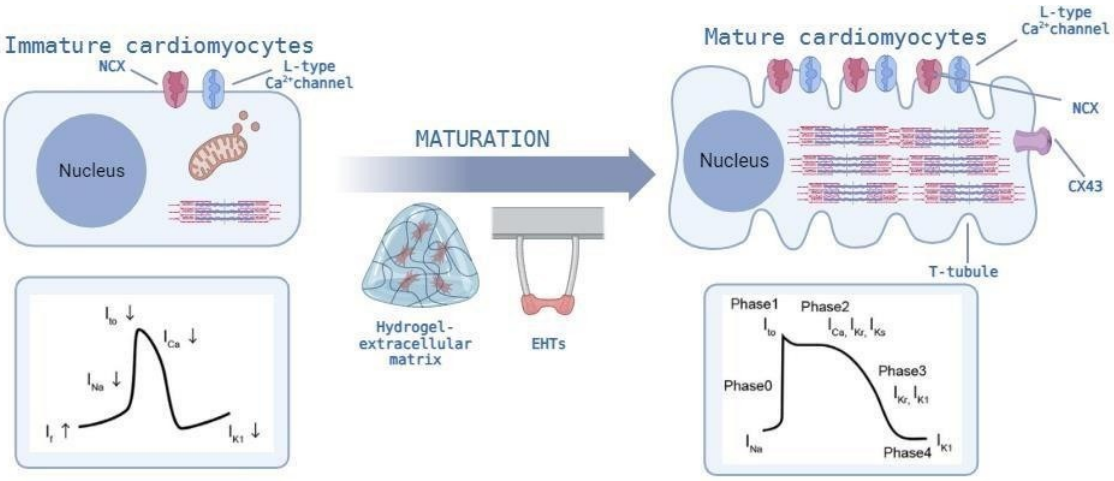

Figure 21. *Strategies to improve cardiomyocytes maturation: engineered heart tissues generation.*

1.5 Towards precision medicine and preclinical testing using hiPSC-cardiomyocytes

Inherited cardiomyopathies are among the most common cause of morbidity and mortality in young people worldwide. Cardiac alterations associated with cardiomyopathies include electrical, myocardial and structural impairment secondary to specific mutations that occur in contractile proteins. The management and diagnosis of the different categories of inherited cardiac diseases is greatly varied, depending on symptoms severity, disease progression and patient-specific risk stratification. Clinical manifestations of cardiomyopathies are heterogeneous and include dyspnoea, palpitations, dizziness and syncope, culminating in heart failure or sudden cardiac death (SCD). Classic pharmacological strategies involve the use of a combination of drugs to minimize symptoms, including β-blockers, calcium antagonists, oral anticoagulants, diuretics or ACE-inhibitors. Although classical therapies may treat efficiently cardiomyopathy-associated symptoms and acute complications, no current drugs or surgical interventions can affect the pathophysiological mechanisms underlying this disorder. Considerable progresses have been made in the development of new and innovative pharmacological compounds to be used as valuable treatment options to treat inherited cardiomyopathies. Moreover, the majority of mutations associated with cardiomyopathies impair the contractile proteins of sarcomere, including troponin I or T, myosin or titin. For these reasons, pharmacological treatment targeting sarcomere proteins may provide a useful tool to alter the pathophysiology of inherited cardiomyopathies. Therefore, pharmacological

treatments and clinical targets change with the evolving natural history of the disease, in relation to different pathological manifestation depending on each patient. In fact, genetic testing of familial screening has highlighted a very early stage in HCM pathogenesis (Stage I), characterized from individuals carrying HCM malignant mutations but not yet showing the associated pathological phenotype. However, in the stage II, hypercontractility appears with a fully expressed hypertrophic phenotype in absence to fibrotic replacement. In this specific stage, the most common cause of symptoms is represented by left ventricular tract obstruction (LVOTO). Whit the progression of the disease, the stage III is characterized from dangerous remodelling, including left ventricular fibrosis, worsening diastolic and systolic functionality and ejection fraction (EF) of 50-65%. Finally, in the late stage of disease (stage IV) patients manifest severe left ventricular systolic dysfunction with EF < 50% (Argirò A. et al., 2023). In each of these stages, pharmacological targets differ and consequently also the therapeutic approaches (Figure 22).

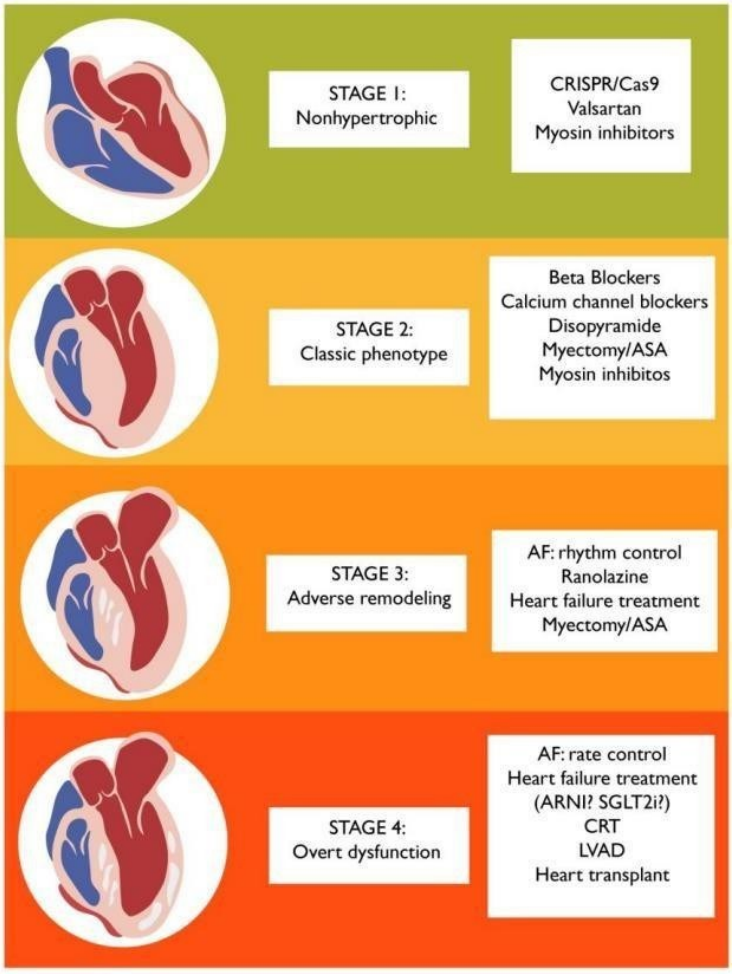

***Figure 22**. Different specific stage of hypertrophic cardiomyopathy and Stage-specific pharmacological treatments (Stage-specific therapy for hypertrophic cardiomyopathy, Argirò A. et al., 2023).*

HCM, may lead to a pathological increase of sarcomere force, specific myosin inhibitors may address myocardial hypercontractility, restoring the normal energetic cost of contraction. As a member of the myosin-inhibitors class, mavacamten (MYK-461) reduces sarcomere contractility in hypertrophic cardiomyopathy (HCM), targeting cardiac myosin and stabilizing the SRX conformation of myosin (Anderson R. et al., 2018). This compound exerts an allosteric inhibition of myosin, the major force-producing protein in cardiac muscle (Zampieri M et al., 2021). Moreover, in vivo preclinical studies on cardiomyocytes obtained from rodent models of HCM, the treatment with Mavacamten reduced fractional shortening, cardiac fibrosis and cardiomyocytes disarray, associated with no changes in Ca^{2+} transients (Green E. M. et al., 2016; De Rio C. L. et al., 2017). During the conversion from weakly to strongly bound conformation of myosin, MYK-461 determines a consistent reduction in the number of myosin heads available for interaction with actin. Mavacamten causes a decrease of ATPase activity, resulting in a reduction of the general force exerted by sarcomere, that result from the product of single force generated by each single myosin head (Teekakirikul P. et al., 2010). Also, the positive effect of MYK-461 was evaluated in mouse cardiac strips (Awinda P. et al., 2020) and human samples (Sewanan L. et al., 2021), resulting in the increase of ADP release rate from myosin. Therefore, in the phase III MAVERICK-HCM trial (Ho C. et al., 2020), Mavacamten has shown promising effects on the majority of patient enrolled; moreover, the phase III EXPLORER-HCM trial highlighted that mavacamten treatment significantly reduced left ventricular mass and wall thickness, with no modifications of markers of cardiac fibrosis, as compared with placebo (Saberi S et al., 2021). In addition, other functional alterations may be considered as valuable targets for the pharmacological treatment of inherited cardiomyopathies. Electrophysiological defects associated with changes in specific current densities cause action potential (AP) alterations, culminating in arrhythmic events in obstructive HCM (oHCM) patients. The electrical alterations of HCM myocytes result into an impaired cardiac function in HCM patients. Several lines of evidence showed that late sodium current ($I_{Na\text{-}L}$) is enhanced in HCM (Coppini R. et al., 2013), highlighting a possible target for pharmacological intervention. This is the case of ranolazine, an anti-anginal drug that acts by inhibiting the late sodium current ($I_{Na\text{-}L}$) (Antzelevitch C. et al., 2004), decreasing intracellular Na^+ concentration which, in turn, promotes the activity of NCX exchanger and decreases intracellular calcium concentration, ameliorating diastolic function and normalizing cellular electrical function. Indeed, in human HCM cardiomyocytes ranolazine improved diastolic function and reduced

arrhythmic triggers (Coppini R. et al., 2013). Therapeutic targets for medical therapy are rapidly evolving. In fact, novel pharmacological approaches include the use of “off-label” drugs, showing beneficial effects outside of their main mechanism of action. In this context, a class of SGLT2 inhibitors, called gliflozins, have demonstrated to act as cardioprotective agents, although the underlying mechanisms are still unclear. Dapagliflozin may reduce the risk of hospitalization and heart failure complications in patients affected by type 2 diabetes. Starting from these promising results, the randomized clinical trial DAPA-HF (Dapagliflozin and Prevention of Adverse Outcomes in Heart Failure) have highlighted the efficacy of SLGT2 inhibitors also in patients affected by heart failure and reduced ejection fraction, regardless of the presence or absence of diabetes. In conclusion, innovative pharmacological approaches based on new molecular targets, such as late current inhibition, metabolic modulation or myosin inhibition, potentially provide an improvement in the quality of life of patients with inherited cardiomyopathies, resulting in a reduction of clinical complications and a milder disease progression (McMurray JJV et al., 2019).

Chapter 2

2 AIM OF THE THESIS

Inherited cardiomyopathies are congenital disorders of the myocardium, accounting for the main cause of sudden death in young individuals worldwide. Familial hypertrophic cardiomyopathy (HCM) and dilated cardiomyopathy (DCM) associated with Duchenne Muscular Dystrophy (DMD) are caused from several mutations occurring in specific genes associated with cardiomyocyte contraction. To date, pharmacological strategies to manage patients with inherited cardiomyopathies are focused on minimizing the symptoms associated with the progression of cardiac impairment, such as dyspnoea, palpitations, heart failure, as well as on the prevention of arrhythmogenic events, which can culminate in sudden cardiac death (SCD). Currently, a number of drugs are administrated for the treatment of inherited cardiomyopathies. The typical approach to the treatment of cardiomyopathy patients involves the use of of β-blockers, calcium antagonists or antiarrhythmic agents and, in the most severe cases, the implantation of a defibrillator, a surgical operations or cardiac transplantation. In this context, the development of novel and innovative pharmacological treatments is fundamental to address patient-specific therapies, in terms of personalized medicine based on the specific molecular mechanisms that are altered in different forms of inherited cardiomyopathies. In particular, cardiomyopathies are caused from several mutations occurring in different genes, mainly encoding for sarcomere proteins. The most common mutations associated with HCM are located in the myosin-binding protein C (cMyBP-C) and β-myosin heavy chain (β-MHC), encoded by MYBPC3 and MYH7 genes, respectively, and causing a particularly severe form of hypertrophic cardiomyopathy. On the other hand, DMD is caused from truncated mutations located in DMD gene (Δ exons 46-48; Δ exon 50; Δ exon 51), resulting in the total absence of dystrophin in males and leading to the increase of mechanical stress exerted on cardiomyocytes and skeletal muscle cells during contraction.

In this thesis, we will investigate the specific mutations associated with HCM and DMD, to evaluate their mechanical and electrophysiological effects on cardiomyocytes. The development of induced pluripotent stem cells (hiPSCs) represents a useful tool to study the main pathological mechanisms underlying inherited cardiomyopathies. In fact, the possibility to obtain hiPSCs from HCM and DMD patients and to perform their differentiation into cardiomyocytes, represents an innovative platform for the in vitro study of these two inherited cardiac disorders. We derived 3D engineered heart tissues (EHTs), suitable models to achieve

an increased cardiomyocyte maturation, allowing us to perform mechanical evaluations of cardiac muscle contraction.

The main goal of this study was to use of hiPSC-CMs as a model to study inherited cardiomyopathies, using cardiomyocytes derived from patient specific hiPSCs, obtained from the following patients:

- HCM patients carrying a mutation in:
  - Cardiac myosin binding protein C (MYBPC3);
  - β-myosin heavy chain (β-MHC);

- DMD patients carrying a mutation in:
  - Δ exons 46-48 (DMD gene);
  - Δ exon 50 (DMD gene);
  - Δ exon 51 (DMD gene).

To improve the immature phenotype of induced pluripotent stem cells-derived cardiomyocytes, we used different experimental approaches. A previous study from our group (Pioner et al., 2022) highlighted an increase of intracellular calcium handling maturation in cardiomyocytes derived from DMD-hiPSCs, achieved by using a long-term culture in association with culture substrates with different stiffness (PEG and DEG).

Engineered heart tissue to model hypertrophic cardiomyopathy. Induced pluripotent stem cells derived engineered heart tissues were used to investigate the cellular mechanisms leading to the progression of HCM. In particular, we performed mechanical recordings of EHTs contraction in auxotonic conditions, starting from lines carrying the MYBPC3:c.772G>A, to investigate changes occurring during cardiomyocyte maturation. Moreover, at a later-stage of EHT maturation, we evaluated contraction in isometric conditions, to assess active tension and twitch kinetics.

Pharmacological treatments. In addition, we performed a long-term treatment with a novel allosteric myosin inhibitor, Mavacamten, in clinical use for the treatment of symptomatic obstructive HCM patients (Olivotto I. et al., 2020), using mutated and isogenic-corrected hiPSC-EHTs. Finally, to assess HCM-specific electrophysiological modifications, we carried out simultaneous measurements of action potentials and calcium transients, by using two specific fluorescent dyes and a confocal microscope (Fluovolt, Cal630).

Mechanical evaluation of R403Q-hiPSCs-CMs. hiPSC-CMs carrying a R403Q mutation (heterozygous and homozygous), a pathological substitution in β-myosin heavy chain (β-MHC), were used to perform shortening and calcium transient evaluations, thought optical measurements (IonOptix system) associated with calcium fluorescent dye incubation (FURA-2). Moreover, we tested pathological HCM-alterations via functional recordings at different calcium concentrations and stimulation frequencies, to evaluate the changes that occur in relation to different frequencies and calcium concentrations. In addition, since the R403Q mutation occurs in one of the most important contractile proteins, resulting in contractile impairment, evaluation of actin-myosin sliding (In Vitro Motility Assay, IVMA) was performed at a later-stage of cardiomyocyte maturation.

Induced pluripotent stem cell- derived cardiomyocytes and skeletal cellular muscle cells to model Duchenne Muscular Dystrophy. In the second part of this thesis, we focused on the characterization of Duchenne Muscular Dystrophy, a neurodegenerative disorder that leads to progressive muscle weakness, often associated with a severe form of dilated cardiomyopathy, which represents the main cause of death in these patients. To investigate the mechanical impairment of DMD-cardiomyocytes, we used engineered heart tissues derived from different male DMD patients carrying deletions in the DMD gene (Δ exons 46-48; Δ exon 50; Δ exon 51), all resulting in total absence of dystrophin. On each EHTs, we performed twitch contraction recordings at specific time points and a later-stage of maturation (~ day 60). Furthermore, electrophysiological evaluations were performed by using fluorescent dyes, to investigate action potential and calcium transient modifications.

In addition, to better understand how pathological changes occurring in early stages of cellular development may alter cellular function in skeletal muscle cells, a specific differentiation protocol was used to obtained viable myotubes starting from DMD- and control- hiPSCs. Initially, at each phase of differentiation, we performed immunofluorescence acquisitions to evaluate the expression of specific differentiation markers (Pax7, MyoD, MyoG, MHC). Once the myotubes were obtained, we carried out calcium transient evaluations under acetylcholine stimulation, by using a fluorescent dye for calcium ion (Cal520).

Pharmacological treatment. The lack of dystrophin leads to an important cellular impairment, associated with an increase of mechanical stress on the membrane of cardiomyocytes during contraction, resulting in calcium handling alterations and cellular death. Starting from this evidence, we performed a treatment with a Poloxamer 188 (P188), a copolymer that is capable

of intercalating between the membrane phospholipids, leading to membrane structural repair. Long-term treatment was performed for 20 days in culture on DMD-hiPSC-CMs, to investigate the effect of this drug on the contractile capacity of dystrophin deficiency cardiomyocytes.
Moreover, preliminary results show promising effect of Dapagliflozin on EHTs derived from DMD hiPSC lines, but more evidence is required. In addition, since several electrophysiological alterations may occur in DMD cardiomyocytes, we performed acute treatment on DMD-EHTs with Ranolazine, an anti-anginal drug that acts by inhibiting late sodium current ($I_{Na\text{-}L}$), potentially mitigating the ionic imbalance associated with this disorder.

Acute treatment of cardiomyocytes isolated to human ventricular surgical samples derived from HCM and aortic stenosis patients. Gliflozins have been recently demonstrated to ameliorate cardiovascular function through a pleiotropic mechanism. In particular, Dapagliflozin was shown to reduce the risk of hospitalization in heart failure patients, also in the presence of preserved ejection fraction (DAPA-HF; DELIVER) and was recently introduced in all international HF guidelines (McDonagh T.A. et al., 2023). The molecular mechanisms underlying these beneficial effects are still not entirely known, and likely involve some direct effects on cardiac cells, probably mediated by different molecular targets. Starting from this evidence, we performed an acute treatment with Dapagliflozin on cardiomyocytes isolated from human surgical biopsies (provide from Careggi hospital), derived from HCM and aortic stenosis patients at two different concentrations (1 and 5 μM). We performed patch clamp measurements to evaluate the effects of the drug on the electrophysiological features of action potential (AP), in particular on its duration (APD), as well as on late sodium currents ($I_{Na\text{-}L}$).

Several mutations lead to the pathogenesis of inherited cardiomyopathies, including hypertrophic and dilated cardiomyopathy. The knowledge of the molecular effect of these pathological alterations possibly leads to a better understanding of disease progression, allowing the development of mutation-specific therapeutical approach. Therefore, the use of hiPSC-EHTs may provide a good model to investigate early-stage modifications that occur during cardiomyocytes development, before the onset of symptoms. Moreover, despite inherited cardiomyopathies can often evolve into different pathological phenotypes, some mechanisms may be in common, thus pharmacological interventions can be inserted into different pathological contexts. In fact, several pharmacological compounds, including gliflozins, may act transversally on different cardiovascular disorders, providing the basis for personalized medicine and patient specific interventions.

Chapter 3

MATERIALS AND METHODS

3.1 Induced pluripotent stem cell lines generation

Patient-derived somatic cells and stem cell lines generation. Urine-derived cells from a healthy donor and DMD patients were reprogramming into hiPSC lines (UC3-4 A1), by using a lentiviral vector carrying Oct3/4, Sox2, Klf4 and c-Myc. In particular, we used cell lines derived from DMD patient carrying a deletion of the exon 50 located on DMD gene (UC72039, DMDΔ50), compared with a control donor (UC3-4) (Guan et al., 2014) and its isogenic (positive control) cell line (c.263delG, UC1015-6), generated from the donor line using the Crispr/Cas9 technique to delete the 5' of Exon 1 in DMD gene (Pioner et al., 2020).

In addition, using blood mononuclear cells (PBMCs) extracted from the peripheral blood of 2 additional DMD patients, we generated other 2 different patient-derived Duchenne lines, DMD1C11 and DMD3C1, carrying mutations in exon 46-48 and in exon 51, respectively. PBMCs were isolated at Careggi University Hospital (Florence, Italy) from patient blood samples using a specific density gradient centrifugation method (Ficoll). A solution containing sodium diatrizoate, polysaccharides, and water, at a density of 1.08 g/ml, was blended with equal volume of whole blood diluted in PBS and centrifugated for 40 minutes at 400-500 x g. The resulting PBMCs ring was collected at 2 x 106 cell/ml in a solution with 20% dimethyl sulfoxide (DMSO) and 90% Fetal Bovine Serum (FBS) (Life Technologies) and placed inside a freezing container (Nalgene Mr. Frosty) at -80°C, overnight, to allow progressive gradual cooling. The following day, cells were moved to liquid nitrogen and shipped to the University of Washington at Seattle for reprogramming. The newly generated hiPSCs lines had been previously characterized for the absence of the full-length dystrophin (Dp427) (Guan et al., 2014; Macadangdang et al., 2015; Pioner et al., 2020; Bremner et al., 2022). Mutated lines were compared with control lines (WTC11, UC3-4), derived from healthy donors.

In addition, PBMCs obtained from patients with hypertrophic cardiomyopathy carrying the MYBPC3 c.772G>A mutation were also shipped to the University of Washington for reprogramming through the CytoTune®-iPS 2.0 Sendai Reprogramming Kit (Gibco), followed by quality control tests on newly generated iPSCs colonies (karyotyping, citometry for pluripotency markers). The hiPSC lines we used to perform studies on HCM include the WT-C11 line engineered by Dr. Bruce Conklin (The Gladstone Institute), the ID3 hiPSC line (AOUC-HCM4 with the MYBPC3-c.772G>A mutation) and the corrected ID3 isogenic negative-control line (obtained from the ID3 HCM line after correction of the mutation).

Moreover, during my fellowship to the University of Washington with professor Regnier group (Bioengineered department, University of Washington, Seattle, USA), I used two different HCM lines, R403Q-Het and R403Q-Homo lines, carrying a cardiac myosin-heavy chain (MYH7) point mutation of Arg^{403} to glutamine (R403Q) (Volkmann et al., 2005), edited using the CRISPR/Cas9 method, in comparison with isogenic control (MYH7-WT), to investigate the main mechanical characteristics underlying HCM due to myosin mutations.

3.1.1 Cardiac differentiation from induced pluripotent stem cells

Induced pluripotent stem cells were expanded in serum-free conditions and maintained in culture in mTeSR medium (StemCell Technologies) on a Corning® Matrigel hESC-Qualified Matrix (StemCell Technologies), at 37°C with 5% CO2. After achieving of 70-80% confluence in hiPSC colonies, in order to induce cardiac differentiation, we performed a differentiation protocol on monolayer using a specific Cardiomyocyte Differentiation Kit (Life Technologies). During this process, hiPSC colonies were chemically dissociated with Tryple 1X (Life Technologies) and incubated for 5 minutes, at 37°C, to obtain single cells. After dissociation, cells were collected and centrifugated at 200 x g for 4 minutes and pellet was resuspended in a solution containing m-TeSR medium with the addition of supplement and ROCK inhibitor (Y-27632 StemCell Technologies), to minimize cellular death. Then, cells were seeded in each well of a 24-well plate at cell density (90.000-100.000 cells/well, depending on the optimal cell density of each cell line). The medium was changed the following day to remove ROCK inhibitor and, when cells showed ~70% of confluency (~2 days after dissociation), the medium was replaced with Cardiomyocyte Differentiation Medium A (day 0 of the differentiation protocol). Two days later, Medium A was replaced with Cardiomyocyte Differentiation Medium B (day 2 of the differentiation protocol); after a further 2 days the medium was replaced with Cardiomyocyte Maintenance Differentiation Medium C (day 4), which was subsequently changed every 2 days, until spontaneous beating appear (approximately at day 8-10 of differentiation). On day 12 from cardiac induction, Medium C was replaced with RPMI medium supplemented with B-27 (Life Technologies). Cardiomyocytes differentiated from induced pluripotent stem cells (hiPSC-CMs) can be cultured until day 12-15 for dissociation and/or cryopreservation or kept in culture to perform long-term differentiation.

Moreover, several differentiation protocols are used to induce cardiac differentiation from hiPSCs. A particularly efficient protocol, as differentiation protocol I used in University of

Washington, include the use of specific factors to induce cardiomyocytes specification. In particular hiPSCs lines were growth until the achievement of confluence (~75 %) and detached by using versene solution supplemented with Rock Inhibitor (Y-27632, StemCell Technologies). After determining the right cellular density (75.000/100.000) cells were plated on Corning® Matrigel coated dishes (StemCell Technologies) and after 24 hours medium was replaced with m-TesR medium supplemented with Chiron 99021 (1 µM) and incubated overnight at 37°C, 5% CO_2. The day after, Chiron concentration was increased to 4 µM in a RPMI medium containing bovine serum albumin (BSA) and ascorbic acid (this medium is designed as RBS medium); after 2 days, medium was replaced with RBA supplemented with WNT C-59* (2 µM). At day 4, medium was replaced with RBA medium without WNT C-59* and after other two days, medium was aspirate and replaced with RPMI supplemented with insulin (RPMI supplement, B-27). Initial beating is usually observed between days 6-7 but can be observed later. After the obtainment of viable cardiomyocytes, a specific purification protocol was performed. Medium was replaced with DMEM medium without glucose plus lactate (4 mM), using the capacity of cardiomyocytes to use lactate rather than glucose, leading the elimination of possible undifferentiated cells.

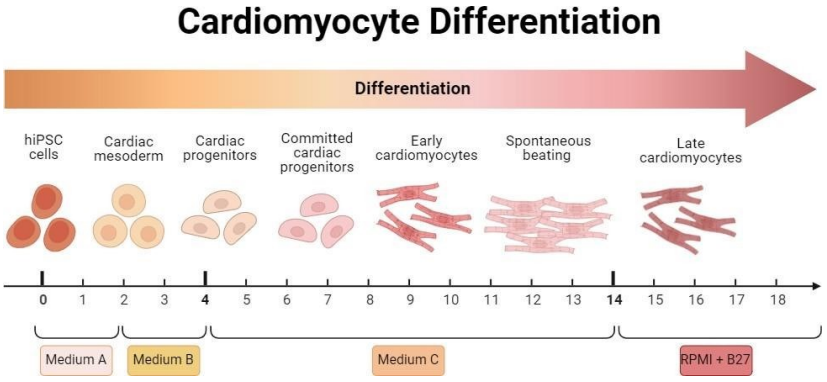

Figure 23. *Cardiomyocytes differentiation protocol on monolayer. Starting from hiPSCs, cardiac induction was induced through the addition of three different differentiation medium (medium A+B+C). Around day 11-14 post differentiation, spontaneous beating appears.*

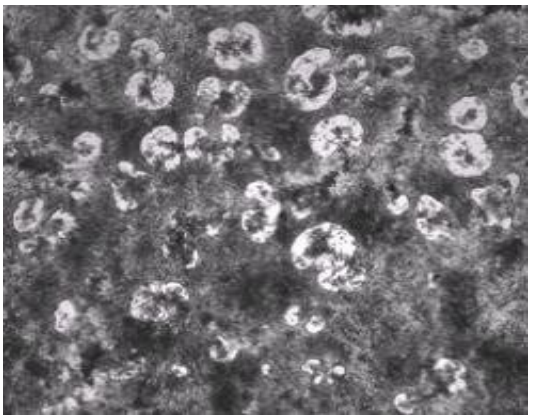

***Figure 24**. Optical acquisition (EVOS) of cardiomyocytes differentiated from induced pluripotent stem cells (day 15 p.d., 4X of magnification).*

3.1.2 Single cells plating

Around day 20 post differentiation (p.d.), cardiomyocytes obtained from induced pluripotent stem cells were detached from each well and seeded on glass slides to perform single cells studies. In particular, cells were dissociated with Tryple 1X and incubated for 10-15 minutes. After incubation, cells suspension was diluted into RPMI medium supplemented with FBS (50% RPMI, 50% FBS) to stop Tryple activity and centrifuged at 1000 rpm for 5 minutes at room temperature. Pellet was resuspended in a solution containing RPMI medium, 10% FBS and ROCK inhibitor and plated on Matrigel-coated glass slides.

3.1.3 Plating on PDMS stamps

To increase distribution and allow the optimal cellular alignment, hiPSC-CMs were plated on specific matrigel-coating PDMS (polydimethylsiloxane) molds, with previously formed parallel grooves with 15 μm spacing. After an appropriate sterilization with ethanol 100%, we performed the transfer of matrigel disks onto the circular grooved PDMS cover glasses through the formation of a" sandwich"; we then affixed a specific weight (~ 50g) on the top of the sandwich for 5-10 minutes to allow the moulding of the Matrigel surface, and stored it in the fridge. The following day, cardiomyocytes were washed with PBS 1X, dissociated in single cells with a solution of tripsin-EDTA and incubated at 37°C for 3 minutes. Then, cells were diluted in a solution of DMEM/F12 supplemented with 20% of FBS and centrifuged at 1000 rpm for 5 minutes at room temperature. Pellet was resuspended in RPMI/B27 plus ROCK Inhibitor (1:1000) and gently plated on Matrigel-coated grooved PDMS cover-glasses at a density of 1.500.000c/ml. Finally, we verified the alignment and spaceing of cardiomyocytes.

As shown in figure 25, the spacing is optimal to perform single cell measurements and this plating procedure provides an increased degree of cardiomyocyte maturation.

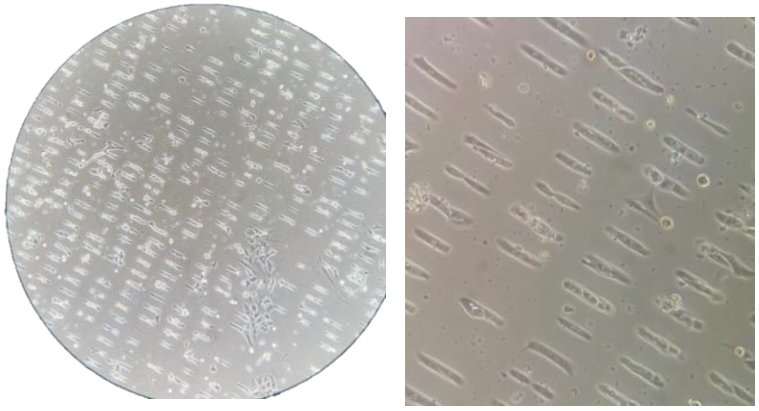

Figure 25. *Induced pluripotent stem cells derived cardiomyocytes plated on Matrigel PDMS stamps.*

3.1.4 Cellular Shortening and calcium fluorescent recording (FURA-2)

Single hiPSC-CMs were used to perform shortening and calcium transient acquisition measurements through an IonOptix system, featuring a video-microscopy setup to measure the degree of cardiomyocyte shortening during contraction, as well as intracellular Ca-fluxes. Mature cardiomyocytes (day 30 p.d.) derived from hiPSCs were incubated at 37°C with Fura-2 at 0.15 μM for 15 minutes in a Tyrode Solution containing (in mM): $MgSo_4.7H_2O$ 1.2, KCl 3.7, NaCl 138, KH_2PO_4 1.2, HEPES 10, Glucose 5. Then, solution was replaced with fresh Tyrode solution without Fura-2, where cells were left for 12 minutes before starting measurements. Cells were maintained at 37°C and perfused in continuous with Tyrode solution with increasing calcium concentration (in mM) (0.8, 1 and 1.8) and pacing stimuli at different frequencies (0.5, 1, 1.5 and 2 Hz). For stimulation, voltage was set at 20 V and pulse waveform duration was set at 4.0 ms. Shortening acquisition was carried out with an objective magnification of 40X. Recordings were analysed with IonWizard Software.

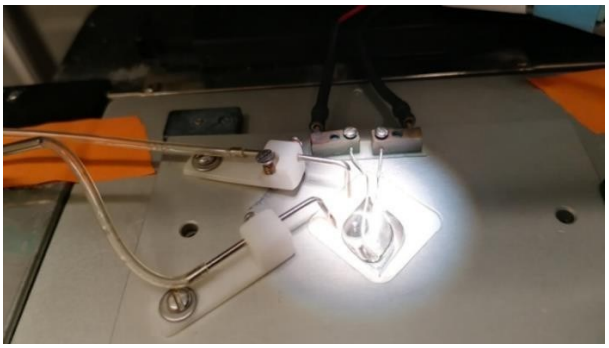

Figure 26. *Experimental chamber for the measurements of cell fractional shortening and calcium fluorescence under imposed external pacing in a perfused Tyrode solution at constant temperature of 37°C.*

3.1.5 Mechanical evaluation of contractile proteins

Myosin isolation from hiPSC-CMs. At a later stage of maturation (day 50 p.d.), myosin was extracted from hiPSC-CMs to perform in vitro motility assays (IVMA). Initially, cells were washed with PBS 1x, dissociated with trispin-EDTA for 4 minutes and diluted with DMEM/F12, supplemented with 10% of FBS. After a spinning of 1000 rpm for 5 minutes, cold extraction buffer (KCl 0.3 M, Imidazole 1.15 M, $Na_4P_2O_7$ 10 mM, $MgCl_2$ 1 mM and DTT 2 mM) was added to cellular suspension and solution was gently mixed in ice for 20 minutes. Then, cells were centrifuged with TLA 120.2 rotor at 75.000 rpm for 1h at 4°C to remove residuals and actin. Subsequently, cells were moved in a solution containing 3ml of water and DTT 0.1 M and left on ice for > 1h to allow myosin precipitation. Finally, we performed an extra round of centrifugation with TLA 100.4 rotor at 4°C and the resulting pellet was finally resuspended with Buffer C (KCl 0.6 M, $MgCl_2$ 2 mM, DTT 5 mM, Imidazole 10 mM, pH 7.4). The extracted myosin is then quantified with spectrophotometer to calculate the optimal concentration to be used during the assay.

In Vitro Motility Assay (IVMA). To prepare the In Vitro Motility Assay chamber, coverslips were washed with ethanol and a solution of 0.1% of nitrocellulose was prepared. Initially, 22X60 mm coverslips (VWR Scientific) were rinsed with ddH_2O and we coated the middle half of each coverslip with 0.1% of nitrocellulose. After a complete drying, the assay chamber was created by using two -2 mm-wide strips mounted 2 mm apart in the nitrocellulose-covered area, parallel to the long axis. Then, we placed an 18 mm coverslip (Corning) on the strips.

To perform IVMA, myosin was added onto nitrocellulose coverslip for 1 min and washed with bovine serum albumin (BSA) (0.5 mg/ml) in motility buffer to block unspecific sites. Immediately, unlabelled actin was used to block rigor heads and incubate for 30 sec. Then, to release filaments of actin from functional myosin heads, MgATP in motility buffer was added, leading the block of only “rigor” heads, followed by rinsing with motility buffer to remove the excess of MgATP. Finally, Phalloidin rhodamine-labelled F-actin was added to coverslip for 30 s and rinsed with motility buffer. IVMA was performed at 37 °C, in motility buffer with 1mM MgATP, 0.5% methylcellulose and oxygen scavengers (3 mg/ml glucose, 0.1 mg/ml glucose oxidase, 0.18 mg/ml catalase). Actin sliding was observed using a fluorescent inverted microscope and motility data were recorded and digitized for analysis, thought a software that allow a characterization of the entire field without bias, determining mean velocity via a Gaussian analysis.

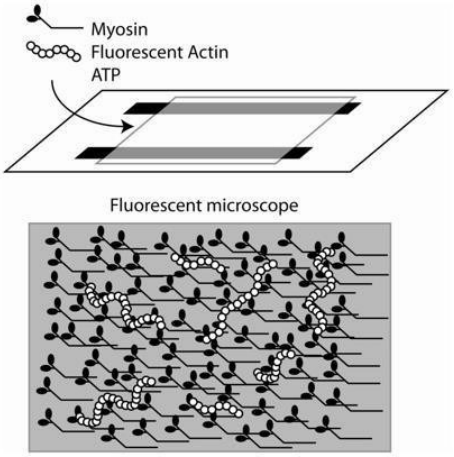

Figure 27. *In Vitro Motility Assay technique. Nitrocellulose-covered chamber with myosin preparation, fluorescent actin, and ATP.*

3.2 Engineered heart tissues (EHTs) generation

Engineered heart tissues (EHTs) were generated from hiPSC-CMs following a previously described protocol (Weinberger F. et al., 2017). Agarose casting moulds were formed in a 24-well tissue culture plate using 2% agarose (Life Technologies) dissolved in PBS 1X and the solution was heated to dissolve the agarose powder. Agarose moulds were generated by inserting Teflon spacers (EHT Technologies GmbH) in the wells; after agarose solidification (~10 min), Teflon spacers were removed and silicone PDMS racks (EHT Technologies GmbH) were positioned in the middle of each agarose well. At day 15 post cardiac induction, starting from beating monolayers, cardiomyocytes were washed with PBS 1X and dissociated with Tryple for 10 minutes at 37°C. Then, the cell suspension was moved into a centrifuge tube containing RPMI/B27 medium and FBS (50% RPMI, 50% FBS) and centrifuged at 1000 rpm for 5 min. HiPSC-CMs were resuspended in RPMI/B27 medium supplemented with 10% of FBS and ROCK inhibitor (1:1000).

Each EHT were generated with 100µl of mixed solution, consisting of 1 x 10^6 cells in RPMI/B27, 5 mg/ml of fibrinogen derived from bovine plasma (Sigma-Aldrich) and 3 U/mL of Thrombin (Sigma-Aldrich). The mixed solution of fibrinogen and thrombin was pipetting into the agarose mould and incubated for 80 min at 37°C, 5% CO2, to allow fibrin tissue polymerization. Subsequently, each well was covered with a small amount of RPMI/B27 (300uL) and incubated for 10 minutes to easily remove the tissue from the agarose stamps. Finally, the PDMS structure were carefully removed from the wells and transferred to wells

containing the EHT-medium, consisting of the RPMI plus B27 with insulin, 10% FBS, as well as 33µg/ml Aprotinin (Sigma-Aldrich) to minimize proteolytic degradation. The following day, the medium was replaced with RPMI/B27 supplemented with Aprotinin without FBS. Usually, engineered heart tissues start spontaneous beating around day 3-4 after tissue formation.

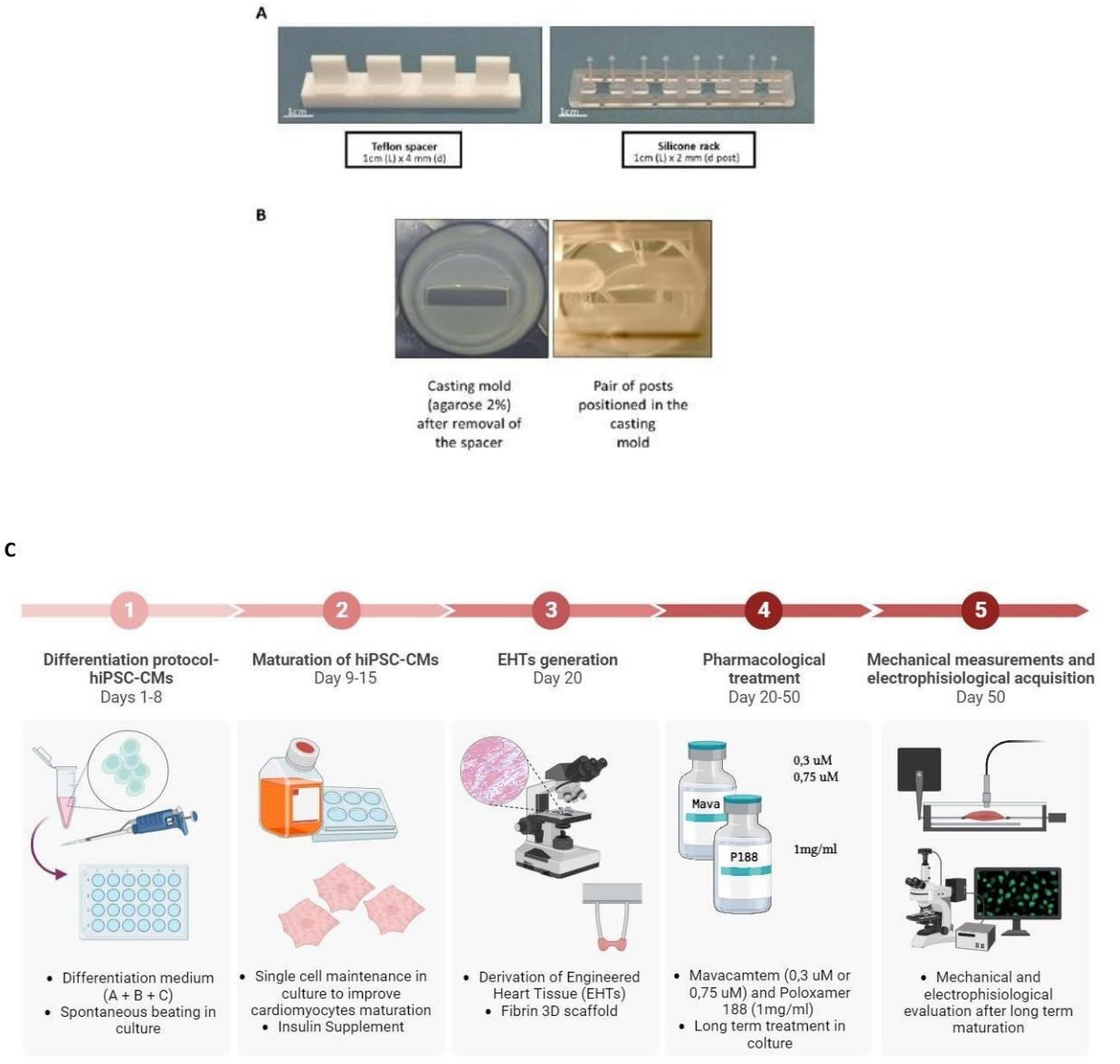

Figure 28. *Agarose casting mold preparation.* ***A)*** *Teflon spacer to perform agarose casting molds and a silicone PDMS rack.* ***B)*** *Generation of agarose casting molds and pillar insertion (Mannhardt et al., 2017);* ***C)*** *EHTs generation from hiPSC-CMs and chronic in vitro treatment.*

3.2.1 Spontaneous auxotonic recordings

Spontaneous auxotonic tension and beating frequency were regularly measured at specific time points during maturation (from day 20 to 50 p.d.) by optical tracking of the flexible post deflection at 10x of magnification (Olympus) using an Evos FL2 auto system (20 second recordings at 33 frames/sec) (Life Technologies). The system was associated with an on-stage incubator connected to a BenchPro 2100 Plasmid Purification System (Invitrogen) that allow the maintenance of culture condition of 37°C, 5% CO_2. Measurements were performed in the RPMI/B27 culture medium with ~0.4mM of Ca^{2+}. The relationship between the deflection of the individual pillars and force is 0.28 µN/µm. Tension was analyzed using a customized Labview analysis program and tissue cross-sectional area was calculated assuming an elliptical cross section (A= π/4 x width x thickness) for force normalization.

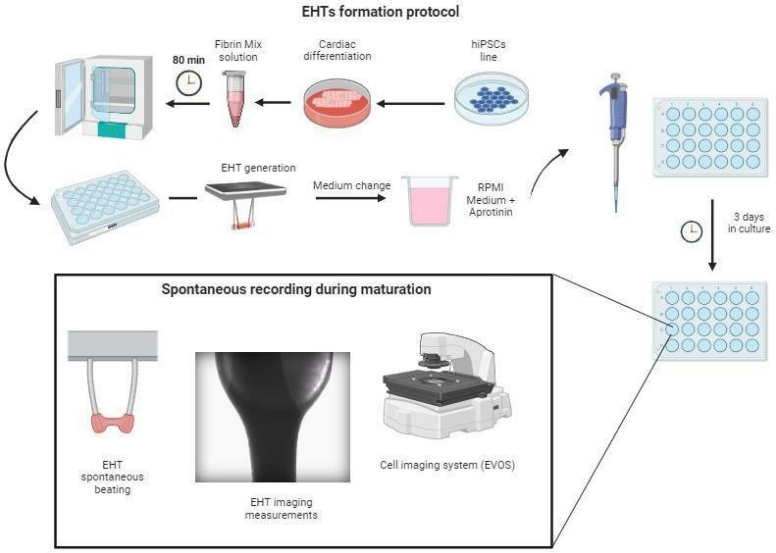

Figure 29. *Spontaneous auxotonic measurements by recording of flexible pillars deflection during EHTs maturation.*

3.2.2 Isometric force measurements

At a later stage of maturation (day 50 p.d.), EHTs were detached from the silicon pillars and immediately transferred into Krebs/Henseleit solution, containing (in mM) 119 NaCl, 4.7 KCl, 2.5 CaCl2, 1.2 MgSO4, 1.2 KH2PO4, 25 NaHCO3 with the addition of BDM (20mM). Then, the EHT was mounted between a force transducer (KG7A, Scientific Instruments Heidelberg, Germany) and a motor (Aurora Scientific Inc. Aurora, Canada), controlled by a custom Labview (National Instruments, Austin, Texas) program. Tissue dimensions (length and width)

were determined using a stereomicroscope with a calibrated reticule in the eyepiece and then tissue length was slowly increased in approximately 3% strain increments, while passive force was continuously recorded. The tissues were perfused with Krebs/Henseleit solution, without BDM, at pH 7.4 with 95%O2:5%CO2. Isometric force was recorded at 35±2°C and EHTs were stimulated at increasing pacing rates (from 0.2 to 2.5 Hz). Moreover, measurements were performed at different Ca^{2+} concentrations (0.5, 0.8, 1, 1.2, 1.8, 2, 3 and 4mM). Isometric force was recorded via custom LabView software and was calculated using the same cross-sectional area as for the spontaneous recording.

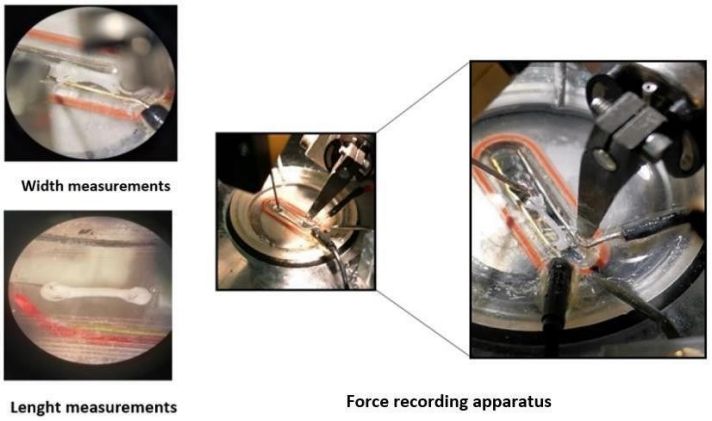

Figure 30. **Isometric contractions recording.** Images of mounting the EHT between a force transducer and a motor arm and width and length measurements before recordings.

3.2.3 Action potential and calcium transient evaluation by using a confocal microscope

At day 50 post cardiac induction, EHTs were incubated with two specific fluorescent dyes for membrane voltage and calcium (Fluovolt and Cal630, respectively) in Tyrode Solution, containing (in mM) 5 HEPES, 10 Glucose, 140 NaCl, 5.4 KCl, 1.2 $MgCl_2$, 1.8 $CaCl_2$ (pH = 7.3) supplemented with 10µM blebbistatin, Time of incubation was for 40 minutes. After this time, Tyrode buffer was replaced with fresh solution without dyes and mounted on a cellular stage of a confocal microscope (NikonEclipse T:2) supplemented with a multicolor light LED source. The EHTs were stimulated at difference frequencies (0.1, 1, 2 Hz) and maintained in perfusion with Tyrode solution at a controlled temperature of 37°C.

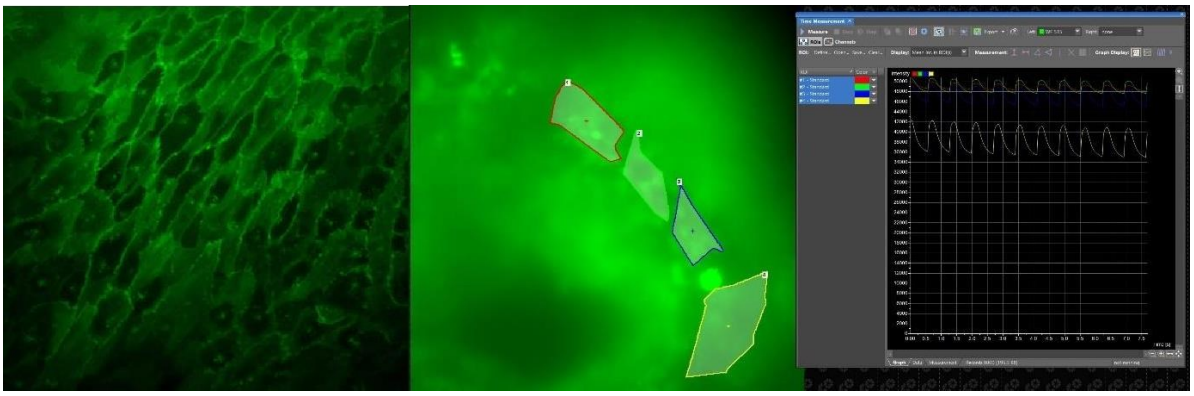

Figure 31. *Representative image of induced pluripotent stem cells derived engineered heart tissue (hiPSC-EHTs) loaded with a fluorescent day (Fluovolt) by using a confocal microscope.*

3.3 Cardiomyocytes isolation from human surgical samples

Starting from human surgical samples from the atria and ventriculles of selected patients who underwent cardiac surgery, viable cardiomyocytes were obtained using a combination of enzymatic and mechanic digestion, as described before (Coppini et al. Circulation 2013). In particular, cardiac tissue was cut into small pieces ($1mm^3$) in a cardioplegic solution, containing (in mM) KH_2PO_4 50, $MgSO_4$ 8, HEPES 10, Adenosine 5, Glucose 140, Mannitol 100 and Taurine 10. After cutting, the tissue was rinsed with Ca^{2+} -free dissociation buffer (HEPES 1o mM, Glucose 10 mM, taurine 20 mM, pyruvate 5 mM, NaCl 120 mM, KH_2PO_4 1.2 mM, KCl 10 mM, $MgCl_2$1.2 mM, pH 7.2). Enzymatic digestion was performed using collagenase Type V and protease Type XXIV (Sigma) at 0.4 mg/ml and 0.2 mg/ml, respectively, for extracellular matrix degradation, in association with a mechanical digestion, using a custom-made apparatus. Subsequently, the tissue was subjected to additional digestion cycles with collagenase, to allow the release of single cardiomyocytes. During digestion, the buffer containing cardiomyocytes was collected at the end of each cycle and the enzyme action was stopped with an equal volume of KB solution (glucose 20 mM, creatine 5 mM, taurine 5 mM, EGTA 0.5 mM, succinic acid 5 mM, K_2-ATP 2mM, pyruvic acid 5 mM, β-hydroxybutyric acid 5 mM, KCl 85 mM, K_2HPO_4 $7H_2O$ 5mM).

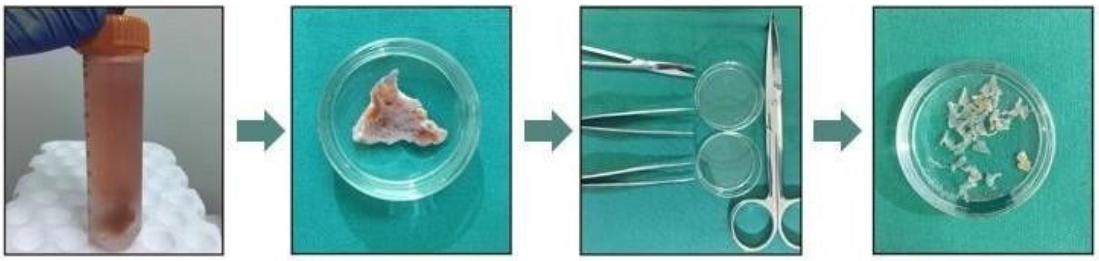

Figure 32. Viable cardiomyocytes isolation from human surgical samples. *Cardiac tissue is divided into small pieces and fibrotic and fat tissues were removed.*

Then, a small amount of cellular suspension was observed under microscope to evaluate the number and morphology of obtained cardiomyocytes, that should be as follows: rod-shaped, presence of visible stripes, well-defined cellular edges, absence of visible vacuolization or inclusions, absence of spontaneous beating. Once we obtained viable cardiomyocytes, the cellular suspension derived from all cycles of digestion was centrifuged at 700 x g for 5 minutes and pellet was resuspended in a Ca-free Tyrode solution supplemented with 1 mg/ml albumin and 0.1 mM $CaCl_2$. Finally, cardiomyocytes were gradually adapted at physiological calcium concentration by gradually adding $CaCl_2$ until we reached a final concentration of 0.6 mM. At this point, cardiomyocytes can be used to perform functional measurements, such as patch clamp and calcium fluorescence recordings.

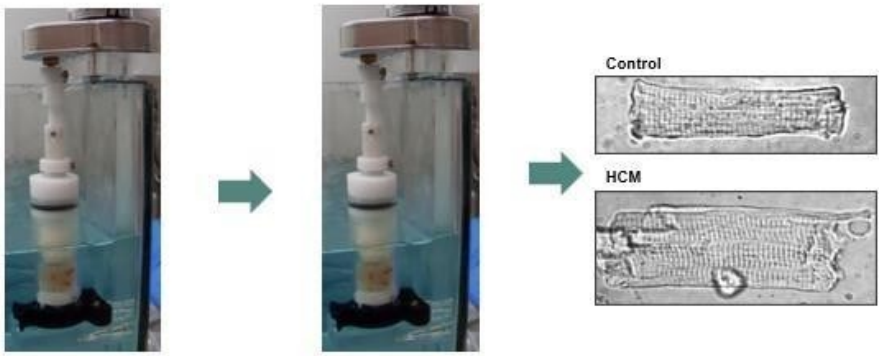

Figure 33. Enzymatic and mechanical digestion to obtain viable cardiomyocytes. *Cardiomyocytes were obtained using a custom-made tritur with a solution of collagenase and protease.*

3.3.1 Electrophysiological evaluation using patch clamp measurements

Cardiomyocytes isolated from human surgical samples of interventricular septum of patients affected from hypertrophic cardiomyopathy (HCM) were used to perform patch clamp

measurements, aiming to characterize the electrophysiological alterations in the presence of cardiomyopathies. Using a custom-made six-way perfusion system, we tested the acute effects of different compounds at different concentrations on the same cardiomyocytes, in comparison with the basal condition. With regards to electrophysiological measurements, isolated cells were placed on a cellular stage maintained at a temperature of 35±2 °C to perform current-clamp and voltage-clamp recordings aimed at evaluating the characteristics of action potentials, transmembrane currents, and intracellular calcium. Action potentials (APs) were measured using the perforated-patch configuration (amphotericin-B method). APs were activated with short depolarizing stimuli, and data were analysed using the Clampfit Software.

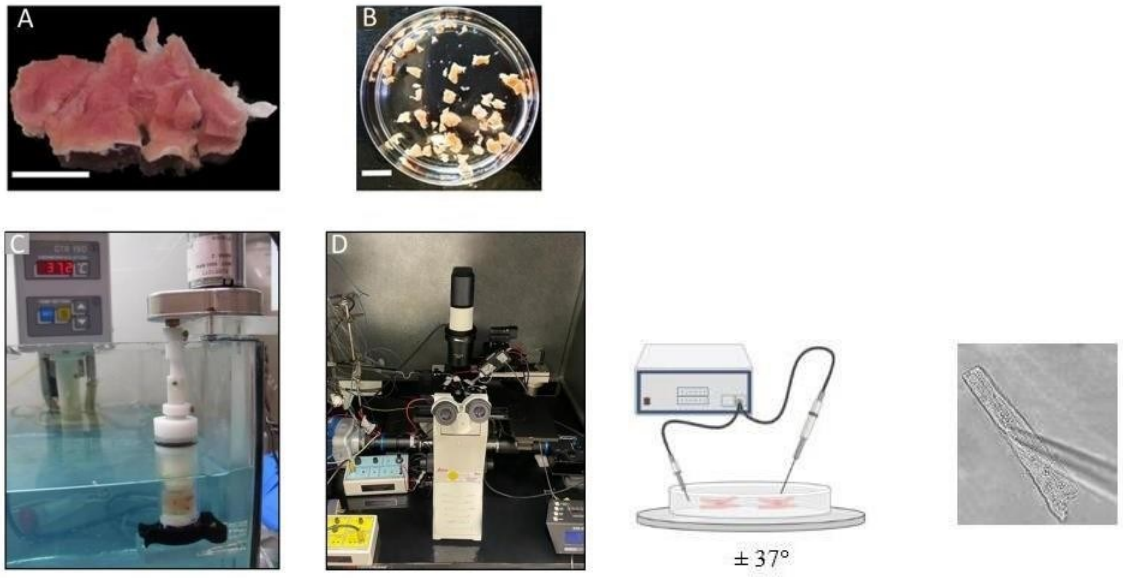

Figure 34. *Schematic representation of isolating procedure to obtain viable cardiomyocytes and patch-clamp measurements. A) Ventricular cardiac tissue derived from surgical myectomy. B) Cutting of cardiac tissue and fibrotic and fat tissues removal. C) Mechanical and enzymatic digestion. D) Patch-clamp measurements.*

3.4 Skeletal muscle differentiation from human induced pluripotent stem cells (hiPSCs)

Human induced pluripotent stem cells were obtained by reprogramming monocytes derived from a healthy donor and from a Duchenne patient carrying a deletion of exon 46-48, resulting in total absence of dystrophin (DMD1C11; ΔExon46-48). When hiPSCs reached 80% of confluence in culture, they were dissociated with ACCUTASE and incubated for 5 min at 37°C. Then, cellular suspension was dilute in Skeletal Muscle Induction medium 1 (SKM-01) and centrifugated at 1200 rpm for 4 minutes. Pellet was resuspended in SKM-01 medium and cells were plated at density of 20.000 cells/dish, to start the differentiation towards skeletal muscle

cells. To obtain 90% of confluency, the skeletal muscle precursors were detached with trypsin and incubated for 5 minutes; cells were diluted in KO-DMEM supplemented with 10% of KO-Serum and centrifuged for 4 minutes at 1200 rpm. Cells obtained were plated in a mw-24 (10.000 cell per dish) in Skeletal Muscle Myoblasts medium (SKM-02). Cells were then cultured until 90% of confluence, when skeletal precursors became myoblasts. To induce the conversion from myoblasts to myotubes, the SKM-02 medium was replaced with Skeletal Muscle Myotube medium 3 (SKM-03).

At each phase of differentiation, skeletal muscle precursors, myoblasts and myotubes, cells were detached and fixed with paraformaldehyde (PFA) at 4% to perform immunofluorescence staining for the main markers of each stage of differentiation (Pax7, MyoD, Miogenin, MHC). In addition, at the later stage of maturation (~ day 30 p.d.), calcium transient evaluation was performed by using a specific fluorescent dye (Cal520), to evaluate the calcium handling of both lines tested, under acetylcholine stimulation.

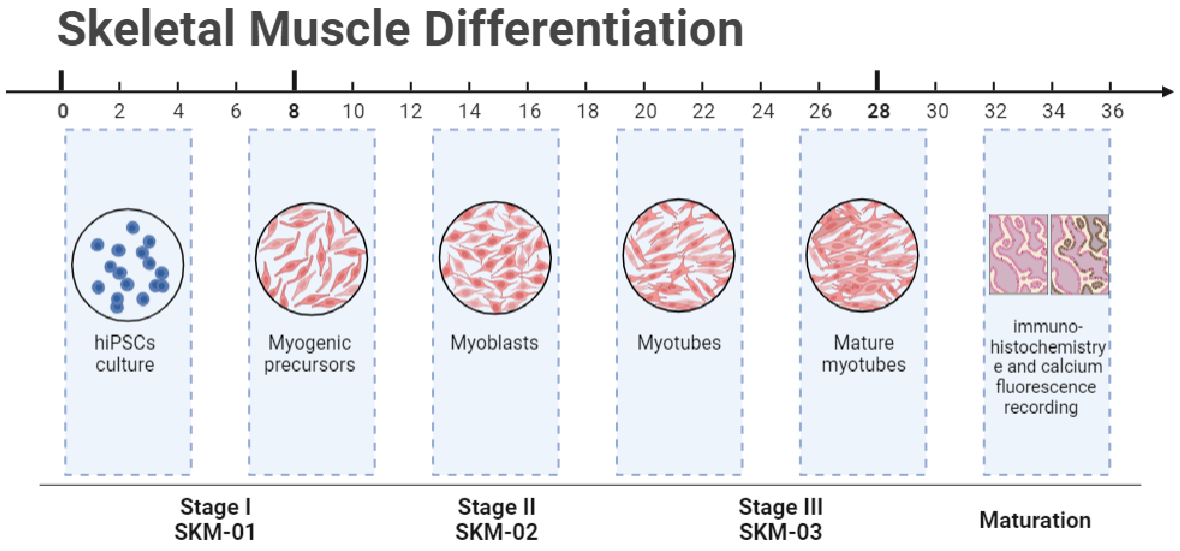

Figure 35. *Schematic representation of skeletal muscle differentiation protocol in vitro. Differentiation was performed in SKM-01/SKM-02/SKM-03 medium, and skeletal muscle cells were kept in culture at 37°C, 5% CO_2.*

Chapter 4

RESULTS

4.1 Modelling Hypertrophic cardiomyopathy using Engineered Heart Tissue (EHTs)

Hypertrophic cardiomyopathy (HCM) is commonly associated with an important sarcomere dysfunction, leading to cardiac muscle hypercontractility and specific myocardial impairment. In a normal heart, the actin-myosin interaction involves less than 10% of all myosin heads (Spudich JA et al., 2014), while the remaining heads are in a super relaxed state conformation where ATP-binding domains are sterically inhibited and unable to bind actin. In this view, HCM mutations lead to an increased number of active myosin heads involved in each cardiac cycle, increasing cardiac actin-myosin interaction, leading to increased energy consumption and hypercontractility.

To date, appropriate and specific pharmacological treatments for HCM are not available. In fact, current strategies provide for reducing arrhythmia occurrence, managing atrial fibrillation and improving left ventricular filling, by using beta-blockers and diuretics (Elliott P.M et al., 2014). Since cardiomyocyte hypercontractility represents a suitable target for HCM treatment, Mavacamtem, a novel first-in-class cardiac myosin inhibitor, may reverse the fundamental abnormalities of HCM myocardium (Zampieri M. et al., 2021). In a phase III clinical trial on patients with obstructive hypertrophic cardiomyopathy (Olivotto I. et al., 2020), Mavacamtem demonstrated efficacy in mitigating left ventricular outflow tract obstruction, improved the exercise capacity of patients, their NYHA functional class, and their health status. Moreover, the phase II MAVERICK-HCM trial showed improved indexes of cardiac function in HCM patients without obstruction (Ho CY et al., 2020)

4.1.1 MYBPC3 mutation associated with hypertrophic cardiomyopathy

Most of the mutations involved in the pathogenesis of HCM affect sarcomere and at least 80% of familial HCM is caused by mutation in two contractile proteins: myosin-binding protein C (MYBPC3) and myosin heavy chain (MYH7). MYBPC3 gene was the first mutation described as a cause of dilated cardiomyopathy, restrictive cardiomyopathy and left ventricular non-compaction (Hershberger RE et al., 2010; Yuan et al., 2017), MyBPC maintains the sarcomere integrity through interaction with actin, myosin, and titin (Flavigny J et al., 2003). Mutations in MYBPC3 gene lead an acceleration of cross-bridge kinetics, increasing energetic cost of contraction. Also, electrophysiological modifications, such as slower action potentials and prolonged calcium transients, occur in HCM patients carrying MYBPC3 mutation (Pioner et

al., 2023). In particular, somatic cells from a patient carrying the *MYBPC3*: c.772G>A variant (p.Glu258Lys, E258K) have been used to derive a induced pluripotent stem cells (iPSCs) line. Since induced pluripotent stem cells derived cardiomyocytes (hiPSC-CMs) are capable to mimic cardiomyocytes at a developmental stage (Marchiano' et al., 2019), the use of hiPSC-CMs can be predictive to model modifications that occurs in a very early stage of the disease, when overt cardiac abnormalities are still absent. In addition, to better understand the role of this particular sarcomere mutation on cellular contractility, engineered heart tissues (EHTs) were derived from the *MYBPC3*: c.772G>A line. An isogenic line derived from Crispr/Cas9 technique was used as control. Initially, to evaluate the effects of mavacamtem on sarcomere function in HCM, we performed an acute exposure of the c.772G>A line to the drug, followed by a long-term treatment for 20 days in culture. To analyse the pathological changes occurring during cardiac development, we performed an evaluation of auxotonic contractions at specific time points of maturation in EHTs (days 25, 30, 35, 40, 45, 50), through video-microscopy recordings of the deflection of the flexible silicon pillars attached to the muscles. Analysis of spontaneous contractions of EHTs was performed during culture in RPMI/B27 medium at 37°C, 5% CO_2, with and without Mavacamten (0.3 and 0.75 µM).

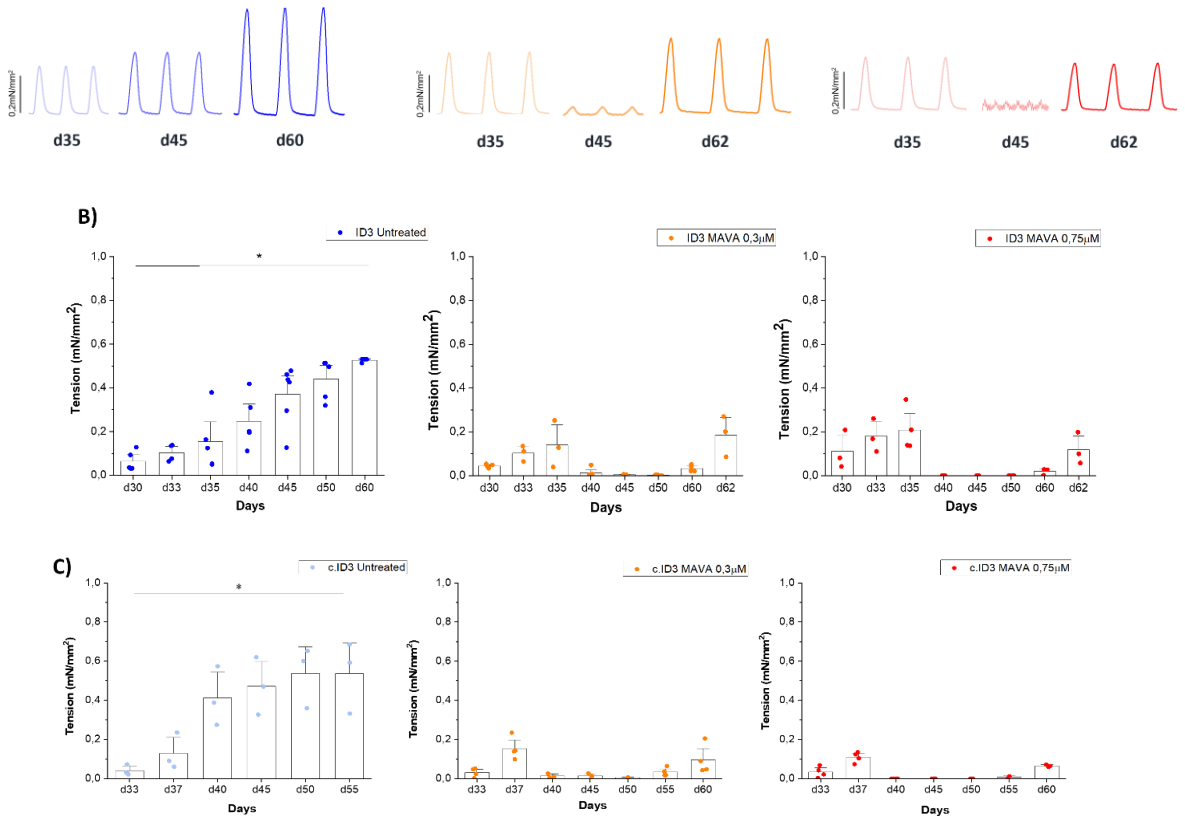

Figure 36. Chronic treatment with Mavacamten. *Chronic treatment of EHTs from day 40 to day 60 p.d. Analysis of spontaneous contractions of EHTs was performed during culture with and without Mavacamten by optical tracking of flexible pillar deflection. EHTs were kept in culture in RPMI/B27 medium at 37°C, 5% CO_2*

Recordings of spontaneous auxotonic twitches highlighted that Mavacamtem treatment determined a partial reduction of contractile force at 0.3µM, while the higher concentration (0.75µM) was sufficient to completely abolish spontaneous contractions. Furthermore, as a result of wash-out protocols, tension slowly recovered reaching pre-treatment levels. In addition, at a later stage of maturation (day 50), EHTs were detached from the pillars and mounted on a custom-made apparatus to perform measurements of tension and contraction kinetics in isometric conditions. EHTs were subjected to pacing stimuli at specific frequencies (0.2-0.5-1-1.5-2 Hz) and were exposed to different extracellular calcium concentrations (0.5 - 1.8 - 4 mM). Measurements were performed with a continuous perfusion with Krebs-Henselheit solution at 37C.

Our results show that long-term treatment with Mavacamtem (0,75µM) induces a significant reduction in isometric twitch force in HCM lines and control. In addition, Mavacamten induces an acceleration of twitch contraction and relaxationin mutated EHTs, but no effects on kinetics were observed in control muscles.

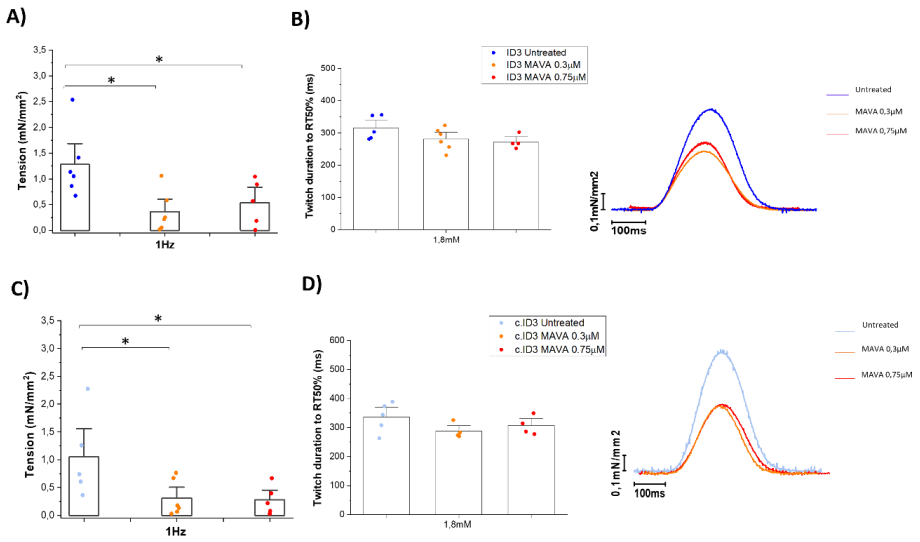

Figure 37. Isometric measurements of active tension. *Mechanical recordings of HCM-EHTs at day 60 p.d Analysis of spontaneous contractions of EHTs was performed during culture with and without Mavacamten by optical tracking of flexible pillar deflection. EHTs were kept in culture in RPMI/B27 medium at 37°C, 5% CO_2.*

4.1.2 Fluorescent evaluation of action potential by using confocal microscope

To assess the effect of long-term treatment with Mavacamten on HCM-EHTs, on the same tissue, we performed a fluorescent evaluation of action potential, by using a specific fluorescent dye able to work as a voltage indicator (Fluovolt). In particular, we compared untreated with treated HCM-EHTs and, through a confocal miscroscope, we perform action potential (AP) measurements.

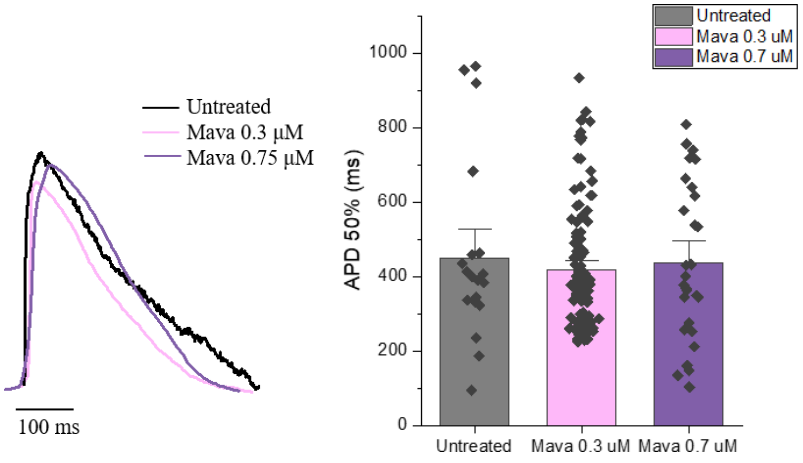

Figure 38. *Action potential recording using FluoVolt as a voltage indicator. Untreated EHTs were compared with those treated with Mava (0.3µM) for action potential at 50% of duration (APD50, ms). Measurements were performed at 1Hz at 37°C in Tyrode solution with 1.8mM of extracellular calcium and Blebbistatin 5µM. (Untreated N=3 n=22; Mava 0.3 µM N=6 n=125; Mava 0.75 µM N=2 n=26)*

4.2 R403Q mutation: mechanical alterations of myosin motility in hypertrophic cardiomyopathy

Approximately 70% of all HCM cases are linked to single point mutations, including mutation that occur in β-myosin heavy chain (MHC), resulting in myosin motor function alterations. One of the most severe MHC mutations is the R403Q mutation, with 50% of the affected individuals dying by 40 years of age in the first case series reported. To investigate the effect of the R403Q mutation on the mechanical properties of myocardium, cardiomyocytes were differentiated from induced pluripotent stem cells Crispr-Cas9 engineered to carrying R403Q mutation in heterozygosis and homozygosis (Het-R403Q and Homo-R403Q, respectively), using a differentiation protocol as previously described. Around d30 post cardiac induction, cellular shortening, contraction time (time to 50% peak), relaxation time (time from peak to 50% baseline) were measured through an automated video-based detection software (IonOptix, USA). Contractility measurements were included when cardiomyocytes followed field stimulation and spontaneous beating did not occur. In addition, on the same day of maturation (day 50 p.d.), we performed a single molecule mechanical assay on cardiac myosin isolated from hiPSC-CMs.

Shortening measurements. To evaluate how R403Q mutation can affect cardiomyocytes contractility, we performed shortening and calcium fluorescence evaluation on long-term cultures of hiPSC-CMs, carrying the R403Q mutation in heterozygosis or in homozygosis (Het-R403Q and Homo-R403Q, respectively). Cardiomyocytes were perfused at 37 C, with Tyrode solution supplemented with different calcium concentration (0.5mM-0.8mM-1mM-1.8mM) under imposed stimuli at different frequencies (0.5Hz-1Hz-1.5Hz-2Hz).

Optical evaluations were performed in Tyrode solution perfusion at physiological calcium concentration (1.8 mM) at 1 Hz stimulation rate and showed a marked decrease of cellular shortening percentage (%) of Het-hiPSC-CMs and Homo-hiPSC-CMs in comparison with control cardiomyocytes, associated with a more pronounced decrease in heterozygous compared to homozygous and control cells (Figure 39.B). Moreover, twitch contraction kinetics, in terms of time to peak 50% and time to 50% of relaxation, highlighted no significant differences in both lines tested compared to control (Figure 39.C). In addition, at the same experimental conditions and a field stimulation of 1 Hz, does not occur any significant differences in both lines tested, compared to control (Figure 39.D).

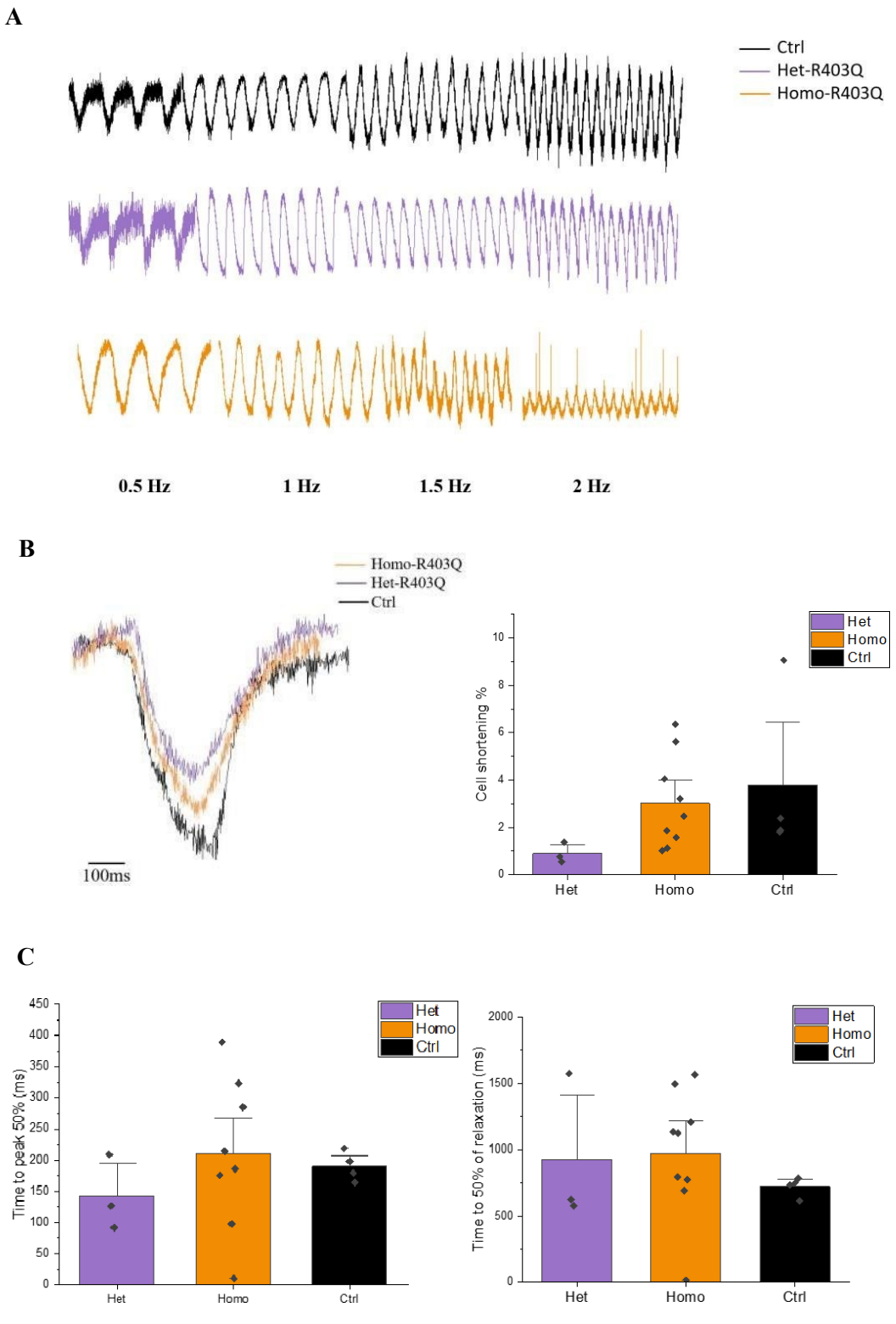

Figure 39. Shortening measurements using IonOptix evaluation. ***A)*** *Representative traces of hiPSC derived cardiomyocytes under imposed stimuli of (0.5, 1, 1.5 and 2 Hz).* ***B)*** *Het-hiPSC-CMs, Homo-hiPSC-CMs and ctrl-hiPSC-CMs shortening evaluation. Recordings were performed at d50, in Tyrode solution supplemented with* $CaCl_2$ *(1.8 mM) under imposed stimulus of 0.5 Hz. Cardiomyocytes were kept in culture in RPMI/B27 medium at 37°C, 5%* CO_2.

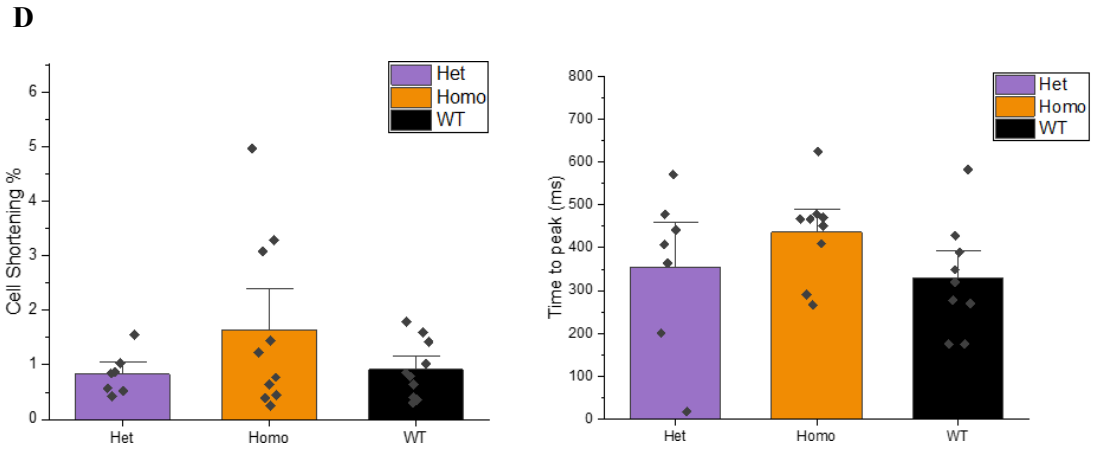

Figure 40. Shortening measurements via IonOptix technique*. Het-hiPSC-CMs, Homo-hiPSC-CMs and ctrl-hiPSC-CMs shortening evaluation (shortening percentage, time to peak, time to 50% of relaxation). Recordings were performed in Tyrode solution supplemented with* $CaCl_2$ *(1.8 mM), 37°C, under imposed stimulus of 1 Hz. Het-hiPSC-CMs: N=3 n=7; Homo-hiPSC-CMs: N=4 n=12; ctrl-hiPSC-CMs: N=4 n=11.*

Calcium transient evaluations. Calcium plays a fundamental role in cardiomyocytes function, triggering excitation-contraction coupling and modulating several electrophysiological and mechanical processes. Previous findings show evidence that contractile activity is dependent on cytosolic Ca^{2+} levels, with low concentrations (1-10 mM) of calcium that led mechanical activation but inhibiting this process to high concentrations (> 10 mM) (Fabiato and Fabiato 1972; Fabiato 1983). To assess how HCM cardiomyocytes can adapt their mechanical activity in relation to the variation in intracellular calcium concentration, we performed optical evaluation (IonOptix, USA) by changing calcium concentrations in solution (0.5-0.8-1-1.8 mM). Measurements were performed on Het-hiPSC-CMs, Homo-hiPSC-CMs and control at d50 p.d, in continuous perfusion with Tyrode solution and a different stimulation frequency (0.5-1 Hz), as previously described.

IonOptix evaluation highlighted that cellular shortening (%) is lower in both mutated cardiomyocytes compared to control, at 0.5 Hz of stimulation (Figure 41,B), but with an increase in the shortening percentage of Homo-hiPSC-CMs in comparison to Het-hiPSC-CMs and ctrl-hiPSC-CMs (Figure 41,C), at 1 Hz of field stimulation. This preliminary data may be explained with the hypercontractility characteristic by β-myosin heavy chain mutation, such as R403Q mutation.

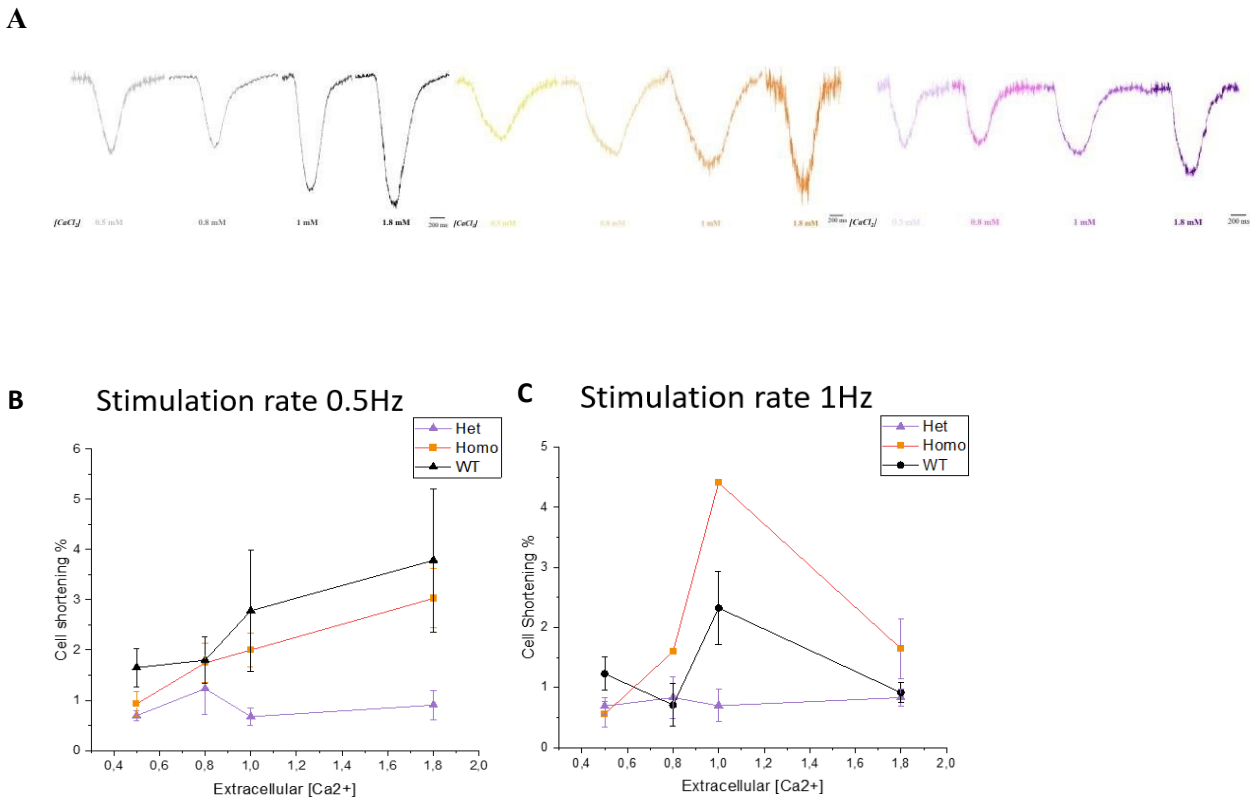

Figure 41. Shortening measurements via IonOptix tecnique*. Het-hiPSC-CMs, Homo-hiPSC-CMs and ctrl-hiPSC-CMs shortening evaluation (%) Recordings were performed in Tyrode solution supplemented with different calcium concentration (0.5-0.8-1-1.8 mM), 37°C, under imposed stimulus (0.5-1 Hz).* ***A)*** *Cardiomyocytes shortening (%) at different calcium concentration under imposed stimulus of 0.5 Hz.* ***B)*** *Cardiomyocytes shortening (%) at different calcium concentration under imposed stimulus of 1 Hz.*

In addition to shortening evaluations, at the same day of maturation (d50), we performed calcium transient measurements by using a ratiometric fluorescent dye for calcium (FURA-2). Calcium transient kinetics evaluations highlighted a significant reduction in time to peak (ms) and time to 50% of relaxation (ms) in homozygous and heterozygous cardiomyocytes compared to control line, at 0.5 and 1 Hz of field stimulation (Figures 42.B). Moreover, the same trend was maintained also for higher frequencies of stimulation (Figures 42.C).

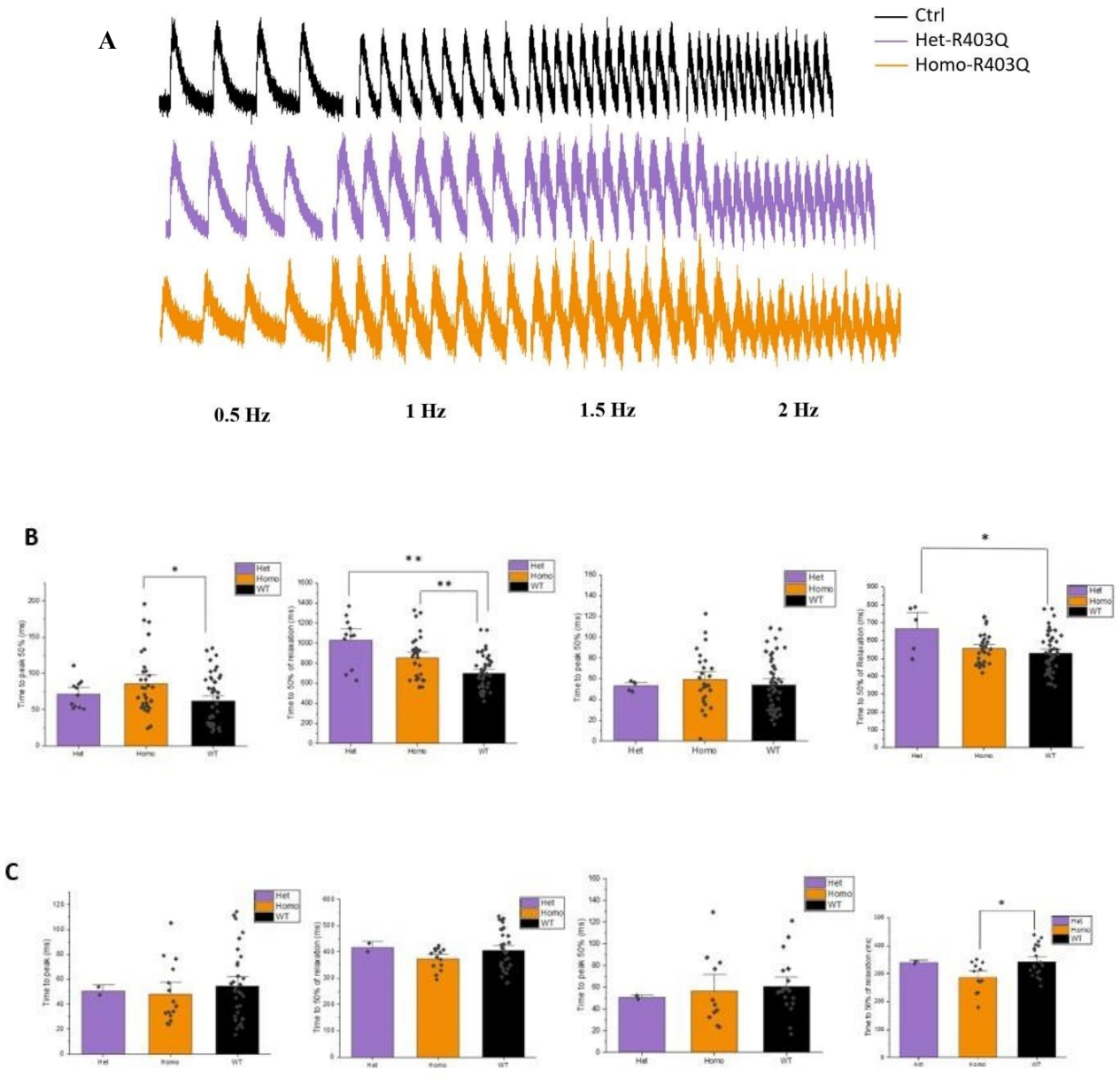

Figure 42. Calcium fluorescent measurements using FURA-2 fluorescent dye. *Het-hiPSC-CMs, Homo-hiPSC-CMs and ctrl-hiPSC-CMs calcium transient evaluation (time to peak, time to 50% of relaxation). Recordings were performed in Tyrode solution supplemented with $CaCl_2$ (1.8 mM), 37°C, under field stimulation. Het-hiPSC-CMs: N=1 n=11; Homo-hiPSC-CMs: N=3 n=32; ctrl-hiPSC-CMs: N=3 n=49.* ***A)*** *Calcium transient kinetics recorded under imposed stimulus of 0.5 Hz.* ***B)*** *Calcium transient kinetics recorded under imposed stimulus of 1 Hz.* ***C)*** *Calcium transient kinetics recorded under imposed stimulus of 1.5 Hz.* ***D)*** *Calcium transient kinetics recorded under imposed stimulus of 2 Hz.*

Moreover, calcium handling evaluation by using FURA fluorescent dye on Het-hiPSC-CMs, Homo-hiPSC-CMs and ctrl-hiPSC-CMs showed a significant reduction in calcium transient amplitude in both mutated lines, compared to control line, at all stimulation frequencies tested (0.5-1 Hz), highlight a possible alteration in calcium handling associated with the R403Q mutation (Figure 43).

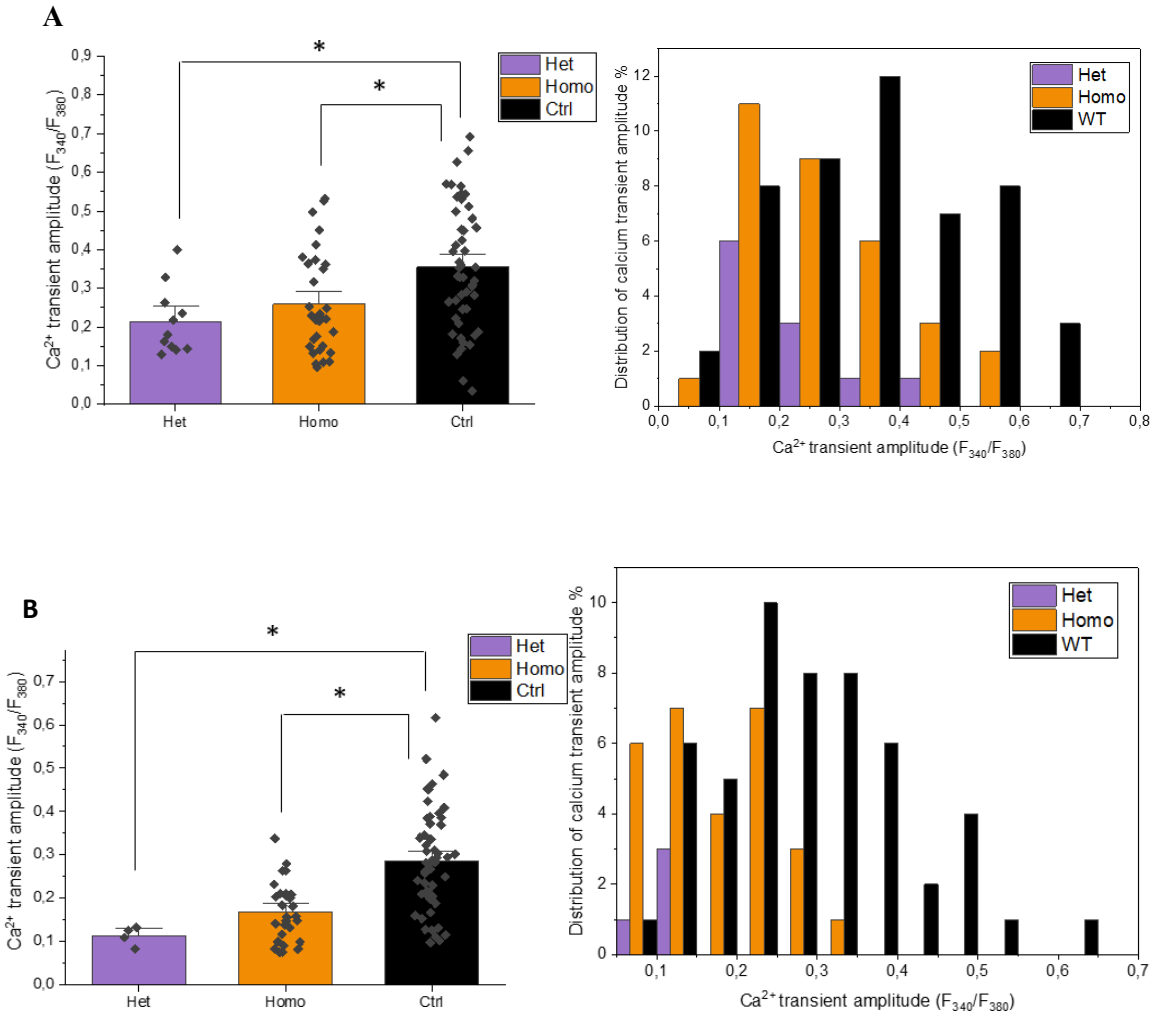

Figure 43. Calcium fluorescent measurements using FURA-2 fluorescent dye. *Het-hiPSC-CMs, Homo-hiPSC-CMs and ctrl-hiPSC-CMs calcium transient amplitude evaluation. Recordings were performed in Tyrode solution supplemented with $CaCl_2$ (1.8 mM), 37°C, under field stimulation. Het-hiPSC-CMs: N=1 n=11; Homo-hiPSC-CMs: N=3 n=32; ctrl-hiPSC-CMs: N=3 n=49.* ***A)*** *Calcium transient amplitude recorded under imposed stimulus of 0.5 Hz.* ***B)*** *Calcium transient amplitude recorded under imposed stimulus of 1 Hz.*

Fluorescent evaluation of sliding actin-myosin velocity: In Vitro Motility Assay (IVMA). In Vitro Motility Assay (IVMA) technique provide a powerful tool to lead many important fundamental observations about the mechanism of actin and myosin interaction. The IVMA protocol allowed us to observe fluorescently labelled actin filaments gliding over a cover slip that has been coated with myosin in the presence of ATP. The actin-myosin movement is captured with a sensitive video camera and velocity is estimated using a specific analysis software. Moreover, the rate of movement of actin results independent of the concentration of myosin or on the length of the actin filament, then the movement occur at the peak velocity when the threshold of myosin density is achieved.

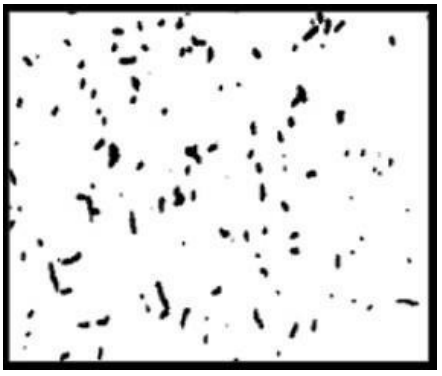

Figure 44. *Representative image of sliding actin-myosin recording using In Vitro Motility Assay performed via fluorescent microscope, in presence of photo labelled actin.*

Several studies show evidence that R403Q mutation can increase cross-bridge relaxation kinetics, in association with an increase of energetic cost of sarcomere tension generation, representing one of the causes of hypertrophic cardiomyopathy (Belus et al Circ res 2009).

To investigate the effects of R403Q mutation in cross-bridge formation and on actin-myosin kinetics, we performed IVMA on myosin isolated from mutated hiPSC-CMs (Het R403Q, Homo R403Q), in comparison with control. At day 50 p.d. we applied a specific myosin extraction protocol, obtaining myosin from each lines tested (Het R403Q, Homo R403Q and Ctrl) and performed IVMA in presence of 100% ATP (2mM) and 50% ATP/ADP (1mM ATP, 1mM ADP).

Our results highlight an evident reduction in filament velocity (µm/s) in moving non-erratic filaments in mutated lines, when 50% ATP was applied, in comparison with 100% ATP (Figure 45, B). Moreover, Het R403Q myosin showed a reduction of sliding velocity in comparison with the control line.

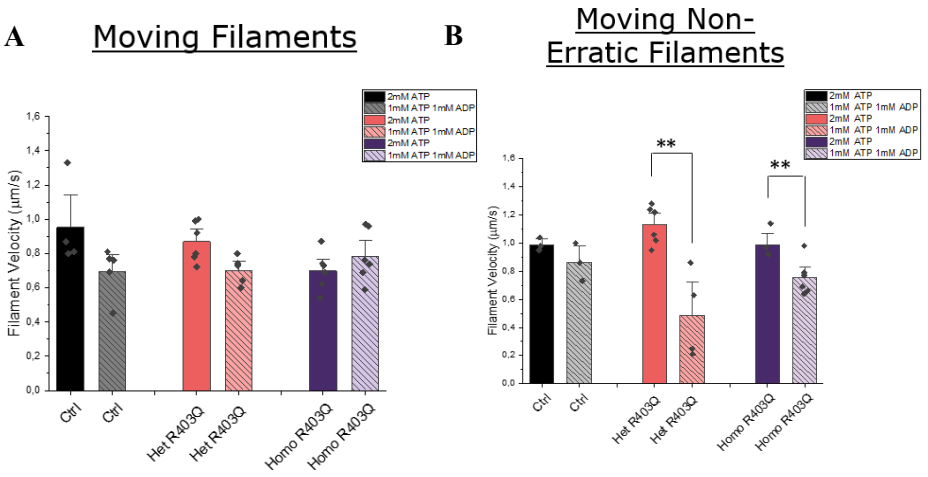

Figure 45. In Vitro Motility Assay fluorescent evaluation. *Myosin was extracted from Het-hiPSC-CMs, Homo-hiPSC-CMs and ctrl-hiPSC-CMs at day 50 after cardiac induction. Measurements were performed at 37°C, with a fluorescent microscope equipped with a sensitive camera. Het-hiPSC-CMs: N=2 n=6; Homo-hiPSC-CMs: N=2 n=6; ctrl-hiPSC-CMs: N=2 n=4.* ***A)*** *Sliding velocity of moving filaments* ***B)*** *Sliding velocity of moving non-erratic filaments. [Myo] Het R403Q= 0.43 mg/ml; 0.63 mg/ml. [Myo] Homo R403Q= 0.37 mg/ml; 0.59 mg/ml. [Myo] Ctrl= 0.20 mg/ml; 0.47 mg/ml.*

4.3 Electrophysiological evaluation of surgical human samples derived from HCM and aortic stenosis

Despite the advance in new therapies, cardiovascular disease remains the largest cause of illness and death worldwide. One considered a rare inherited cardiac disease, hypertrophic cardiomyopathy (HCM) is one of the most common heart diseases, with an incidence of 1:500 in the general population and characterized by cardiac dysfunction and heart failure (Maron B. J. Et al., 2022). Effective pharmacological interventions have significantly reduced HCM mortality and morbidity and include the use of angiotensin-converting enzyme inhibitors, angiotensin II receptor blockers, diuretics and beta blockers.

In the recent years, sodium-glucose cotransporter-2 inhibitors (SGLT2-Is), known as gliflozins, first identified as anti-diabetic medication, were introduced as "off-label" use for the treatment of cardiovascular events. The mechanisms underlying the cardioprotective effects of SGLT2-Is are still unclear, but a role in the activation of anti-inflammatory and oxidative stress pathways has been proposed (Tomasoni D. et al., 2019). To date, clinical trials highlight a possible key role of dapagliflozin in cardiac electrophysiology. In fact, recent clinical evidence from a post-hoc analysis of the Dapagliflozin effect on cardiovascular events (DECLARE-TIMI 58) demonstrated a reduction of relative risk of atrial fibrillation, reducing heart failure (HF) and hospitalization, even in non-diabetic patients with HF (EMPEROR-Reduced trial).

Starting from this evidence, we tested Dapagliflozin on cardiomyocytes isolated from surgical biopsies derived from patients undergoing myectomies affected by HCM and aortic stenosis (Careggi University Hospital, Florence). Aortic stenosis a classic example of secondary hypertrophy, caused by a reduction of aortic valve opening capability representing an obstruction to the physiological outflow of blood between the left ventricle and the aorta during systole, resulting in loss of pressure and heart failure symptoms.

To investigate the effect of Dapagliflozin on the myocardium electrophysiological profile, cardiomyocytes were isolated from surgical samples of the interventricular septum extracted from patients with HCM or aortic stenosis. To obtain single cells, we used a mechanical and enzymatic digestion, as previously described (Coppini et al, Circulation 2013). Subsequently, we performed acute treatment with Dapagliflozin at two different concentrations: 1 μM, very similar to the concentrations obtained in the plasma of patients during clinical use, and 10 μM, to assess potential cardiotoxic effects of this drug. During treatment, cardiomyocytes were perfused with Tyrode solution and maintained at 37°C. Action potentials were recorded in current clamp configuration at different frequencies (0.2, 0.5, 1 Hz).

Patch clamp measurements in HCM cells highlighted a significant reduction of action potential duration at 90%, compared to basal, at all stimulation frequencies tested (0.2-0.5-1 Hz). Moreover, this decrease was more pronounced with the increase of stimulation frequency and with the increase of drug concentration (1 µM vs 10 µM), showing a possible and dose-dependent and frequency-dependent effect (Figure 45). Moreover, the same effect has been observed on action potential duration at 90% in cardiomyocytes isolated from surgical samples of patients with aortic stenosis (Figure 46).

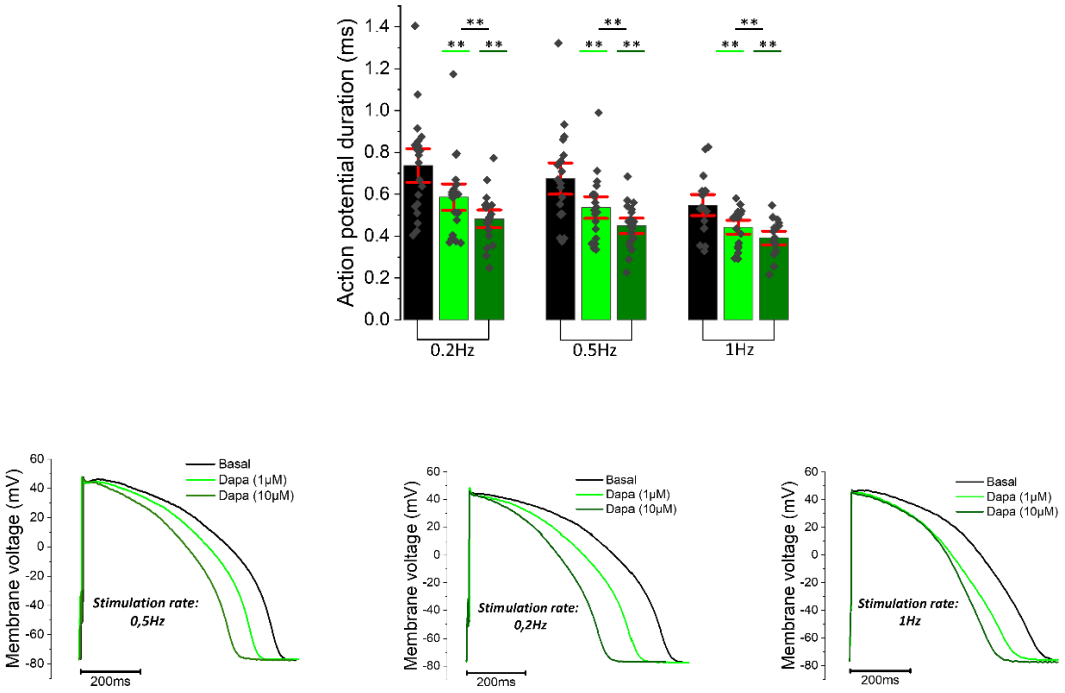

Figure 46. Effect of Dapagliflozin on action potential kinetics of ventricular cardiomyocytes isolated from hypertrophic cardiomyopathy surgical samples: current clamp configuration. A) *Action potential duration at 90% repolarization (APD90%) recorded during stimulation at 0.2Hz, 0.5Hz and 1Hz in human ventricular cardiomyocytes isolated from hypertrophic cardiomyopathy (HCM) surgical samples.* ***B)*** *Superimposed representative action potential traces recorded in human ventricular cardiomyocytes isolated from hypertrophic cardiomyopathy (HCM) surgical samples during stimulation at 0.2hz, before drug exposure (black traces) and during exposure to different Dapagliflozin at the concentration of 1 µM (light green traces) and 10 µM (dark green traces).* ***C)*** *Superimposed representative action potential traces recorded in human ventricular cardiomyocytes isolated from hypertrophic cardiomyopathy (HCM) surgical samples during stimulation at 0.5Hz, before drug exposure (black traces) and during exposure to different Dapagliflozin at the concentration of 1 µM (light green traces) and 10 µM (dark green traces).* ***D)*** *Superimposed representative action potential traces recorded in human ventricular cardiomyocytes isolated from hypertrophic cardiomyopathy (HCM) surgical samples during stimulation at 0.2hz, before drug exposure (black traces) and during exposure to different Dapagliflozin at the*

*concentration of 1 µM (light green traces) and 10 µM (dark green traces). Mean ± SEM from 8 patients (20 cardiomyocytes). * *= p<0.01*

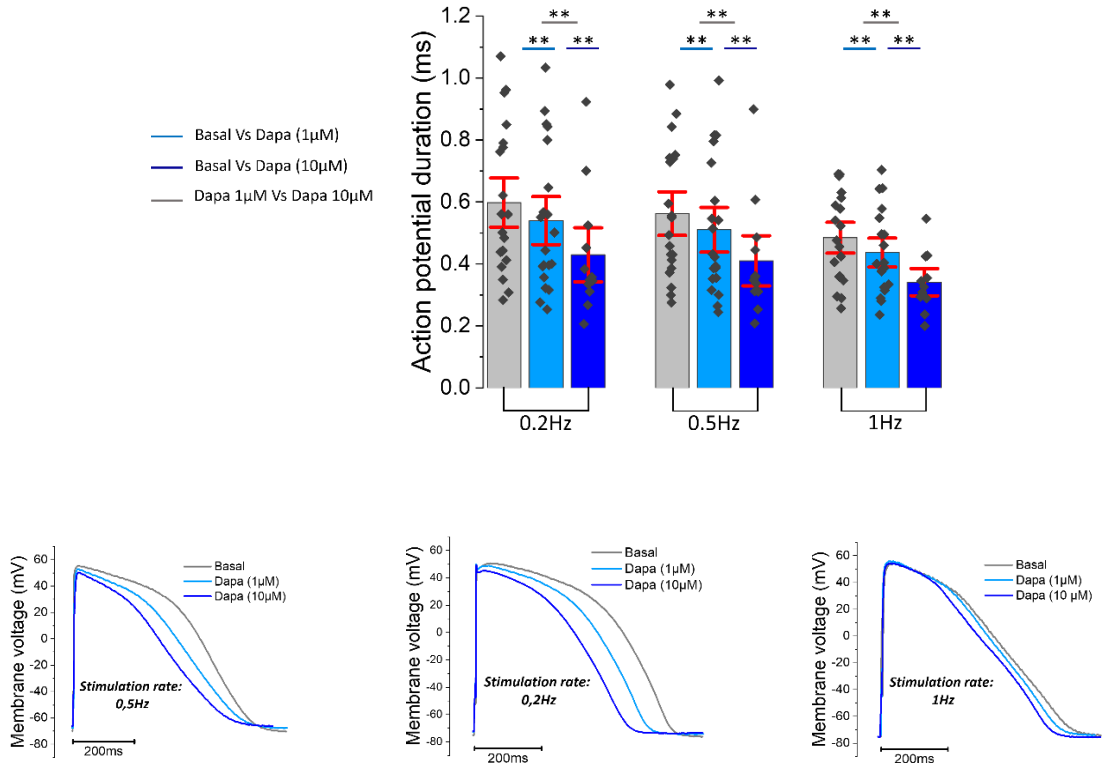

Figure 47. Effect of Dapagliflozin on action potential kinetics of ventricular cardiomyocytes isolated from aortic stenosis surgical samples: current clamp configuration. A) *Action potential duration at 90% repolarization (APD90%) recorded during stimulation at 0.2Hz, 0.5Hz and 1Hz in human ventricular cardiomyocytes isolated from aortic stenosis (AOS) surgical samples.* ***B)*** *Superimposed representative action potential traces recorded in human ventricular cardiomyocytes isolated from aortic stenosis (AOS) surgical samples during stimulation at 0.2hz, before drug exposure (black traces) and during exposure to different Dapagliflozin at the concentration of 1 µM (light green traces) and 10 µM (dark green traces).* ***C)*** *Superimposed representative action potential traces recorded in human ventricular cardiomyocytes isolated from aortic stenosis (AOS) surgical samples during stimulation at 0.5hz, before drug exposure (black traces) and during exposure to different Dapagliflozin at the concentration of 1 µM (light green traces) and 10 µM (dark green traces).* ***D)*** *Superimposed representative action potential traces recorded in human ventricular cardiomyocytes isolated from aortic stenosis (AOS) surgical samples during stimulation at 0.2hz, before drug exposure (black traces) and during exposure to different Dapagliflozin at the concentration of 1 µM (light green traces) and 10 µM (dark green traces). Mean ± SEM from 8 patients (20 cardiomyocytes). * *= p<0.01*

Moreover, acute treatment with dapagliflozin does not show any significant differences in maximum rise slope of action potentials measured in ventricular cardiomyocytes isolated from oHCM and aortic stenosis surgical samples, compared to the baseline conditions (Figure 47).

Then, these results highlight that cardioprotective effect of Dapagliflozin is explained on the action potential, via the reduction of action potential duration (APD). Moreover, this reduction, in association to the absence of effect on the peak sodium current, even at high concentration (10 µM), may induce a decrease of arrhythmic events occurrence.

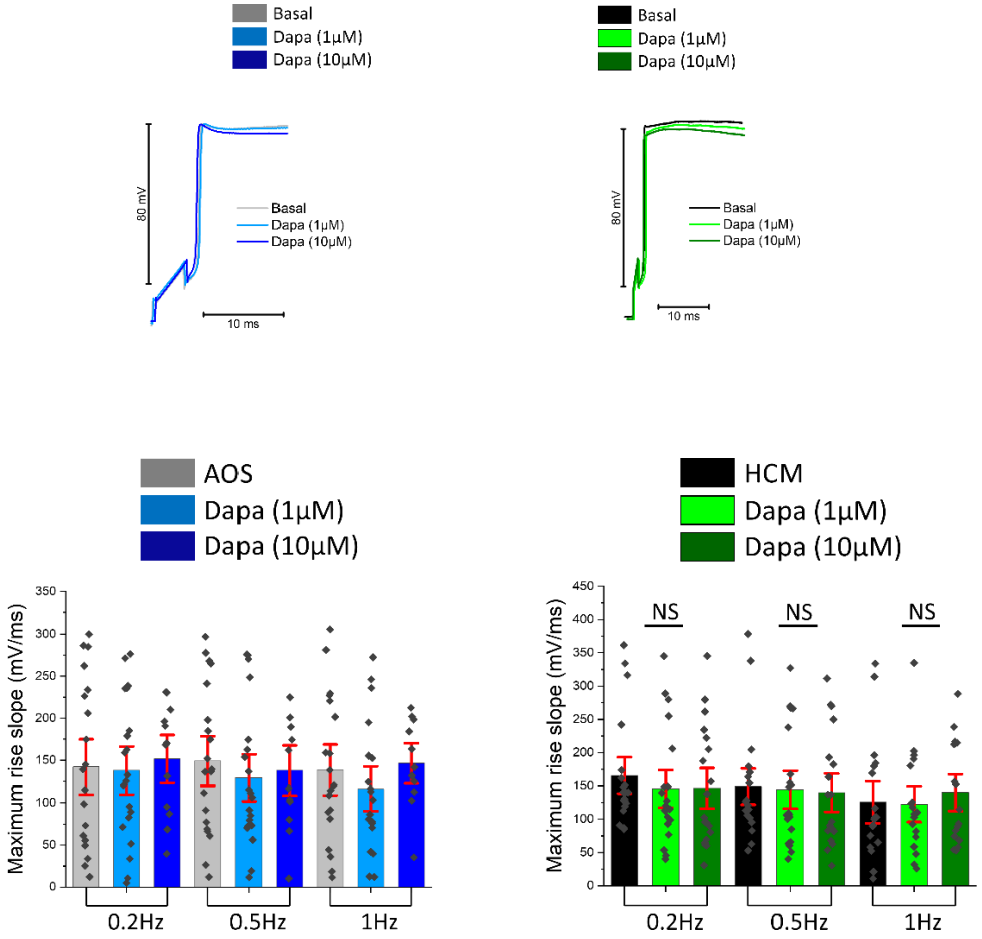

Figure 48. Effect of Dapagliflozin on action potential kinetics of ventricular cardiomyocytes isolated from hypertrophic cardiomyopathy and aortic stenosis surgical samples: current clamp configuration. ***A)*** *Maximum upstroke speed of action potential recorded in ventricular cardiomyocytes from oHCM patients at 0.2Hz, 0.5 and 1Hz, before and after exposure to different Dapagliflozin concentrations (1 µM and 10 µM). Mean ± SEM from 8 patients (20 cardiomyocytes).* ***NS****= Not Significant.* ***B)*** *Maximum upstroke speed of action potential recorded in ventricular cardiomyocytes from AOS patients at 0.2Hz, 0.5 and 1Hz, before and after exposure to different Dapagliflozin concentrations (1 µM and 10 µM). Mean ± SEM from 6 patients (20 cardiomyocytes).* ***NS****= Not Significant.*

4.4 Engineered heart tissue to modelling dilated cardiomyopathy associated to Duchenne muscular dystrophy

Idiopathic dilated cardiomyopathy (DCM) represents one of the most common causes of heart failure worldwide, with an estimated prevalence of 40 cases per 100.000 individuals in the general population. Clinically, DCM is manifested as an abnormal dilatation of ventricular chambers, often associated with cardiac dysfunction and sudden cardiac death (SCD) in young subjects, representing a leading indication for cardiac transplantation (K. Lakdawala et al., 2023) or implantation of implantable cardioverter-defibrillators (ICDs). DCM may be a consequence of several types of inherited myopathies, including Duchenne Muscular Dystrophy (DMD). DMD is a neuromuscular disorder affecting 1:3500 male individuals (Romitti PA et al., 2015), manifesting with progressive loss of muscles mass and function associated with fatal outcome within the third decade of life. Cardiac and respiratory complications remain the main cause of death in DMD patients. Genetically, DMD is caused by mutations in the gene encoding for dystrophin, a regulatory protein involved in the protection of sarcolemma from mechanical stress occurring during contraction. As a result, cardiomyocyte membrane-fragility occurs, causing ruptures that allow extracellular Ca to enter muscle cells, culminating in myocardial damage and cellular death (Sun C. et al., 2019).

Initially, to evaluate the main mechanisms underlying dilated cardiomyopathy associated with Duchenne Muscular dystrophy, we derived engineered heart tissue (EHTs) from cardiomyocytes differentiated from three different Duchenne hiPSC lines:

- **4.4.1 Δ exons 46-48 (DMD1-c11)**, derived from a eighteen-years old patient with heart failure (LVEF= 29%) and implanted defibrillator;
- **4.4.2 Δ exon 50 (UC-72039)**, carrying a deletion of exon 50 resulting in total absence of dystrophin (Guan X., Stem Cell Res, 2013; Pioner JM, Cardiovasc Res., 2019);
- **4.4.3 Δ exon 51 (DMD3),** derived from a seventeen-year old patient with a sever cardiac impairment and manifested dilated cardiomyopathy.

We performed measurements of tension by contraction of flexible pillars, at specific time points, to assess the mechanical proprieties of mutated lines, in comparison with the control line, derived from a healthy donor.

Our results highlight that tension increased during maturation in the control line; however, this increase was less pronounced in DMD lines at the same days of maturation (Figure 49.A).

Moreover, spontaneous beating frequencies tended to decrease with the progression of maturation in both lines tested (Figure 49.B).

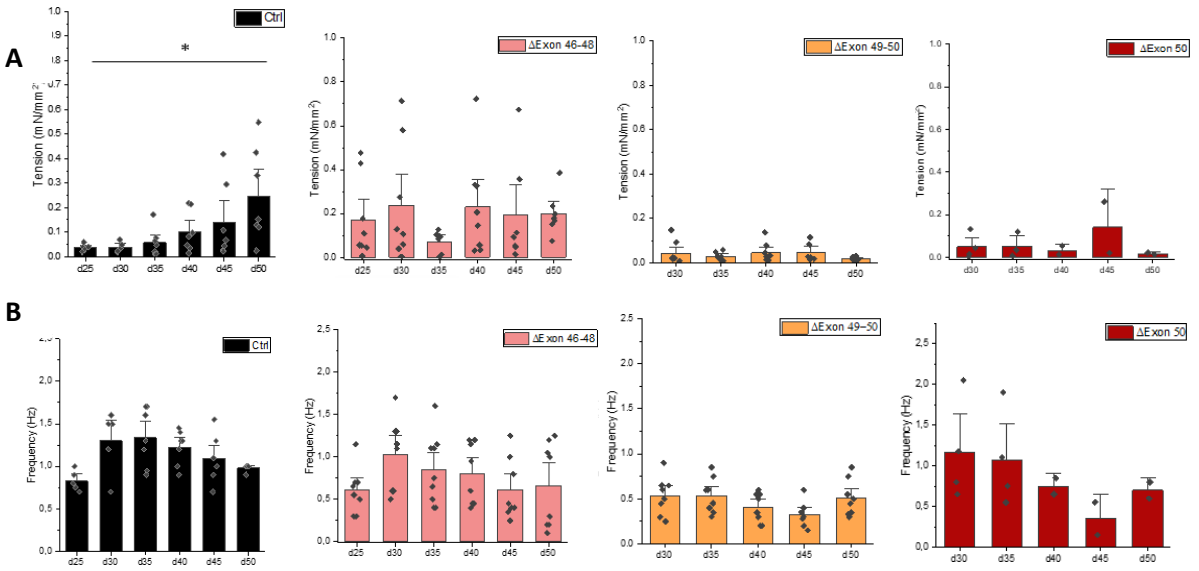

Figure 49. Auxotonic spontaneous recording of frequency and tension in DMD-EHTs *(Δexon 46-48, Δexon 49-50, Δexon 50 and control) from day 25 to day 50. 37°C, RPMI Medium, [Ca^{2+}] 0.4mM. One-way analysis of variance (ANOVA) with a Tukey post-hoc test was used to compare the different time points. * $p < 0.05$ and ** $p < 0.01$.* ***A)*** *Spontaneous recording of tension (mN/mm²) measured at different time points of EHTs maturations;* ***B)*** *spontaneous frequency (Hz) of EHTs contraction during maturation.*

In addition, we performed an evaluation of active tension in isometric conditions at a later-stage of maturation (d50), under field stimulation at 1Hz. These results highlighted a significant reduction of active tension in DMD lines (Δ exons 46-48, Δ exon 50, Δ exon 51), compared to controls (figure 50). Moreover, twitch duration does not change significantly in all lines tested (Figure 51).

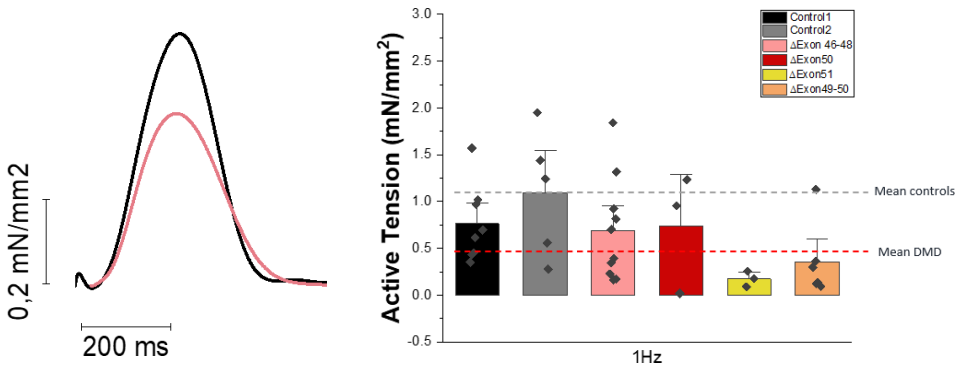

Figure 50. Active tension measurements in isometric conditions of DMD-hiPSC-CMs compared to control. *Δ exons 46-48, Δ exon 50, Δ exon 51, compared to ctrl. Stimulation pacing 1Hz, 1.8mM [Ca^{2+}].*

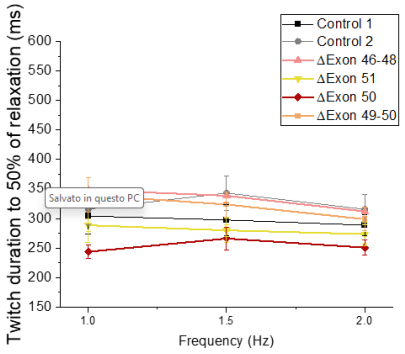

Figure 51. Twitch duration to 50% of relaxation on DMD-EHTs compared to control. *Different frequencies of stimulation (1Hz, 1,5Hz, 2Hz, 1.8mM [Ca^{2+}].*

4.4.1 Chronic treatment with Poloxamer 188 (P188)

To date, pharmacological interventions to treat DMD are focused on optimizing muscle growth and reducing muscle inflammation by using corticosteroids, ventilatory support with positive pressure ventilation and cardioprotective treatments (general HF treatment with ACE-inhibitors and beta-blockers), to improve survival. However, these treatments have several limitations and adverse effects, and fail to delay the progression of the disease. Nowadays, novel therapeutic strategies have been proposed for the treatment of DMD, including gene therapy to restore dystrophin production (Konieczny P. et al., 2013), mechanisms focused on restoring the integrity of membrane (Malik V. et al., 2012) and strategies to enhance muscle regeneration (Motohashi M. et al., 2014). In terms of increasing membrane stability, a valid approach may be the use of compounds that repair membrane damage in DMD cardiomyocytes during contraction. In fact, the triblock copolymer class of membrane-interacting compounds called poloxamers or pluronics, have shown promising results in numerous biological applications, such us lysis detergents (Krylova O. et al., 2004), drugs delivery adjuvants and membrane stabilizers (Yasuda S. et al., 2004). Poloxamers are non-ionic amphiphiles molecules consisting of a linear structure formed by a hydrophobic core of polypropylene oxide (PPO) elongated on both sides with two hydrophilic chains of polyethylene oxide (PEO). The hydrophobic region is able to insert inside specific membrane areas with reduced tension, such as damaged areas of the sarcolemma in DMD cells (Cai C. et al., 2009). Poloxamer 188 (P188), with a molecular weight of 8400 and a PPO/PEO ratio of 0.20, is the most widely studied copolymer. Previous

finding from Yasuda et colleagues (Yasuda S. et al., 2004) highlighted that acute treatment with P188 in isolated myocytes from dystrophic mdx mice restored membrane function though the block of anormal calcium entry through the sarcolemma.

To evaluate the effects of Poloxamer 188 on the mechanical proprieties of DMD hiPSC lines, we performed chronic treatment with 1mg/ml of P188 for 20 days in culture. During P188 exposure, recording carried out on DMD-EHTs in auxotonic conditions showed an increase in tension in treated EHTs compared to untreated muscles (figure 52).

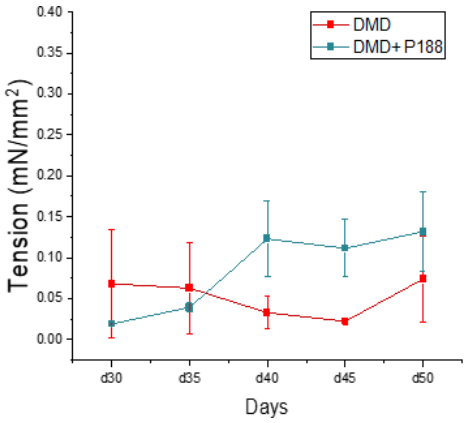

Figure 52. Auxotonic spontaneous contraction of treated with P188 (1mg/ml) versus untreated DMD-EHTs from day 30 to day 50 of maturation. *Measurements were performed at 37°C, 5%CO_2 in RPMI+B27 medium containing ~[Ca^{2+}] 0.4mM.*

Furthermore, at day 50 post differentiation (p.d.), EHTs were detached from the pillars, and we measured active tension through a force transducer, in isometric conditions. Recordings were performed in a Krebs-Henselheit solution supplemented with different extracellular calcium concentration (0.5mM, 1.8mM, 4mM). Our results show a significant increase of active tension at all calcium concentrations in treated DMD-EHTs, compared to untreated DMD muscles (Figure 53).

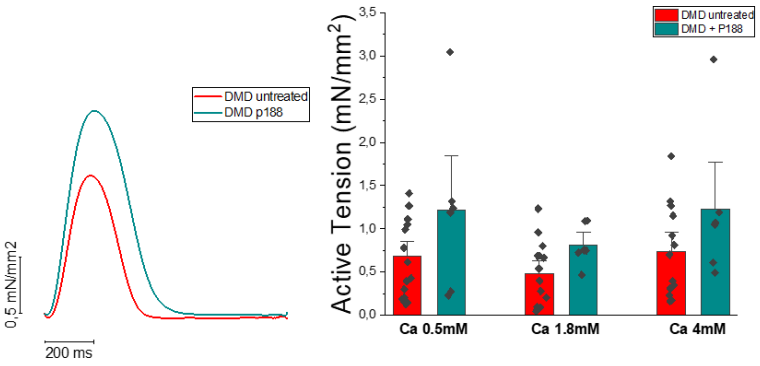

Figure 53. A) *Representative traces of tension of treated versus untreated DMD-EHTs. 37°C, day 50 p.d., Krebs solution* ***B)*** *Measurements of active tension performed at different calcium concentrations (0.5mM, 1.8mM, 4mM).*

4.4.2 Evaluation of Ranolazine acute treatment on DMD engineered heart tissues (DMD-EHTs)

Electrophysiological abnormalities are caused from changes occurring in specific current density cause action potential (AP) alterations, culminating in arrhythmic events in obstructive HCM (oHCM) patients. Moreover, several evidence showed that late sodium current ($I_{Na\text{-}L}$) result enhanced in HCM (Coppini R. et al., 2013), resulting in a possible target to pharmacological interventions. This is the case of ranolazine, an anti-anginal drug that act inhibiting the late sodium current ($I_{Na\text{-}L}$) (Antzelevitch C. et al., 2004). The increase of $I_{Na\text{-}L}$ current density lead Na^+ overload which, in turn, decreases intracellular calcium concentration and promotes the activity of NCX exchanger, with the increment of exchange of intracellular Na^+ with extracellular Ca^{2+}, worsening calcium overload. These electrical alterations result in an impaired cardiac function in HCM patients. Moreover, Ranolazine has shown to improve diastolic function in vitro, reducing arrhythmic events occurrence in impaired cardiomyocytes (Coppini R. et al., 2013). In addition, several studies highlight a safe and affective role of Ranolazine to the treatment of fibrosis developed from patients affected by non-ischemic dilated cardiomyopathy (Vizzardi E. et al., 2013; Poglajen G. et al, 2016). In fact, DCM myocardium is vulnerable to electrical instability, including re-entry mechanism, caused from the onset of fibrotic tissue and low left ventricle ejection fraction. Based on this evidence, we perform acute-treatment with ranolazine (10 μM) on DMD-EHTs at later stage of maturation (day 50) at high calcium concentration (4 mM).

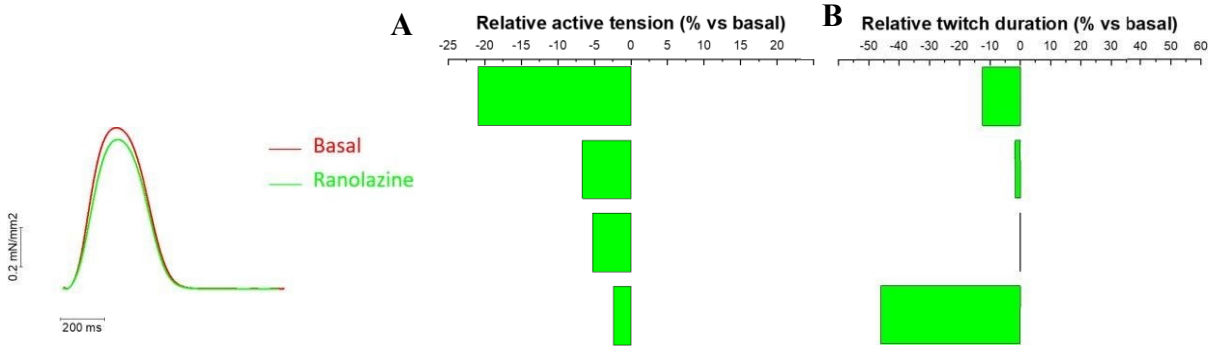

***Figure 54**. **Acute treatment with Ranolazine (10 µM) in isometric conditions and high calcium concentration (4 mM). A)** Relative active tension (% vs basal) of EHT-DMD measured at day 50 p.d. and representative trace. **B)** Relative twitch duration (% vs basal). EHTs were measured in isometric conditions at 37°C in the Krebs-Henselheit solution with 4mM of [Ca^{2+}] under imposed pacing. One-way analysis of variance (ANOVA) with a Tukey post-hoc test was used to compare the different time points. * $p < 0.05$ and ** $p < 0.01$. (N=4)*

One of the most accredited hypotheses is the possible effect of Ranolazine on calcium overload. In fact, previous studies suggest a role of this drug in a mitigation of calcium overload, often associated to dilated cardiomyopathy (DCM). Moreover, another additional effect of Ranolazine is the modulation of NCX exchanger activity, leading an additional calcium removal from citosol of DMD cardiomyocytes. Our results showed that, after acute treatment with Ranolazine, active tension and twitch duration (%) of DMD-EHTs result decrease in comparison to control (Figure 54), highlight a possible additional effect of this drug on the weakness capacity of contraction machinery of DMD impaired cardiomyocytes.

4.5 Gliflozins: a new potential pharmacological treatment for inherited cardiomyopathies

Sodium-glucose cotransporter 2 (SGLT2) inhibitors (SGLT2-Is), known as gliflozins, represent a novel class of oral drugs, currently used for the treatment of type 2 diabetes and heart failure. To date, SGLT2 inhibitors are associated with an increase of glycaemic control and reduction in body mass and blood pressure.

Glucose transporters are part of a protein family consisting of four members, encoding from the SLC-5 gene. The two main members of this family are represented by the sodium/glucose carrier proteins SGLT-1 and SGLT-2, which are expressed in the kidneys, having a crucial role in renal glucose resorption and intestinal glucose absorption. In this contest, SGLT-2 inhibitors act by blocking glucose reabsorption in the renal proximal convoluted tubule, through the inhibition of SGLT-2 transporter, which is responsible for approximately 90% of renal glucose reabsorption. In addition, several studies show that SGLT2-Is may reduce the renal threshold for glucose excretion from 10 mmol/L (180 mg/dL) to 2.2 mmol/L (40 mg/dL) (De Fonzo R.A: et al., 2013). This mechanism promotes a consequent increase of urinary glucose elimination under normal plasma glucose concentrations, leading to a reduction of blood glucose levels and improving body sensitivity to insulin (Merovci A. et al., 2015). The ancestor of SGLT inhibitors, Phlorizin, was discovered in 1835 starting from the apple tree root and its benefits on glycosuria was identified just a century later (Chasis H. et al., 1933). To date, several other compounds have been derived, including dapagliflozin, canagliflozin, empagliflozin, ertugliflozin, ipragliflozin, sotagliflozin, remogliflozin etabonate, luseogliflozin, and tofogliflozin. Despite the large number of SGLT2-Is developed, only dapagliflozin, canagliflozin, empagliflozin and ertugliflozin have been approved for clinical use in type 2 diabetes patients in Europe.

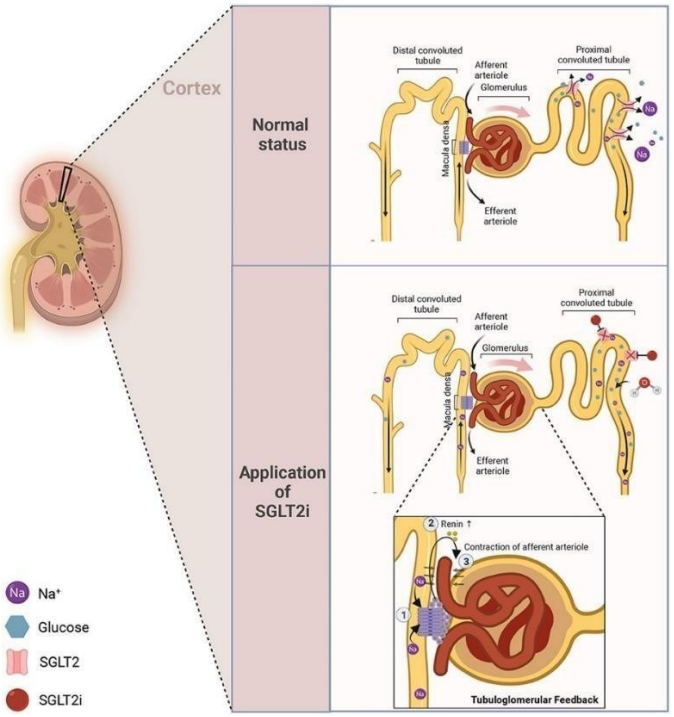

Figure 55. *Anti-hyperglycemic mechanism of SGLT2 Inhibitor (SGLT2i). Normally, glucose and Na^+ can be efficiently reabsorbed at the site of the proximal convoluted tubule to maintain glucose homeostasis. After SGLT2i treatment, reabsorption will be inhibited, thereby leading to diuresis and natriuresis.*
(New insights and advances of sodium-glucose cotransporter 2 inhibitors in heart failure, Yang X et al., 2022 frontiers in neurology).

In addition to their hypoglycemic effect, SGLT2-Is may prevent renal damage and cardiovascular events, including heart failure. These unexpected effects of cardiovascular protection have led to an increase in scientific interest and to significant changes in the treatment guidelines for heart failure. In fact, in several cardiovascular trials, SGLT2-Is have shown to improve cardiovascular and renal outcomes, such as the reduction of risk of cardiovascular death or heart failure progression (Salvatore T. et al., 2022). In particular, in a large, randomized, placebo-controlled trial, EMPA-REG-OUTCOME, the SGLT2 inhibitor empagliflozin have shown marked cardiovascular benefits and improved survival. Subsequently, focused studies were conducted on heart failure patients recruited regardless of the presence or absence of diabetes. In the international, multicentre, parallel group, event-driven, randomized, double-blind, placebo-controlled study DAPA-HF (J.J.V. McMurray et al. 2019), dapagliflozin was tested on patients with heart failure and reduced ejection fraction (HFrEF); treated patients showed a reduction of the risk of cardiovascular death and worsening heart failure (HF). In addition, in the phase III trial DELIVER, researchers observed that the

effects of gliflozins were not changed by the initial FE value, with promising outcome on cardiovascular events and hospitalization in patients with heart failure with slightly reduced or preserved ejection fraction (EF), compared to placebo.

Currently, the guidelines of the American Heart Association, suggest the use of gliflozins for the treatment of chronic heart failure with reduced, moderately reduced or preserved ejection fraction, with a Class IIA recommendation and evidence of level B. Moreover, the results obtained in the DELIVER trial could induce a review of the recommendation levels and provide further guidance on the guidelines, in favour of a wider use of gliflozins in clinical practice. Therefore, dapagliflozin and empaglioflozin are currently approved for the baseline therapy of heart failure in the EU and USA, while sotagliflozin is approved for heart failure treatment only in the USA.

To evaluate the effects of gliflozins on inherited dilated cardiomyopathy, we performed acute treatment procedures in DMD-EHTs. Force evaluations were carried out on EHTs resulting from our DMD-hiPSC-line carrying a deletion of Exon 51 (ΔExon51) resulting in the total absence of dystrophin. The measurements were performed under isometric conditions, at day 50 of maturation, in continuous perfusion with Krebs-Henselheit solution, at 37 $°C$ and at different stimulation frequencies (1-1.5-2 Hz). In addition, EHTs were subjected to an acute perfusion with 1 μM and 5 μM Dapagliflozin, to assess the effects of this drug on force generation and contraction kinetics.

Our preliminary results show a reduction in the duration of contraction recorded at 90% of the relaxation phase, an effect that became progressively larger with the increase of stimulation frequency and of drug, concentration, highlighting a possible interaction of Dapagliflozin with the myocardium contraction kinetics (Figure 56.B). In addition, relative active tension increases after treatment with the drug, at both concentrations tested (Figure 56. A), suggesting a possible mechanism of action of this drug to increase the contraction force of cardiomyocytes, which is extremely reduced in dystrophin-deficiency cardiomyocytes.

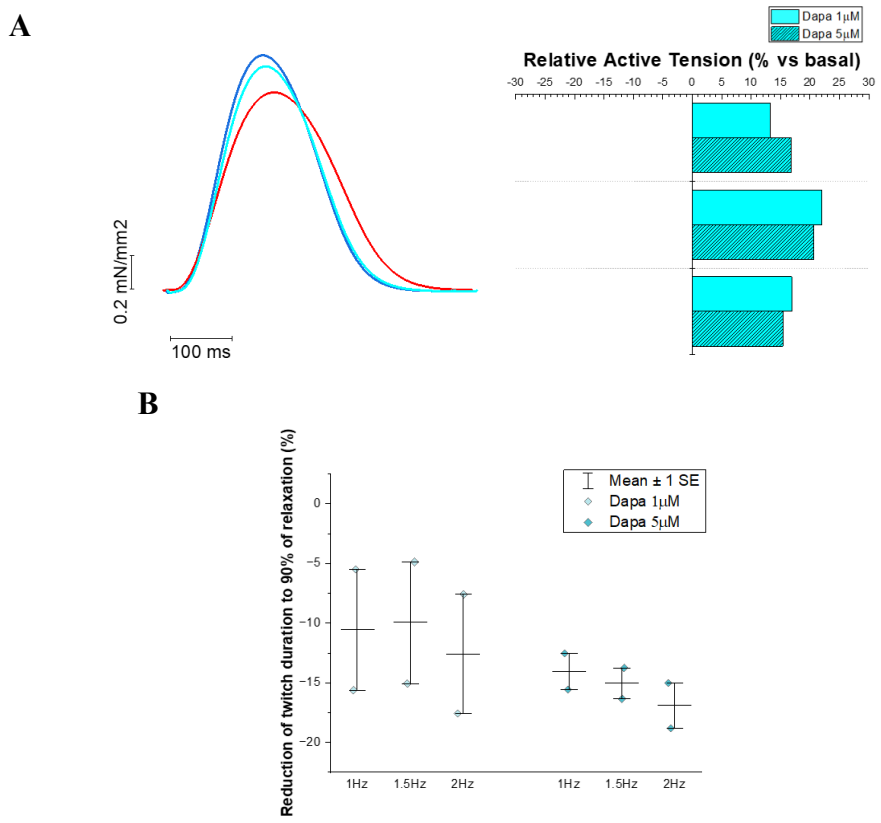

Figure 56. Acute treatment with Dapagliflozin (1 and 5 µM) in isometric conditions. A) *Relative active tension (% vs basal) measured at day 50 p.d. and representative trace (DMD-EHTs, ΔExon51).* ***B)*** *Twitch duration to 90% of relaxation at different frequencies (1-1.5-2 Hz) recording on DMD-EHTs (ΔExon51) untreated compared to treated (Dapagliflozin 1µM and 5µM). EHTs were measured in isometric conditions at 37°C in the Krebs-Henselheit solution with 4mM of [Ca^{2+}] under imposed pacing. One-way analysis of variance (ANOVA) with a Tukey post-hoc test was used to compare the different time points. * $p < 0.05$ and ** $p < 0.01$. (N=3).*

4.6 Simultaneous measurements of action potential and calcium transient by fluorescent recordings

During each cardiac cycle, action potential (AP) leads the modifications that occur in transmembrane electrical potential in cardiomyocytes, depending on time- or voltage-dependent changes in several channels, exchangers or pumps. After isometric measurements, on the same EHTs we performed simultaneous acquisition of AP and Ca^{2+} transient, through a confocal microscope. To evaluate the electrophysiological characteristics of AP in relation to pathological modification that occur in dilated cardiomyopathy associated to Duchenne Muscular Dystrophy, at later stage of maturation (day 60) we incubated each EHTs with two specific fluorescent dyes targeting membrane voltage and calcium (Fluovolt and Cal630, respectively).

Preliminary data of confocal acquisitions of AP and calcium transient kinetics showed no significant differences in DMD-EHTs, in comparison to control (Figure 57).

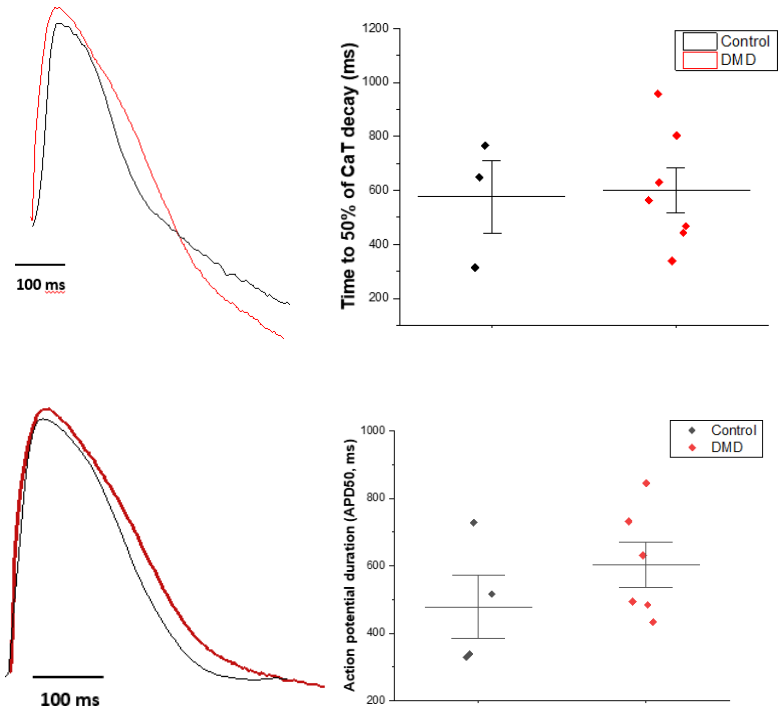

***Figure 57**. Simultaneous recording of action potential 50% (action potential duration, APD50, ms) and calcium transient kinetics (time to 50% of CaT decay, ms). Measurements were performed at 37°C, in Tyrode solution supplemented with blebbistatin (10 µM) (control N=3; DMD=7).*

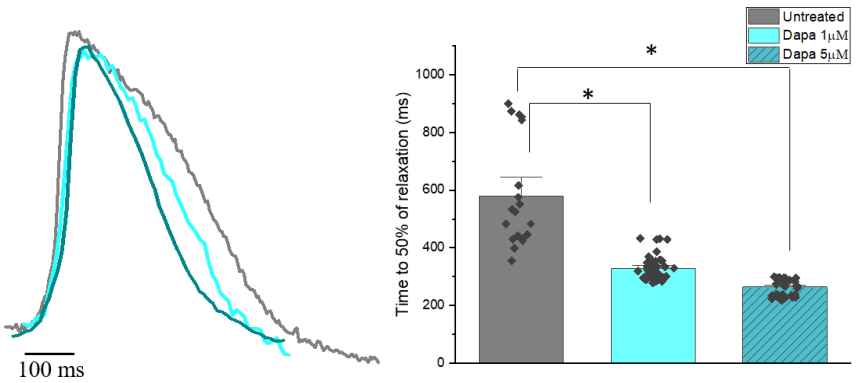

***Figure 58**. Measurements of action potential kinetics after acute treatment with Dapagliflozin (1 and 5 µM). Time to 50% of relaxation (ms) recorded on DMD-EHTs treated compared to untreated. Measurements were performed at 37°C, in Tyrode solution supplemented with blebbistatin (10 µM) (untreated N=4 n=23; Dapa 1 µM N=1 n=42; Dapa 5 µM N=2 n=42).*

4.7 Induced pluripotent stem cells derived skeletal muscles as model to study skeletal muscle disease in Duchenne Muscular Dystrophy

The absence of dystrophin in Duchenne Muscular Dystrophy (DMD) leads to the onset of membrane fragility in muscle fibres, culminating with muscle damage, muscle weakness and cellular death. In DMD, muscle regeneration is compromised due to the degeneration of myocytes associated with the depletion of satellite cells pool (Lu et al., 2014). In fact, loss of dystrophin results into an alteration of polarity and abnormal differentiation of satellite cells (Dumont et al., 2015), leading to an impairment of the capacity to replace muscle fibres and to the substitution of healthy tissue with fibrotic tissue (Alvarez et al., 2002).

Skeletal myogenesis occurs early during the first stage of embryonic development, after gastrulation, and continues in mammals, until the end of postnatal growth. The transition from muscle precursor to multinucleated muscle fibres is associated with a significant change in the synthesis and accumulation of specific proteins. During the specification phase, intra- and extracellular events progressively restrict the fate of mesodermal cells, increasing their capability to respond to paracrine signals. Initially, specific paracrine factors induce myoblasts to synthesize proteins that lead the formation of muscle fibres, including MyoD (Maroto M. et al., 1997). As long as growth factors are present, especially FGFs, myoblasts are able to proliferate without differentiation (Buckingham and Rigby, 2014). Instead, when FGFs are exhausted, the myoblasts exit the cell cycle, and proliferation ends. During differentiation, the second phase of skeletal muscle formation, an increase of synthesis of myofibrillary proteins is observed, including skeletal muscle actin, heavy and light chains of myosin, muscle isoforms of tropomyosin and troponin. In addition, activity of intracellular enzymes increases, such as muscle creatine phosphokinase and glycogen phosphorylase, de novo synthesis of acetylcholinesterase and acetylcholine receptor.

The final stage is the fusion of myoblasts in myotubes, in which myoblasts get longer and metabolic modifications occur. before melting, myoblasts lengthen and undergo metabolic changes, including an increase in the number of mitochondria and sarcoplasmic reticulum development. When myoblasts become able to melt, another myogenic protein, myogenin, becomes active; in addition, MyoD and Myf5 act in specifying muscle cells, while myogenin acts on the differentiation. When myoblasts enter the differentiating pathway, indicated by the activation of myogenin and the irreversible arrest of the cell cycle, phenotypic differentiation begins, indicated by the synthesis of contractile proteins such as the heavy chain of myosin

(MHC) and the formation of the syncytial myotube. Then, during the final stage of myogenesis the maturation of the muscle fibre occurs and the myotubes become excitable and able to contract spontaneously. Finally, muscle fibres acquire acetylcholine (Ach) sensitivity through the expression of the specific receptor (AchR). In more detail, AchR appears early in myogenesis: it is present in myoblasts in small quantities and strongly increase during maturation. In fact, Ach is a specific neurotransmitter of skeletal muscle cell, resulting in the activation of all biochemical and metabolic changes that lead to muscle contraction.

To study the role of the absence of dystrophin on the skeletal muscle development, induced pluripotent stem cells represent a valid tool, for their capability to differentiate into any cell type. In fact, human pluripotent stem cell-derived muscle models show great potential for translational research, displaying structural and functional properties of native human tissue and allowing disease modelling and drug screening. HiPSCs can be differentiated towards skeletal muscle, as shown previously. Compared with other techniques, the recapitulation of skeletal muscle development in vitro with various molecules allow hiPSCs to differentiate into skeletal muscles, mimicking the process of in vivo development. In particular, starting from undifferentiated pluripotent stem cells (indicating as day 0), we use a differentiation protocol on monolayer to lead to the activation of undifferentiated stem-cell precursors, bringing them towards the state of activated satellite cells, characterized by the expression of the typical marker for this phenotype (PAX7+). Subsequently, satellite cells were committed toward myoblasts, the embryonic muscle cells from which the muscle fibres derive. Subsequently, myoblasts combine with each other to form elongated multi-nucleate structures called myotubes. To assess the expression of specific skeletal muscle proteins, characteristic of each phase of skeletal differentiation, that is, satellite cells, myoblasts and myotubes (Pax7, MyoD, MyoG and MHC, respectively), immunohistochemistry was performed at specific time points of the differentiation protocol. In particular, we used two hiPSC lines: a DMD line, reprogrammed from a patient affected by Duchenne muscular dystrophy (ΔExon 46-48, DMD1C11), compared with a control line, derived from a healthy donor (WTC11). In addition, to evaluate how dystrophin mutations can affect skeletal muscle cells function, around day 30 of differentiation, myotubes were subjected to calcium transient evaluation. More in detail, cells were incubated with a specific fluorescent dye to evaluate intracellular calcium variation (Cal520) and subjected to acetylcholine-mediated activation and to its competitive antagonist hexamethonium. Cells were perfused continuously with Tyrode solution containing 1.8 mM of $CaCl_2$, at 37°C, supplemented with acetylcholine (10μM) or hexamethonium (1mM).

4.7.1 Evaluation of specific differentiation markers for immunofluorescence staining of skeletal cells muscles

Evaluation of Pax7 expression in Duchenne skeletal and control muscle precursors. Skeletal regeneration is attributed to satellite cells, muscular stem cells located below the basal lamina of each muscular fibre, characterized by the high expression of the transcription factor Pax7. In particular, skeletal precursors were fixed in 4% Parafolmaldehyde (PFA) at day 10 post differentiation (p.d.) and marked for Pax7, to assess the level of expression of this specific marker of the early stage of differentiation (Figure 59).

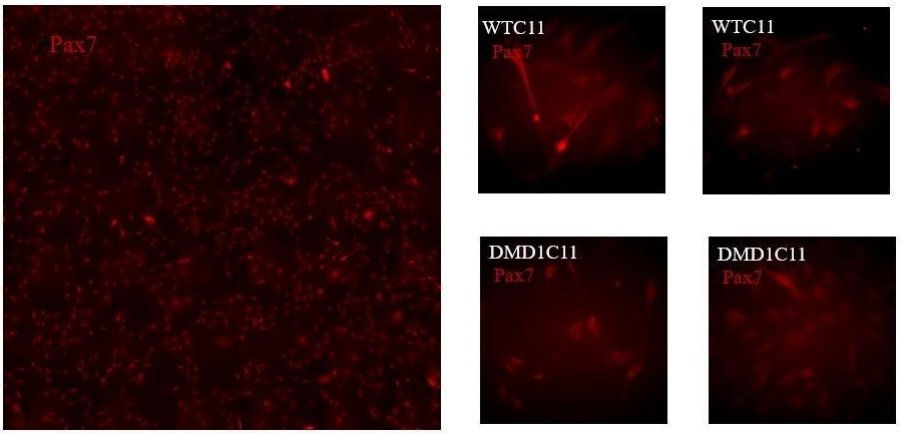

Figure 59. *Myogenic precursors differentiated from induced pluripotent stem cells (DMD1C11 and WTC11) Pax7+.*

Evaluation of MyoD and MyoG expression in Duchenne myoblasts and control. To investigate the obtainment of myoblasts from skeletal precursors, we performed immunostaining for MyoD and MyoG, two specific transcriptional factors of the second stage of skeletal muscle differentiation (Figure 60).

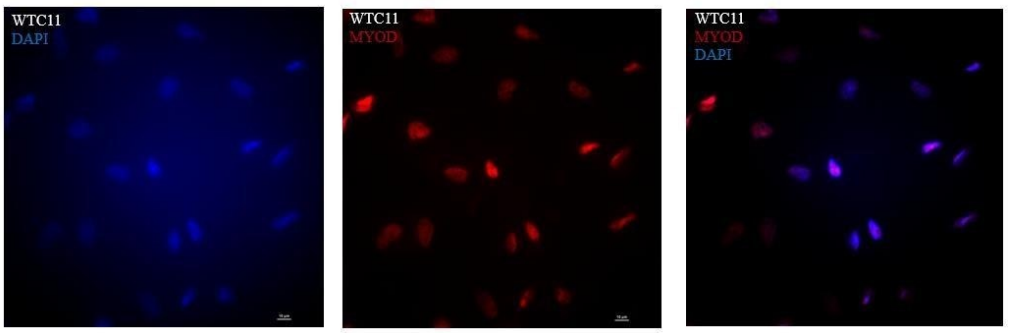

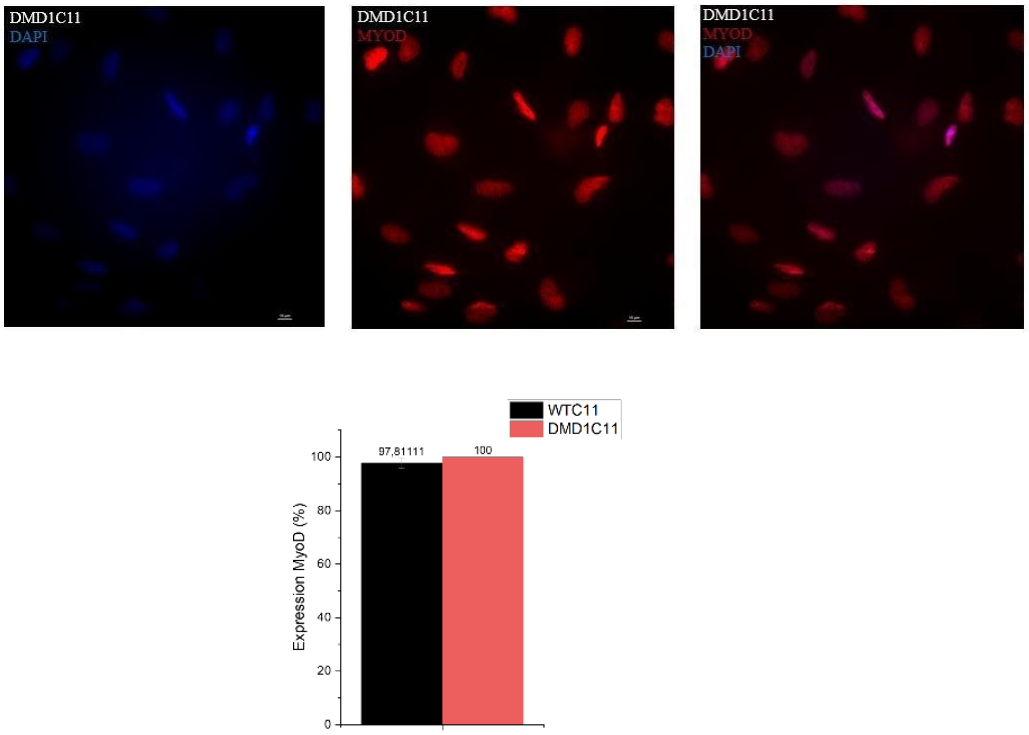

Figure 60. *Differentiated myoblasts from induced DMD1C11 pluripotent stem cells and positive control for MyoD and, at day 20 post differentiation.*

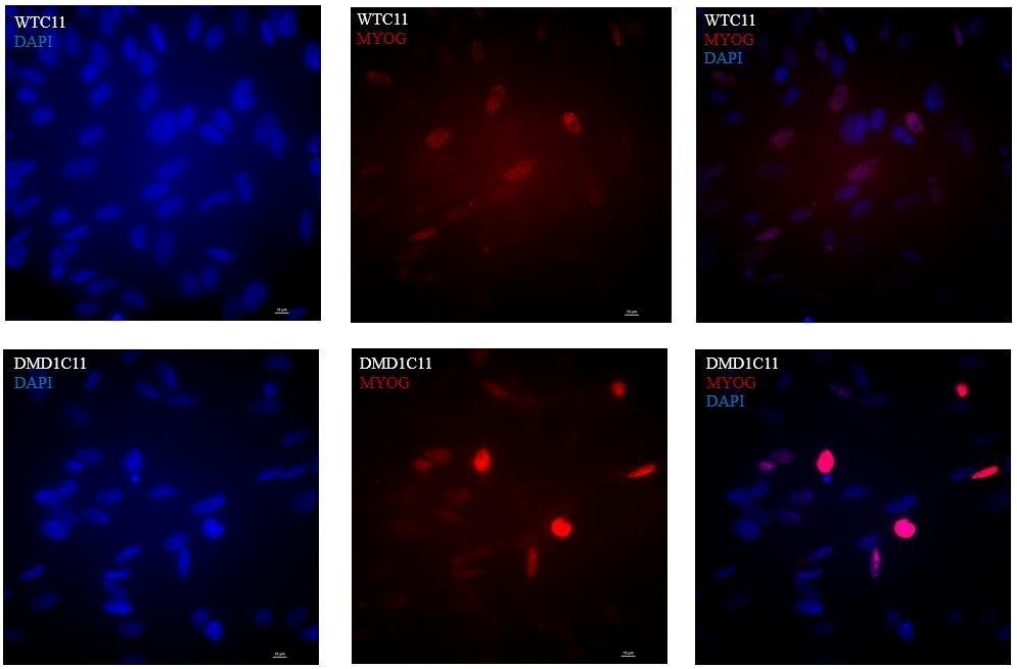

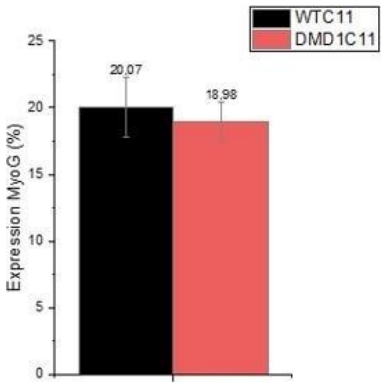

Figure 61. *Immunofluorescent evaluation of early skeletal muscle differentiation markers (MyoG, MyoD) in DMD-hiPSCs-skeletal muscle compared to control.*

Evaluation of MHC expression in Duchenne myoblasts and control

In the last stage of skeletal muscular cells differentiation, elongated myotubes were obtained from both lines tested (DMD vs Control). To investigate the efficiency of maturation, we marked the skeletal muscular cells with an antibody targeting myosin heavy chain (MHC) (Figure 62). Immunostaining investigation showed an increase of cells amount expressed MHC in DMD-line compared to control.

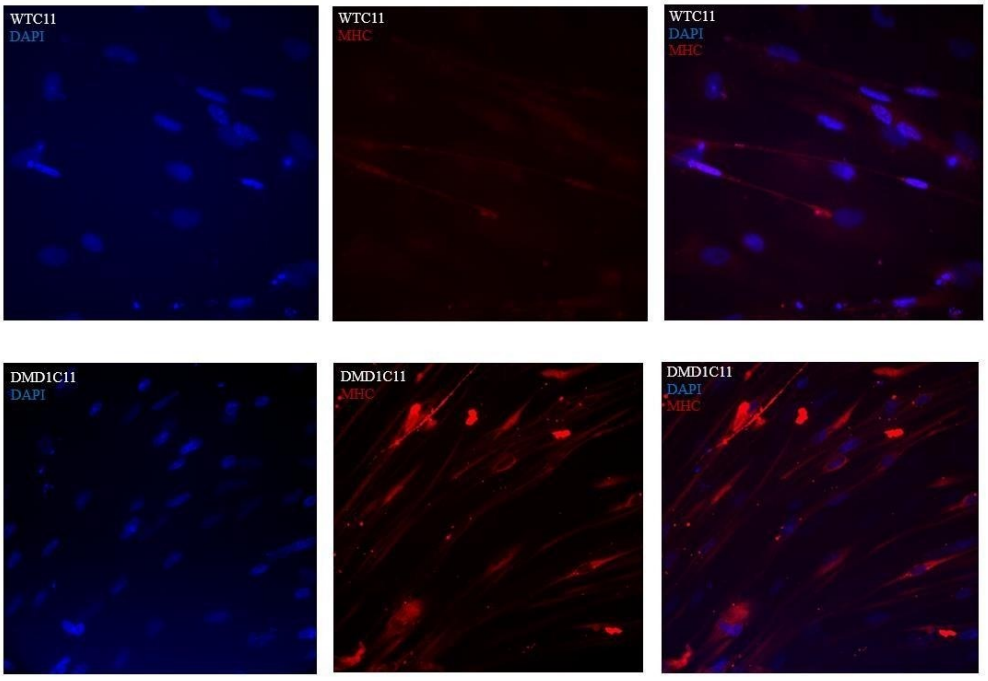

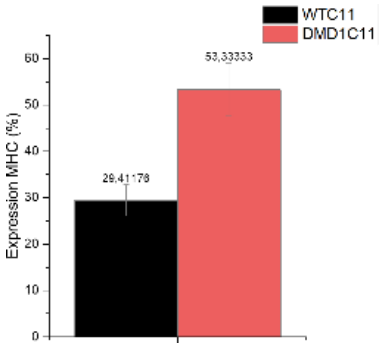

Figure 62. *Differentiated myoblasts from induced DMD1C11 pluripotent stem cells and positive control for MHC at day 28 post differentiation.*

4.7.2 Calcium transient measurements of DMD-myotubes and control

In addition, to evaluate how dystrophin mutations can affect skeletal muscle cells functionality, around day 30 of differentiation, myotubes were subjected to calcium transient evaluation. More in detail, cells were incubated with a specific fluorescent dye to evaluate intracellular calcium variation (Cal520) and subjected to acetylcholine activation and its competitive antagonist hexamethonium. Cells were perfused in continue with TYRODE solution with 1.8 mM of $CaCl_2$, at 37°C, supplemented with acetylcoline (10µM) or hexamentonium (1mM).

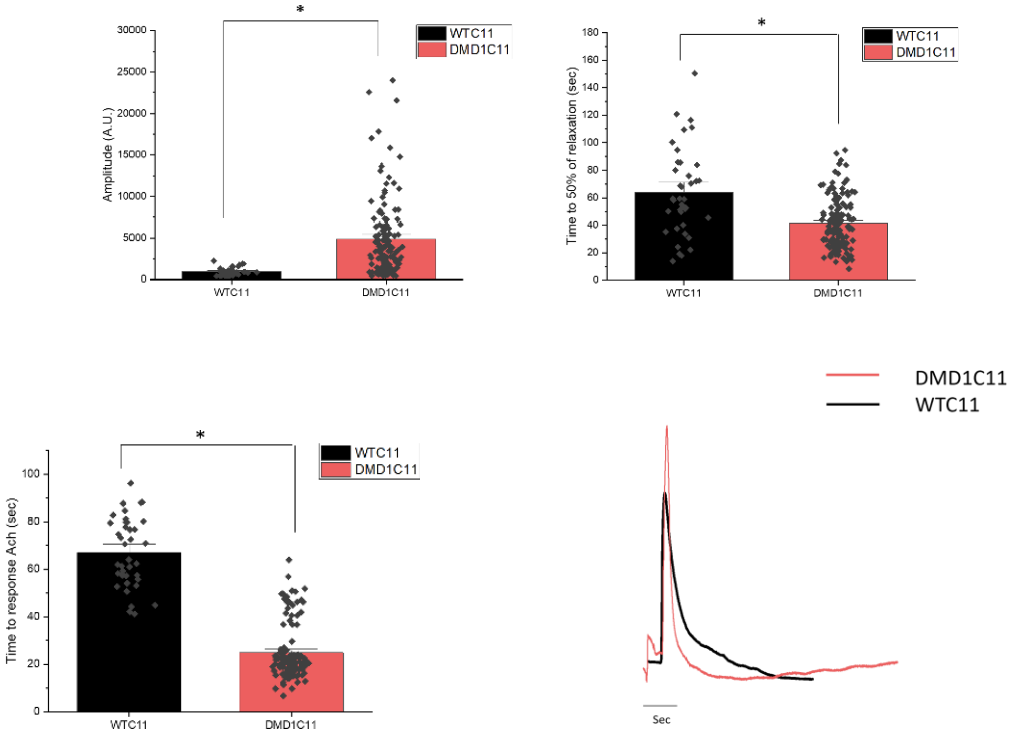

Figure 63. *Electrophysiological evaluation of DMD line, compared to control. Calcium transient evaluation to acetylcholine stimulation of induced pluripotent stem cells derived myotubes (DMD1C11 vs WTC11) (day 30 p.d.). Measurements of amplitude and calcium transient kinetics (time to 50% of relaxation). Representative traces of calcium transient of DMD1C11 and control line. 37°C, Tyrode solution, [Ca^{2+}] 1.8mM. One-way analysis of variance (ANOVA) with a Tukey post-hoc test was used to compare the different time points. * $p < 0.05$ and ** $p < 0.01$.*

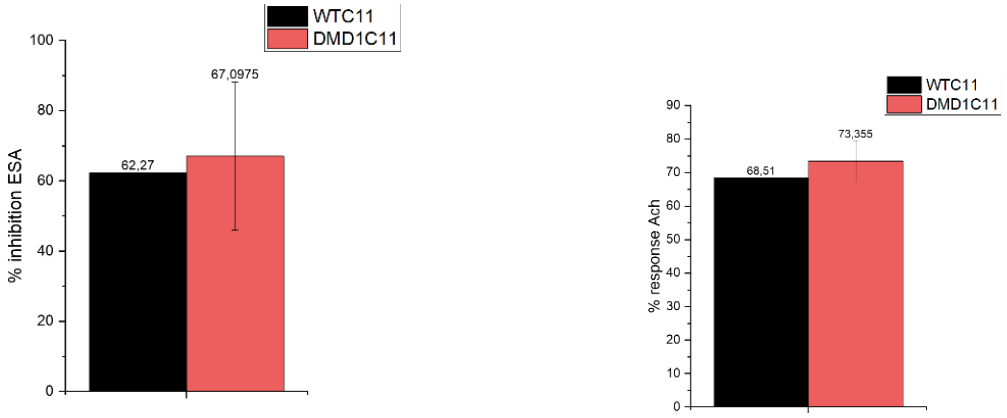

Figure 64. *Evaluation of percentage of inhibition to examentonium (%) and percentage of response to acetylcholine (%) of DMD1C11 line and control. 37°C, Tyrode solution, [Ca^{2+}] 1.8mM. One-way analysis of variance (ANOVA) with a Tukey post-hoc test was used to compare the different time points. * $p < 0.05$ and ** $p < 0.01$.*

4.7.3 Morphological evaluation

Evaluation of morphological characteristics has been used in the past to identify pathological cell populations, test compound or study disease mechanisms (Scheeder et al., 2018; Ziegler et al., 2021). Besides dystrophin mutations represent the main cause of DMD, other pathological factors, including inflammation and impaired regeneration are involved. In particular, the lack of dystrophin leads to mechanical stress, causing an increase in Ca^{2+} intracellular concentration and, consequently, alteration of calcium handling and the structure of sarcolemma (Petrof, B.J. et al., 1993). Fibre size variation is one of the most prominent features in dystrophic muscles. Studies performed on mdx-mouse fibres, provide evidence that, during the first 4 weeks, fibres tended to be smaller and show branching that is not observed in control fibres (Duddy V. et al., 2015).

To investigate changes that occur in morphological features of skeletal muscle fibres during DMD pathogenesis, mature myotubes were visualized on a confocal microscope after staining

with the membrane dye Anneps (in red). Measurements were performed using a software (NIS Element AR Software). More in detail, myotubes differentiated from induced pluripotent stem cells mutated (Δ exons 46-48, DMD1C11) and control (WTC11), at day 28 post-differentiation, were marked with a fluorescent membrane dye (ANEPPS) and displayed to a confocal microscope for morphology and cell size assessments. Our result showed morphological changes in DMD lines compared to control, resulting in increased degree of branching in DMD myotubes, at the same day of maturation (day 30 p.d.) (Figure 65).

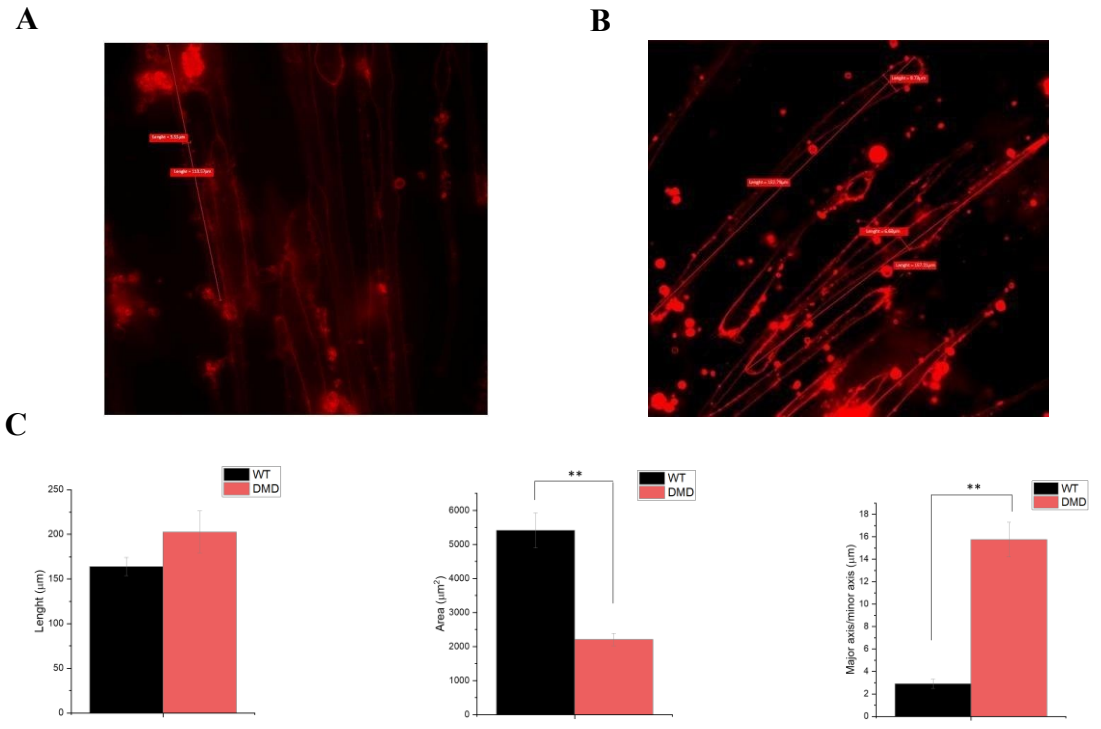

Figure 65. Morphological evaluation of DMD-hiPSC-CMs compared to control line. A) *Representative image of ANNEPS-marked myotubes derived from control line;* ***B)*** *Representative image of ANNEPS-marked myotubes derived from DMD patient.* ***C)*** *Measurements of cardiomyocytes length (µm), area (µm²) and major axis-minor axis ratio, to evaluate the eventual morphological changes that occur in the pathogenesis of DCM associated to DMD. Later-stage of skeletal muscle maturation (day 30 post differentiation, p.d.).*

Chapter 5

Discussion

5.1 Modelling hypertrophic cardiomyopathy using Engineered Heart Tissues (EHTs)

Mutations occurring in MYBPC3 gene are the leading cause of hypertrophic cardiomyopathy (HCM), characterized by left ventricular hypertrophy and hyperdynamic contraction (B. J. Maron 2002, 2004). One of the most dangerous manifestations of HCM is represented by ventricular arrhythmias, that potentially lead to sudden cardiac death (SCD). Several lines of evidence suggest that these electrophysiological alterations depend on functional modifications occurring at the level of cardiomyocytes. The identification of specific cellular target could help to mitigate the progression of HCM, relieve the severity of symptoms and allow personalized therapy. To date, pharmacological treatment for HCM includes the administration of negative inotropic or antiarrhythmic agents, such as non-dihydropyridine calcium channel blockers, disopyramide or β-blockers. In addition, molecular dysregulation associated to HCM-mutation may cause an important increase of energy consumption, leading to an alteration of the metabolic cost of contraction and the typical HCM hypercontractile phenotype. Therefore, the use of specific pharmacological agents targeting contractile proteins can be a valid strategy to normalize this pathological alteration. Recently, Mavacamten, an allosteric reversible myosin inhibitor, was approved by the FDA (Food and Drug Administration) for the treatment of patients with symptomatic obstructive hypertrophic cardiomyopathy (oHCM). Mavacamten modulates the number of myosin heads available for interaction with actin and reduces the probability of cross-bridge formation. Previous findings have demonstrated that Mavacamten can ameliorate the dynamic left ventricular outflow tract (LVOT) obstruction, improve cardiac filling pressure and reduce exertional symptoms in obstructive patients (placebo-controlled phase III EXPLORER-HCM clinical trial, Olivotto I. at al., 2020). Electrophysiological measurements in HCM cardiomyocytes highlighted the occurrence of calcium handling impairment. In fact, calcium concentration increases as a consequence of mutations occurring in sarcomere proteins, likely representing the first pathological modification that occur in HCM myocardium (Coppini R. et al., 2018). In fact, the majority of HCM mutations determine an increase of myofilament calcium sensitivity, resulting in an increase of ATP consumption (Ashrafian et al., 2011). More in detail, the increase of myofilament calcium sensitivity leads to a slower release of calcium from troponin C, prolonging the decay of calcium transients and determining an increased diastolic intracellular calcium (Baudenbacher et al., 2008). Moreover, due to the ATP depletion caused by the inefficient sarcomeres, there is a reduction of the sarcoplasmic reticulum Ca^{2+} ATPase (SERCA) activity (Ashrafian et al., 2003), aggravating

Ca-overload. In addition, HCM cardiomyocytes show abnormalities in action potential duration (APD) and ion current in association with the aforementioned alterations of intracellular calcium handling (Coppini et al., 2013; Ferrantini et al., 2018).

In several studies, researchers have previously investigated the effect of Mavacamten in vitro by using hiPSC-CMs (Halas et al. 2022; Sewanan, Shen, and Campbell 2021). In this study, to understand the mechanism whereby Mavacamten acts for the prevention of upstream arrhythmogenic substrates, we used patient-specific hiPSC-CMs that can recapitulate mechanisms associated to the pre-hypertrophic stages of the disease. More in detail, EHTs were generated starting from hiPSC lines derived from an HCM patient carrying a MYBPC3:c.772G>A mutation, and were analysed in comparison with the isogenic CRISPR-Cas9 isogenic control line (c.ID3) (Pioner JM et al. 2023). EHTs were maintained in culture until day 50 post cardiac induction and measured in isometric conditions, through a force-length recording apparatus, under field stimulation at different frequencies. To investigate the effect of chronic treatment with Mavacamten, we tested HCM-EHTs (ID3 and c.ID3) exposed to two different drug concentrations (0.3 μM and 0.75 μM), compared with DMSO treatment as control.

Initially, we tested the effect of Mavacamten during EHT maturation. The exposure of Mava in the culture medium for 30 days led to a partial contractile force reduction at 0.3 μM and a complete abolishment of spontaneous twitches at 0.75 μM. However, at the later stage of maturation, Mavacamten was washed-out from culture medium for a few days, resulting in an increase of the spontaneous force produced by the EHTs. In addition, in isometric conditions, mutant EHTs and control showed a lower active tension compared to untreated EHTs, likely caused from an impairment of maturation due the reduction of contractility, as a result of prolonged Mavacamten effect. In addition, the hastening of contraction kinetics observed between treated and untreated EHTs could indicate an effect of drug on calcium handling in addition to its effects on cross-bridge formation.

5.2 R403Q mutation: mechanical alterations of myosin motility in hypertrophic cardiomyopathy

The first identified mutation associated to hypertrophic cardiomyopathy (HCM) resulted in a point mutation of arginine to glutamine (R403Q) in the human β-myosin heavy chain (MHC), causing a particularly malignant form of HCM (Geisterfer-Lowrance AA, et al., 1990). Previous studies performed on R403Q myosin, isolated from biopsies of patients, highlighted a strong

decrease in myosin motor function, supporting the idea that LV hypertrophy in HCM is a compensatory response of the myocardium to specific pathological triggers. Researchers showed controversial results while studying cardiomyocyte shortening and while performing in vitro motility assays using samples from different R403Q models. In fact, a mouse transgenic line carrying the R403Q mutation in α-MHC showed an increase of ATPase activity and actin motility at IVMAs. However, the β-isoform is predominant in large mammals and the two isoforms have very different kinetic behaviour, so additional investigations are needed. In particular, Lowey and colleagues have reported a significant reduction in sliding actin motility on beta-myosin isolated from R403Q rabbits and single R403Q myofibrils showed diminished force kinetics and force (Lowey S. et al., 2018). Overall, this evidence led to the hypothesis that this loss-of-function is likely the cause triggering the occurrence of cardiac hypertrophy. On the other hand, different studies highlighted a 30-40% of increase in actin filament velocity in R403Q-β myosin, compared to controls. Considering these conflicting results, we investigated the mechanical features of R403Q mutation using induced pluripotent stem cells derived cardiomyocytes (hiPSC-CMs), carrying R403Q mutation in heterozygosis (Het-hiPSC-CMs) and homozygosis (Homo-hiPSC-CMs), compared to control. We evaluated cardiomyocyte contractility, in term of shortening and calcium transient amplitude and kinetics, using the calcium fluorescent dye FURA-2, under field stimulation at different frequencies and at different calcium concentration. Considering contractile function analysis, the "IonOptix" technique allowed us to record cell- shortening via edge detection using a microscope camera.

Our results showed a reduction in shortening (%) in both mutated lines compared to controls, associated with no significant differences in twitch kinetics. Moreover, since alterations in calcium handling represent the main cause contributing to mechanical dysfunction in HCM failing hearts, we performed calcium transient measurements using fluorescent calcium dyes, while varying the extracellular calcium concentration. In fact, at low frequencies of stimulation (0.5 Hz), we highlighted an increase in the percentage of shortening in all lines tested (Het, Homo, ctrl), especially during the switch from low to high calcium concentration (from 0.5 mM to 1.8 mM). In addition, despite cardiomyocytes from the control and the Homo lines increase in shortening % while increasing external [Ca] in the mutant heterozygous line no significant increment was observed. Instead, at high stimulation rates of stimulation, the homozygous line shows an increased shortening % compared to the other lines tested. In fact, although the HCM-mutation affects mainly the sarcomere proteins, it is possible that the pathological phenotypes observed are determined by secondary effects on calcium handling in R403Q cardiomyocytes. Moreover, the use of single cardiomyocytes plated on specific PDMS substrates, as previously

described, allowed us to evaluate the effects of the R403Q mutation on calcium handling. The evaluation of R403Q cardiomyocytes calcium transient was performed using FURA-2, under field stimulation. In the mutated lines (Het and Homo-hiPSC-CMs), calcium transient kinetics was slower in comparison to controls, especially at low stimulation rates (0.5 and 1 Hz). Also, calcium transient amplitude is decreased in mutated cardiomyocytes compared to the control line. The degree of Ca^{2+} reuptake into the sarcoplasmic reticulum greatly affects cardiomyocytes relaxation kinetics. Therefore, the delayed transient decay kinetics exhibited by both mutated lines, can reflect a delayed rate of calcium reuptake into SR. Moreover, the reduction of calcium amplitude occurring in the R403Q mutation in heterozygosis and homozygosis suggests a reduction in the amount of calcium mobilized during cardiomyocyte contraction. Overall, these observations are all consistent with important calcium handling defects caused by the R403Q mutation, resulting in diastolic dysfunction, commonly associated with hypertrophic cardiomyopathy.

Previous studies investigating the function of β-MHC of R403Q cardiomyocytes and control suggested that mutated myosin act as a "poison protein", resulting in sarcomere disarray that led to the onset of a compensatory cardiac hypertrophy (Straceski et al., 1994; Marian et al., 1995). The functional impact of R403Q mutation has been examined in different models, including myosin backbones (Sweeney et al., 1994), smooth muscle (Yamashita et al., 2000) and human cardiac biopsies or antibody-purified proteins from slow-skeletal muscle biopsies (Cuda et al., 1993). These studies suggest that significant myosin dysfunctions are the main cause of this pathological process; these include a decrease in the actin-binding as measured with the actin-activated ATPase assay, decreased ATPase activity (Sweeney et al., 1994; Sata and Ikebe, 1996), decreased velocity of shortening and force/stiffness ratio (Lankford et al., 1995). At the molecular level, despite in vitro motility assay performed on R403Q have highlighted a reduction in actin filament velocity (Cuda et al., 1993, 1997; Sweeney et al., 1994), additional evidence showed an increase in actin filament velocity in R403Q mutants compared to controls, highlighting that the increase in the non-erratic movement of filaments is associated with the hypercontractility caused by myosin impairment. Indeed, an increase in the affinity of mutated myosin for actin is observed, leading to a greater resistance of actin filaments during the relaxation phase of contraction. Then, these pathological alterations may result in a functional disorder at the level of myosin-actin interface, resulting in myocardial diastolic dysfunction. In fact, these results support the hypothesis that R403Q mutation leads to a decrease in motor function of myosin, inducing the onset of hypertrophy as a compensatory pathological response.

5.3 Electrophysiological evaluation of surgical human samples derived from HCM and aortic stenosis patients

Pharmacological intervention of hypertrophic cardiomyopathy (HCM) is limited by the wide variety of symptoms, such as shortness of breath, chest pain, fatigue, heart failure and the onset of arrhythmic events that may culminate in sudden cardiac death (SCD). Moreover, HCM is characterized by several structural alteration, including left ventricular hypertrophy, myocardial fibrosis, ischemia, and abnormalities in functional cardiomyocytes profile. In particular, several electrophysiological alterations are associated to HCM, especially an increase of diastolic calcium, NCX pump alteration, a reduced expression of SERCA, prolongation of calcium transient decay and increase of CaMKII activity. The most common clinical interventions are focused on the symptoms mitigation and include angiotensin II receptor blockers, calcium inhibitors or β-blockers treatment. Recently, gliflozins, and more specifically Dapagliflozin, a sodium-glucose cotransporter-2 inhibitors (SGLT2-Is) have been indicated as a possible effective compound to treat HCM, showing to ameliorate the relative risk of atrial fibrillation, reducing heart failure (HF) and risk of hospitalization in HF patients (EMPEROR-Reduced trial). The specific mechanism of action through which Dapagliflozin may produce cardioprotective effects is still unclear, then we perform acute treatment on cardiomyocytes isolated from human surgical biopsies derived from HCM and aortic stenosis (AoS) patients, at two different concentrations (1 and 10 μM). Our results showed a reduction of action potential duration (APD) in both group of patients, more strongly in HCM, likely due to the higher degree of hypertrophy occurring in this disease that led marked changes in the myocardium electrophysiological profile. Moreover, the significative reduction in APD, observed in failure cardiomyocytes, underlies a probably effect of Dapagliflozin on late sodium current ($I_{Na\text{-}L}$), that result increased in the pathogenesis of HCM. In addition, this drug does not affect the initial phase of action potential and then the peak sodium current, that is crucial to the initial phase of action potential. In fact, the modulation of this specific current may lead the onset of lethal arrhythmic events, potentially bringing the patient to cardiac death. Despite other investigations are needed, these findings represent a step forward in understanding the mechanisms underlying the cardioprotective effects of gliflozins, that have already shown to induce clinical benefits not only in diabetic patients but also in non-diabetic patients suffering from heart failure.

5.4 Engineered heart tissue to modelling dilated cardiomyopathy associated to Duchenne muscular dystrophy

Cardiac and striated muscle are constantly subjected to a mechanical stress derived from cellular contraction. Full-length dystrophin (Dp427) is a fundamental component of a big network that covers the majority of the cytoplasmic surface of the plasma membrane, promoting membrane integrity and acting as shock absorber and favouring the direct transferring of mechanical force from the extracellular matrix to the cytoskeleton (Rahimov and Kunkel 2013). The direct consequences of the absence of dystrophin in cardiomyocytes are calcium handling alterations, with mechanisms that remain unclear. Two main hypothesis underlying calcium abnormalities in DMD have been proposed: membrane damage caused by an increase of phospholipid bilayer fragility (Carson et al. 2016) or altered ion channel function associated with the dysregulation of the dystrophin glycoprotein complex (DGC) (Zhan et al. 2014). Over the years, several research has been conducted on DMD animal models, such as the mdx mouse. Unfortunately, these models show important differences when compared with human patients, including different beating rate, electrophysiological and mechanical discrepancies. For these reasons, the development of cell reprogramming techniques and the consequent derivation of induced pluripotent stem cells (hiPSCs) represents a valuable tool to investigate genetic disorder. Due the fundamental role of dystrophin in cellular integrity, it is not surprising that its absence is associated with changes in the expression of different proteins and abnormal calcium handling caused by excessive and unregulated extracellular influx (Fong. P. Y. et al., 1990). Moreover, other authors have investigated the molecular features of excitation-contraction coupling (ECC) in DMD hiPSC-CMs (Jelinkova S. et al., 2020), finding a lower differentiation efficiency in DMD cardiomyocytes and lower rates of calcium transient rise/decay, supporting the idea that dystrophin deficiency causes ECC abnormalities via calcium handling alterations. In addition, Pesl and colleagues found a weaker contraction force in DMD hiPSC-CMs in comparison to control (Pesl M. et al., 2014).

In this study, we performed a basal characterization of a patient specific DMD line (Δ exon 50) (Pioner et al. 2020), compared to control, exploring the differences occurring during maturation in both lines related to changes in substrates stiffness. In particular, we tested the electrophysiological activity of mutated and control lines, in term of calcium transient and action potential evaluation. Recent studies provide evidence of a lower level of actin cytoskeleton turnover, when cardiomyocytes are grown on micropatterned substrates (Macadangdang et al. 2015). Moreover, previous findings reported that the lack of full-length dystrophin determines a reduction of Ca-T kinetics with an important contractility impairment

(Pioner et al., 2019). In this study, the electro-mechanical evaluation of mature DMD hiPSC-CMs evidenced the occurrence of contractile cardiac dysfunction. In fact, calcium transient evaluation was performed at different time points of maturation (60, 75, 90 days post cardiac differentiation) on two custom-made substrates with different stiffness, i.e. PEG and DEG micropatterned surfaces. DMD-line grown on PEG substrates showed lower calcium amplitude and a reduction of post-rest potentiation, in comparison to controls, highlighting a reduced amount of calcium stored into the sarcoplasmic reticulum (SR). Moreover, the same results were confirmed through the caffein-evoked Ca-T, highlighting a significant reduction in SR-calcium content, compared to controls. Also, previous studies have demonstrated an impairment of calcium release via the RyR in DMD disease (Fauconnier et al. 2010; Bellinger et al. 2009. We identified an increased CAMKII activity and phosphorylation state of RyR at phosphor-site S2814 in the mutated line, linked to a higher RyR open probability and, as a consequence, to increased diastolic calcium leakage from the SR (Meyer et al. 2021). Moreover, several studies highlighted that the expression profile of β1 and 2 -adrenergic receptors (AR) in hiPSC-CMs have a strong time-dependent increase (G. Jung et al. 2016). In fact, we tested β-adrenergic pathway in DMD-hiPSC-CMs, using forskolin (FSK), an adenylylcyclase activator, to minimize issues related to different AR expression or reduced AMPc levelsdue the activity of phosphodiesterases (PDEs) (Giannetti et al. 2021) and to investigate the downstream pathway. Our results show that forskolin can increase the calcium transient amplitude in both lines tested (DMD and control), indicating a preserved positive ionotropic mechanism. In addition, the preserved phosphorylation at RyR S2808 site confirmed no alterations of PKA targets.

To evaluate the electrophysiological features associated to DMD-related cardiomyopathy, we incubated cells with a combination of a voltage-sensitive and a calcium fluorescent dye, performing simultaneous recordings of action potentials (AP) and calcium transients. We observed a similar AP profile in the DMD line compared to controls. Moreover, at later stages of maturation, both lines showed a longer plateau phase, compared to early stages. These findings confirm previous observations showing no electrophysiological abnormalities of action potentials in the DMD disease (Jelinkova et al. 2020). Instead, calcium transient evaluation highlights a faster Ca-T decay in the DMD line at day 90, compared to control, reflecting an alteration of calcium recovery mechanisms. In addition, control line shows a gradual increase of Ca-T amplitude during maturation; in DMD cardiomyocytes, however, no significant changes of ca-transient amplitude occur at day 90, suggesting an impairment of

systolic calcium release. Overall, these results could be explained by a poor maturation of SR in the DMD line that can lead to a reduction of calcium storage, causing the absence of Ca-T increase during maturation.

In addition, cardiomyocytes cultivated on stiffer nanopatterned substrates (100% DEG-DA) show functional differences in comparison to those grown on compliant surfaces (PEG-DA). In particular, with the increase of substrates stiffness, we observed a significant increase of Ca-T amplitude in the control line, associated with a smaller increase in mutated cardiomyocytes in the same conditions. Caffeine-induced Ca-T, on stiffer substrates, became slower in DMD line compared to control, indicating a possible reduction in the extrusion of calcium in mutated cardiomyocytes. These results could be explained by a reduction in the function of the NCX exchanger, associated with an increase of RyR open probability, leading to the increase of intracellular calcium levels that can induce the onset of dangerous cellular arrhythmias in DMD cardiomyocytes.

Overall, these results confirm that calcium handling dysregulation is one of the main mechanisms underlying DMD cardiomyocytes impairment, occurring during maturation. Moreover, the stiffness of extracellular matrix (EMC) determines cellular activity, and cardiac tissue regulation, promoting proliferation, migration or differentiation (Engler et al. 2006; Carson et al., 2016). Cellular adhesion of cardiomyocytes to ECM is largely mediated by integrins, linked to the dystroglycan complex, connecting cytoskeleton to the extracellular environmental. Although the pathogenesis of DMD dilated cardiomyopathy is still not fully understood, several studies support the idea that the absence of dystrophin leads to the disruption of the dystroglycan complex, inducing sarcolemma damage in DMD cardiomyocytes. As a consequence, the resulting membrane fragility may lead to adaptative mechanisms, including inflammatory response and cardiomyocyte death, ultimately leading to the progressive substitution of healthy cardiac tissue with fibrotic tissue. This pathological remodelling causes an increase of extracellular matrix stiffness, leading to a further loss of force, owing to the scarce adaptability of DMD cells to changing substrate stiffness. In fact, our results highlight a reduced capacity to induce an efficient calcium extrusion, leading to a potential impairment in the adaptation of DMD cardiomyocytes to changes of matrix stiffness.

Moreover, electrophysiological evaluation of DMD cardiomyocytes compared to control showed that cell maturation is strongly influenced by the extracellular environmental. In particular, substrates with low and high stiffness can provide different levels of external stimuli,

influencing the force of contraction (Querceto et al. 2022). Despite the great potential of nanopatterned surfaces, in vitro models that more closely mimic the physiological features of native cardiac tissue are needed. To date, to evaluate the mechanical properties of mutated cardiomyocytes in relation to changes occurring in extracellular matrix, several 3D models have been developed, including cardiac spheroids, microtissues and cardiac chambers or rings (Beauchamp et al., 2015; Shum et al., 2017; Thavandiran et al., 2020; Tiburcy et al., 2014; Williams et al., 2020). In this context, engineered heart tissues (EHTs) may replicate the ECM characteristics, with different stiffness degrees, and greatly increase maturation of hiPSC-CMs in vitro. In fact, cardiomyocytes were incorporated into a 3D scaffold of fibrin and the tension exerted from pillars on the contraction of growing tissue led to an increase of cellular maturation properties. Moreover, several studies provide evidence that EHTs induce cardiomyocytes alignment and a physiological distribution of cells into the tissue, replicating the composition of native cardiac tissue. Therefore, we generated engineered heart tissues from different hiPSC lines (Δ exons 46-48, Δ exon 50, Δ exon 51) and we kept them in culture until later stages of maturation (day 60). Auxotonic measurements through the detection of flexible pillars movement were performed at specific time points of EHTs maturation (days 25-30-35-40-45-50), allowing the investigation of cardiomyocytes maturation degree, in term of spontaneous beating frequency and tension exerted during in vitro maturation. Control hiPSC-CMs highlight a gradual reduction in spontaneous beating frequencies from early (day 25) to later (day 50) stages of maturation; however, DMD-EHTs does not show any significant decrease of spontaneous beating. In addition, active tension is significant increased during maturation in the control line, but in DMD cardiomyocytes this increase does not occur, underlying a possible cardiac developmental impairment in DMD cardiomyocytes. Moreover, all the DMD lines tested show an important reduction of active tension in isometric condition compared to control, confirming the occurrence of ECC alterations in dystrophin deficient cardiomyocytes.

The inability to handle mechanical stress exerted during contraction is a direct consequence of the absence of the “absorber” protein dystrophin, showing a reduced compliance and an increase in the susceptibility of myocytes to stretch-mediated calcium overload, inducing cellular death (Yasuda S. et al., 2005). Improving membrane stability is a possible therapeutic approach to DMD treatment. In fact, poloxamer 188 (P188) is a compound that is known to stabilize cell membrane (Ballas S. K. et al., 2004). Indeed, it is a non-ionic triblock co-polymer capable of inserting into phospholipid monolayers, resulting in repair damaged membrane. Based on these properties, we performed a long-term treatment with P188 on DMD-EHTs, for

20 days in culture (1 mg/ml). During chronic administration, measurements of auxotonic contraction show an increment of tension in DMD-EHTs treated, compared to untreated. Moreover, the exerted tension is maintained at high levels also at later stages of maturation. We also performed isometric recordings of force contraction in isometric conditions in DMD-EHTs treated with P188, compared to untreated muscles. Our results confirm that the chronic treatment with P188 led an increase of active tension, in comparison with the basal condition, at each calcium concentration tested (0.5 mM, 1.8 mM, 4 mM).

In conclusion, the effects of full-length dystrophin deficiency appear in the early phases of cardiac development and likely before cardiac tissue formation (Jelinkova et al. 2019). Cardiovascular symptoms, including ventricular arrhythmias, conduction abnormalities, fibrosis and fatty replacement of cardiac tissue may strongly impact the quality of life of patients affected by DMD. In addition, the cellular death caused by mutations in the dystrophin gene lead to the typical muscle weakness characterizing DMD patients. In this context, our strategy using cardiomyocytes differentiated from DMD-hiPSCs allowed us to investigate the adaptative alterations that occur in cardiomyocytes during the very early stages of development.

5.5 Induced pluripotent stem cells derived skeletal muscles as model to study skeletal muscle disease in Duchenne Muscular Dystrophy

Several studies have demonstrated the occurrence of a persistent increase of intracellular calcium concentration in skeletal muscle from DMD models undergoing mechanical stress. In fact, Jockusch and colleagues have highlighted a lower stress resistance in DMD and mdx myotubes, compared to control, associated to a dramatic calcium content increase (Menke A. et al., 1995) (Hopf F.W. Et al., 1996). To investigate potential differences occurring in calcium handling in DMD skeletal myocytes compared to control, we performed calcium fluorescent evaluation used a DMD-hiPSC line obtained from a patient carrying a mutation in DMD gene, resulting in the total absence of dystrophin (Δexon 46-48). The stimulation was provided via acetylcholine administration and measurements were performed at later stage of myotubes maturation (day 30 p.d.). Our results showed a significant increase of calcium transient amplitude in mutated myotubes compared to control, highlighting a potential connection between the calcium overload occurring in DMD myocytes and the absence of dystrophin. Moreover, calcium transient kinetics, in term of time to 50% of relaxation phase, is accelerated in DMD myotubes, compared to control. Overall, these pathological modifications may lead a global alteration in the contraction machinery of myocytes, as result of the increase of mechanical stress and the consequent changes of the E-C coupling machinery. Also, time to

response to acetylcholine (Ach) is an indicator of the maturation degree reached from hiPSC derived myotubes. The interaction between acetylcholine and its receptor causes an increase of sarcolemmal permeability to multiple ions, including sodium and potassium, leading to a partial membrane depolarization. Action potential is therefore generated and is quickly transferred inside the myocytes through T-tubules, resulting in the direct activation sarcoplasmic RyR through DHPR-voltage sensors and thus to a marked increase of cytosolic calcium concentration, triggering fiber contraction. The reduction of the time to response to Ach of DMD myotubes may be caused by a maturation impairment occurring in DMD skeletal muscle cells. In addition, morphological variation of skeletal muscle fibres is common in DMD myocytes. In particular, in accordance with previous studies (Duddy W. et al., 2015), DMD myocytes appeared more elongated and thinner at the same day of maturation, compared to controls. More in detail, morphological evaluations performed after staining with a fluorescent dye that interact with myocytes membrane (Anneps) highlighted an increase in cellular length and a reduction in area of DMD myotubes, associated with an increase of cellular ramifications (major axis/minor axis > 1) compared to the control cells, which instead appears more rounded. These modifications could be a direct consequence of the absence of dystrophin in DMD skeletal muscle cells, that may alter the structure of cellular membrane, through mechanisms that likely occur during myocyte maturation.

Chapter 6

Conclusions

In the last two decades, inherited cardiomyopathies are the major cause of mortality in young adult (Lee C.S. et al., 2014), representing the leading causes of heart disease in all age group. A novel classification of cardiomyopathies was recently developed, involving five forms of disease, where hypertrophic cardiomyopathy (HCM) and dilated cardiomyopathy (DCM) are the most common forms in the general population (Maron B.J. et al., 2006). The clinical manifestation, diagnosis and management of patients vary greatly, considering the heterogeneity and the late onset of associated symptoms. In fact, clinical manifestation involve palpitation, panting, heart failure and ventricular arrhythmias, that can lead to sudden cardiac death (SCD). Considering the manifestation of even very serious symptoms, an early diagnosis may prevent severe events and potentially ameliorate the progression of disease, increasing patient quality of life. To date, an improvement in the understanding of pathological events underlying inherited cardiomyopathies has occurred thanks to the advances in genetic, pharmacological, and imaging fields (Teekakirikul P. et al., 2013). As previously described, the discovery of the first cardiomyopathy-associated mutations, more than 20 years ago, has clarified that HCM is a "sarcomere" disorder, linked to several mutations that occur in proteins of the contractile apparatus of cardiomyocytes. In the majority of cases, the HCM pathogenesis is genetic, caused for one fourth to one third of all disease cases of mutations occurring in MYH7 and MYBPC3 genes, encoding for β-myosin heavy chain (β-MHC) and cardiac myosin-binding protein C (cMyBP-C). In vivo evaluation using murine models have showed an increase in contractility and calcium sensitivity in mutated myofilaments (Redwood C.S. et al., 1999). Moreover, structural and functional alterations trigger the onset of cardiac hypertrophy, contributing to diastolic dysfunction characteristic of this disease. In particular, calcium handling abnormalities occur in HCM, due the increment of sarcoplasmic calcium concentration during diastole (Knollmann BC, et al., 2003) and potentially inducing arrhythmic events (Huke S. et al., 2010). Therefore, mutation in myosin or cMyBP-C have the effect to increase the affinity of troponin C for calcium, resulting in an increment of calcium sensitivity (Robinson P. et al., 2007). Therefore, additional cross bridges between thick and thin filaments occur, worsening calcium abnormalities in HCM cardiomyocytes. In fact, the increase affinity of "calcium buffering" protein troponin C has as effect calcium concentration rise during diastole (Kataoka A. et al., 2007). In addition, since cross-bridge cycle accounts for about 70% of ATP consumption in cardiomyocytes, hypercontractility alter cellular energetic balance,

reducing other time-consuming cardiomyocytes activity, including membrane transporter and ion pump such as SERCA, the sarcoplasmic reticulum calcium ATPase.

On the other hand, various advances were made in the study of dilated cardiomyopathy, especially in the knowledge of the genetics of familial DCM (Cahill TJ et al., 2013). DCM represent the main leading cause of sudden cardiac death (SCD) and heart failure (HF), affecting indistinctly young and adult worldwide. The inherited form of DCM derived from mutations occurring in genes encoding proteins of sarcomere, cytoskeleton, or sarcolemma. Moreover, a particularly severe form of DCM is associated to Duchenne Muscular Dystrophy (DMD), due the absence of dystrophin, a fundamental protein that act as mechanical stress adsorber, resulting in an increase in membrane damage of cardiomyocytes. Among the possible disease-causing mechanisms, alterations in intracellular calcium levels have been proposed. In fact, several studies reported the pathological increase in cytosolic calcium and influx from the external environment (Turner et al., 1988). In addition, dystrophin deficiency affects also skeletal muscles, via alteration of structural and functional processes, including susceptibility to membrane damage and branched morphology (Chan and Head, 2011). Also, the increase of membrane fragility leads the abnormal calcium influx that exacerbated muscle fibres damage. Overall, these pathological modifications determine a calcium cycle defects, resulting in Ca^{2+} accumulation inside the cytosol. In this context, calcium dysregulation appears as a pathological mechanism in common with different form of inherited cardiomyopathies, despite this cardiac disorder show very different phenotypes. Then, a better understanding in molecular mechanisms underlying calcium handling alterations may provide the development of novel potential therapeutical targets for HCM and DCM. In this study, the use of induced pluripotent stem cells derived cardiomyocytes (hiPSC-CMs) and the subsequent derivation of engineered heart tissues (EHTs) have provided a useful tool to investigate electrophysiological and contractile alterations in HCM and DCM patients, overcoming the limitations associated to scarce maturation degree of hiPSC-CMs and allowing acute and chronic pharmacological treatments. Currently, there is no curative treatment for HCM or DCM, but the identification of specific targets implicated in the pathogenesis of inherited cardiomyopathies has raised expectations for new form of treatment, including “off-label” compounds that could help to mitigate symptoms associated to these diseases. In this context, novel drugs have been tested for their use in cardiomyopathies. Mavacamten (MYK-461), an allosteric myosin modulator has shown to attenuate hypercontractility in HCM cardiomyocytes (MyoKardia NCT02329184), enhancing calcium uptake by sarcoplasmic reticulum and restoring

intracellular calcium homeostasis. In fact, as previously described, chronic treatment with Mavacamten on HCM-EHTs highlighted a reduction of tension exerted during maturation, with a restoration after "wash-out" protocol, in which drug was eliminated from culture medium. Also, in isometric conditions, the decrease of active tension and contraction kinetics hastened has confirmed the effect of Mavacamten on HCM hypercontractility. Therefore, evaluation of HCM cardiomyocytes carrying R403Q mutation has demonstrated a slight reduction of shortening percentage, a significative reduction of contraction kinetics and calcium transient amplitude, in mutated cardiomyocytes compared to control. These results could be explained with the electrophysiological alteration of R403Q mutation on calcium handling balance of impaired cardiomyocytes.

Moreover, DCM is one of the most common cardiac disorders, usually associated to heart failure, calcium handling abnormalities and the onset of myocardial fibrosis. The functional characterization of DMD-hiPSC-EHTs highlighted a reduction of active tension exerted from dystrophin-deficiency tissues, according to previous evidence. Poloxamer 188 (P188), a copolymer novel compound, has showed to overcome this pathological reduction of active tension in DMD-EHTs. Also, Ranolazine, currently approved for angina or myocardial ischemia, has recently been shown to induce a shortening of action potential duration, reducing arrhythmic events through the inhibition of late sodium current (I_{Na-L}) (Coppini et al., 2013). In fact, acute treatment with Ranolazine showed a reduction of active tension in DMD-EHTs, probably worsening the weakness associated to Duchenne. In this context, novel type 2 glucose transporter inhibitors (SGLT2), Gliflozins, showed promising effect on cardiomyocytes isolated from HCM patients, reducing action potential duration (ADP) and preserved maximum upstroke speed, highlighted promising effect and pharmacological safety. Also, in DMD-hiPSC-EHTs, acute treatment with Dapagliflozin (1 and 5 μM) showed a significant increase of active tension compared to basal condition and a reduction of action potential kinetics. Then, gliflozins could represent a potential innovative pharmacological approach to ameliorate the pathological alteration occurring in HCM and DCM patients. In addition, calcium transient evaluation performed on skeletal muscle cells differentiated from DMD-hiPSCs, showed significative differences between mutated and control line, in term of increase of calcium transient amplitude and accelerated calcium kinetics.

Then, since inherited cardiomyopathies represent the most common cardiovascular issues, affecting millions of people around the world, the extensive knowledge of mutations underlying these diseases could represent a fundamental step forward in clinical practices and

pharmacological therapies. Inherited cardiomyopathies are known to induce cardiac dysfunction and heart failure, culminating in sudden cardiac death. Therefore, molecular effects of pathological modification occurring in inherited cardiomyopathies may provide the basis to the development of patient-specific therapeutical approaches, resulting in sarcomere and sarcolemma mutations responsible for cardiac and skeletal mechanical alteration. Although the genotype-phenotype correlation is expressed through different mechanisms, impaired calcium handling and cardiomyocytes contractile alterations are common mechanisms, representing possible targets in pharmacological novel treatment of these cardiac disorders. Therefore, the early investigation of the genetic defects allows to undertake clinical interventions, including management of patient and pharmacological treatment, reducing risk of incurring in arrhythmic events potentially resulting in sudden cardiac death.

References

- *Alamo L, Ware JS, Pinto A, Gillilan RE, Seidman JG, Seidman CE, Padrón R. Effects of myosin variants on interacting-heads motif explain distinct hypertrophic and dilated cardiomyopathy phenotypes. Elife. 2017 Jun 13;6:e24634. doi: 10.7554/eLife.24634. PMID: 28606303; PMCID: PMC5469618.*
- *Alter P, Rupp H, Stoll F, Adams P, Figiel JH, Klose KJ, Rominger MB, Maisch B. Increased end diastolic wall stress precedes left ventricular hypertrophy in dilative heart failure--use of the volume-based wall stress index. Int J Cardiol. 2012 May 31;157(2):233-8. doi: 10.1016/j.ijcard.2011.07.092. Epub 2011 Sep 8. PMID: 21862155.*
- *Antzelevitch C, Belardinelli L, Wu L, Fraser H, Zygmunt AC, Burashnikov A, Di Diego JM, Fish JM, Cordeiro JM, Goodrow RJ Jr, Scornik F, Perez G. Electrophysiologic properties and antiarrhythmic actions of a novel antianginal agent. J Cardiovasc Pharmacol Ther. 2004 Sep;9 Suppl 1:S65-83. doi: 10.1177/107424840400900106. PMID: 15378132.*
- *Argirò A, Zampieri M, Marchi A, Cappelli F, Del Franco A, Mazzoni C, Cecchi F, Olivotto I. Stage-specific therapy for hypertrophic cardiomyopathy. Eur Heart J Suppl. 2023 Apr 26;25(Suppl C):C155-C161. doi: 10.1093/eurheartjsupp/suad042. PMID: 37125313; PMCID: PMC10132571.*
- *Ashrafian H. Sudden death in young athletes. N Engl J Med. 2003 Dec 18;349(25):2464-5; author reply 2464-5. doi: 10.1056/NEJM200312183492518. PMID: 14681516.*
- *Barefield D, Sadayappan S. Phosphorylation and function of cardiac myosin binding protein-C in health and disease. J Mol Cell Cardiol. 2010 May;48(5):866-75. doi: 10.1016/j.yjmcc.2009.11.014. Epub 2009 Dec 3. PMID: 19962384; PMCID: PMC6800196.*
- *Baudenbacher F, Schober T, Pinto JR, Sidorov VY, Hilliard F, Solaro RJ, Potter JD, Knollmann BC. Myofilament Ca2+ sensitization causes susceptibility to cardiac arrhythmia in mice. J Clin Invest. 2008 Dec;118(12):3893-903. doi: 10.1172/JCI36642. Epub 2008 Nov 20. PMID: 19033660; PMCID: PMC2582931.*
- *Belus A, Piroddi N, Scellini B, Tesi C, D'Amati G, Girolami F, Yacoub M, Cecchi F, Olivotto I, Poggesi C. The familial hypertrophic cardiomyopathy-associated myosin*

mutation R403Q accelerates tension generation and relaxation of human cardiac myofibrils. J Physiol. 2008 Aug 1;586(15):3639-44. doi: 10.1113/jphysiol.2008.155952. Epub 2008 Jun 19. PMID: 18565996; PMCID: PMC2538824.

- *Bers DM. Cardiac excitation-contraction coupling. Nature. 2002 Jan 10;415(6868):198-205. doi: 10.1038/415198a. PMID: 11805843.*
- *Birket MJ, Mummery CL. Pluripotent stem cell derived cardiovascular progenitors--a developmental perspective. Dev Biol. 2015 Apr 15;400(2):169-79. doi: 10.1016/j.ydbio.2015.01.012. Epub 2015 Jan 24. PMID: 25624264.*
- *Blechman I, Arad M, Nussbaum T, Goldenberg I, Freimark D. Predictors and outcome of sustained improvement in left ventricular function in dilated cardiomyopathy. Clin Cardiol. 2014 Nov;37(11):687-92. doi: 10.1002/clc.22331. Epub 2014 Sep 18. PMID: 25236761; PMCID: PMC6649463.*
- *Boreström C, Jonebring A, Guo J, Palmgren H, Cederblad L, Forslöw A, Svensson A, Söderberg M, Reznichenko A, Nyström J, Patrakka J, Hicks R, Maresca M, Valastro B, Collén A. A CRISP(e)R view on kidney organoids allows generation of an induced pluripotent stem cell-derived kidney model for drug discovery. Kidney Int. 2018 Dec;94(6):1099-1110. doi: 10.1016/j.kint.2018.05.003. Epub 2018 Jul 31. PMID: 30072040.*
- *Bremner SB, Mandrycky CJ, Leonard A, Padgett RM, Levinson AR, Rehn ES, Pioner JM, Sniadecki NJ, Mack DL. Full-length dystrophin deficiency leads to contractile and calcium transient defects in human engineered heart tissues. J Tissue Eng. 2022 Aug 17;13:20417314221119628. doi: 10.1177/20417314221119628. PMID: 36003954; PMCID: PMC9393922.*
- *Brigden W. Uncommon myocardial diseases: the non-coronary cardiomyopathies. Lancet. 1957 Dec 21;273(7008):1243-9. doi: 10.1016/s0140-6736(57)91537-4. PMID: 13492617.*
- *Buckingham M, Rigby PW. Gene regulatory networks and transcriptional mechanisms that control myogenesis. Dev Cell. 2014 Feb 10;28(3):225-38. doi: 10.1016/j.devcel.2013.12.020. PMID: 24525185.*
- *Burridge PW, Metzler SA, Nakayama KH, Abilez OJ, Simmons CS, Bruce MA, Matsuura Y, Kim P, Wu JC, Butte M, Huang NF, Yang PC. Multi-cellular interactions*

sustain long-term contractility of human pluripotent stem cell-derived cardiomyocytes. Am J Transl Res. 2014 Nov 22;6(6):724-35. PMID: 25628783; PMCID: PMC4297340.

- *Cahill TJ, Ashrafian H, Watkins H. Genetic cardiomyopathies causing heart failure. Circ Res. 2013 Aug 30;113(6):660-75. doi: 10.1161/CIRCRESAHA.113.300282. PMID: 23989711.*
- *Cai C, Masumiya H, Weisleder N, Matsuda N, Nishi M, Hwang M, Ko JK, Lin P, Thornton A, Zhao X, Pan Z, Komazaki S, Brotto M, Takeshima H, Ma J. MG53 nucleates assembly of cell membrane repair machinery. Nat Cell Biol. 2009 Jan;11(1):56-64. doi: 10.1038/ncb1812. Epub 2008 Nov 30. PMID: 19043407; PMCID: PMC2990407.*
- *Carrier L, Bonne G, Bährend E, Yu B, Richard P, Niel F, Hainque B, Cruaud C, Gary F, Labeit S, Bouhour JB, Dubourg O, Desnos M, Hagège AA, Trent RJ, Komajda M, Fiszman M, Schwartz K. Organization and sequence of human cardiac myosin binding protein C gene (MYBPC3) and identification of mutations predicted to produce truncated proteins in familial hypertrophic cardiomyopathy. Circ Res. 1997 Mar;80(3):427-34. PMID: 9048664.*
- *Chang ACY, Pardon G, Chang ACH, Wu H, Ong SG, Eguchi A, Ancel S, Holbrook C, Ramunas J, Ribeiro AJS, LaGory EL, Wang H, Koleckar K, Giaccia A, Mack DL, Childers MK, Denning C, Day JW, Wu JC, Pruitt BL, Blau HM. Increased tissue stiffness triggers contractile dysfunction and telomere shortening in dystrophic cardiomyocytes. Stem Cell Reports. 2021 Sep 14;16(9):2169-2181. doi: 10.1016/j.stemcr.2021.04.018. Epub 2021 May 20. PMID: 34019816; PMCID: PMC8452491.*
- *Chasis H, Jolliffe N, Smith HW. THE ACTION OF PHLORIZIN ON THE EXCRETION OF GLUCOSE, XYLOSE, SUCROSE, CREATININE AND UREA BY MAN. J Clin Invest. 1933 Nov;12(6):1083-90. doi: 10.1172/JCI100559. PMID: 16694183; PMCID: PMC435965.*
- *Chung J, Smith AL, Hughes SC, Niizawa G, Abdel-Hamid HZ, Naylor EW, Hughes T, Clemens PR. Twenty-year follow-up of newborn screening for patients with muscular dystrophy. Muscle Nerve. 2016 Apr;53(4):570-8. doi: 10.1002/mus.24880. Epub 2015 Sep 10. PMID: 26260293.*
- *Cirulli ET, Goldstein DB. Uncovering the roles of rare variants in common disease through whole-genome sequencing. Nat Rev Genet. 2010 Jun;11(6):415-25. doi: 10.1038/nrg2779. PMID: 20479773.*

- *Coppini R, Ferrantini C, Mazzoni L, Sartiani L, Olivotto I, Poggesi C, Cerbai E, Mugelli A. Regulation of intracellular Na(+) in health and disease: pathophysiological mechanisms and implications for treatment. Glob Cardiol Sci Pract. 2013 Nov 1;2013(3):222-42. doi: 10.5339/gcsp.2013.30. PMID: 24689024; PMCID: PMC3963757.*
- *Coppini R, Ferrantini C. NaV1.8: a novel contributor to cardiac arrhythmogenesis in heart failure. Cardiovasc Res. 2018 Nov 1;114(13):1691-1693. doi: 10.1093/cvr/cvy210. PMID: 30169598.*
- *Denning C, Borgdorff V, Crutchley J, Firth KS, George V, Kalra S, Kondrashov A, Hoang MD, Mosqueira D, Patel A, Prodanov L, Rajamohan D, Skarnes WC, Smith JG, Young LE. Cardiomyocytes from human pluripotent stem cells: From laboratory curiosity to industrial biomedical platform. Biochim Biophys Acta. 2016 Jul;1863(7 Pt B):1728-48. doi: 10.1016/j.bbamcr.2015.10.014. Epub 2015 Oct 31. PMID: 26524115; PMCID: PMC5221745.*
- *Drouin E, Lande G, Charpentier F. Amiodarone reduces transmural heterogeneity of repolarization in the human heart. J Am Coll Cardiol. 1998 Oct;32(4):1063-7. doi: 10.1016/s0735-1097(98)00330-1. PMID: 9768733.*
- *Duddy W, Duguez S, Johnston H, Cohen TV, Phadke A, Gordish-Dressman H, Nagaraju K, Gnocchi V, Low S, Partridge T. Muscular dystrophy in the mdx mouse is a severe myopathy compounded by hypotrophy, hypertrophy and hyperplasia. Skelet Muscle. 2015 May 1;5:16. doi: 10.1186/s13395-015-0041-y. PMID: 25987977; PMCID: PMC4434871.*
- *Dumont NA, Bentzinger CF, Sincennes MC, Rudnicki MA. Satellite Cells and Skeletal Muscle Regeneration. Compr Physiol. 2015 Jul 1;5(3):1027-59. doi: 10.1002/cphy.c140068. PMID: 26140708.*
- *Edelberg JM, Sehnert AJ, Mealiffe ME, Del Rio CL, McDowell R. The Impact of Mavacamten on the Pathophysiology of Hypertrophic Cardiomyopathy: A Narrative Review. Am J Cardiovasc Drugs. 2022 Sep;22(5):497-510. doi: 10.1007/s40256-022-00532-x. Epub 2022 Apr 18. PMID: 35435607; PMCID: PMC9467968.*
- *Eschenhagen T, Fink C, Remmers U, Scholz H, Wattchow J, Weil J, Zimmermann W, Dohmen HH, Schäfer H, Bishopric N, Wakatsuki T, Elson EL. Three-dimensional reconstitution of embryonic cardiomyocytes in a collagen matrix: a new heart muscle*

model system. FASEB J. 1997 Jul;11(8):683-94. doi: 10.1096/fasebj.11.8.9240969. PMID: 9240969.

- *Even-Ram S, Artym V, Yamada KM. Matrix control of stem cell fate. Cell. 2006 Aug 25;126(4):645-7. doi: 10.1016/j.cell.2006.08.008. PMID: 16923382.*
- *Fauconnier J, Pasquié JL, Bideaux P, Lacampagne A, Richard S. Cardiomyocytes hypertrophic status after myocardial infarction determines distinct types of arrhythmia: role of the ryanodine receptor. Prog Biophys Mol Biol. 2010 Sep;103(1):71-80. doi: 10.1016/j.pbiomolbio.2010.01.002. Epub 2010 Jan 28. PMID: 20109482.*
- *Fayssoil A, Abasse S, Silverston K. Cardiac Involvement Classification and Therapeutic Management in Patients with Duchenne Muscular Dystrophy. J Neuromuscul Dis. 2017;4(1):17-23. doi: 10.3233/JND-160194. PMID: 28269790; PMCID: PMC5345647.*
- *Ferlini A, Neri M, Gualandi F. The medical genetics of dystrophinopathies: molecular genetic diagnosis and its impact on clinical practice. Neuromuscul Disord. 2013 Jan;23(1):4-14. doi: 10.1016/j.nmd.2012.09.002. Epub 2012 Oct 30. PMID: 23116935.*
- *Ferlini A, Rimessi P. Exon skipping quantification by real-time PCR. Methods Mol Biol. 2012;867:189-99. doi: 10.1007/978-1-61779-767-5_12. PMID: 22454062.*
- *Ferrantini C, Pioner JM, Mazzoni L, Gentile F, Tosi B, Rossi A, Belardinelli L, Tesi C, Palandri C, Matucci R, Cerbai E, Olivotto I, Poggesi C, Mugelli A, Coppini R. Late sodium current inhibitors to treat exercise-induced obstruction in hypertrophic cardiomyopathy: an in vitro study in human myocardium. Br J Pharmacol. 2018 Jul;175(13):2635-2652. doi: 10.1111/bph.14223. Epub 2018 May 3. PMID: 29579779; PMCID: PMC6003658.*
- *Filipczyk AA, Passier R, Rochat A, Mummery CL. Regulation of cardiomyocyte differentiation of embryonic stem cells by extracellular signalling. Cell Mol Life Sci. 2007 Mar;64(6):704-18. doi: 10.1007/s00018-007-6523-2. PMID: 17380311; PMCID: PMC2778649.*
- *Fong PY, Turner PR, Denetclaw WF, Steinhardt RA. Increased activity of calcium leak channels in myotubes of Duchenne human and mdx mouse origin. Science. 1990 Nov 2;250(4981):673-6. doi: 10.1126/science.2173137. PMID: 2173137.*
- *Fougerousse F, Delezoide AL, Fiszman MY, Schwartz K, Beckmann JS, Carrier L. Cardiac myosin binding protein C gene is specifically expressed in heart during murine*

and human development. Circ Res. 1998 Jan 9-23;82(1):130-3. doi: 10.1161/01.res.82.1.130. PMID: 9440712.

- *Frankel KA, Rosser RJ. The pathology of the heart in progressive muscular dystrophy: epimyocardial fibrosis. Hum Pathol. 1976 Jul;7(4):375-86. doi: 10.1016/s0046-8177(76)80053-6. PMID: 939536.*
- *Freiburg A, Gautel M. A molecular map of the interactions between titin and myosin-binding protein C. Implications for sarcomeric assembly in familial hypertrophic cardiomyopathy. Eur J Biochem. 1996 Jan 15;235(1-2):317-23. doi: 10.1111/j.1432-1033.1996.00317.x. PMID: 8631348.*
- *Gajendrarao P, Krishnamoorthy N, Selvaraj S, Girolami F, Cecchi F, Olivotto I, Yacoub M. An Investigation of the Molecular Mechanism of Double cMyBP-C Mutation in a Patient with End-Stage Hypertrophic Cardiomyopathy. J Cardiovasc Transl Res. 2015 Jun;8(4):232-43. doi: 10.1007/s12265-015-9624-6. Epub 2015 May 14. PMID: 25971843.*
- *Gautel M, Zuffardi O, Freiburg A, Labeit S. Phosphorylation switches specific for the cardiac isoform of myosin binding protein-C: a modulator of cardiac contraction? EMBO J. 1995 May 1;14(9):1952-60. doi: 10.1002/j.1460-2075.1995.tb07187.x. PMID: 7744002; PMCID: PMC398294.*
- *Geisterfer-Lowrance AA, Kass S, Tanigawa G, Vosberg HP, McKenna W, Seidman CE, Seidman JG. A molecular basis for familial hypertrophic cardiomyopathy: a beta cardiac myosin heavy chain gene missense mutation. Cell. 1990 Sep 7;62(5):999-1006. doi: 10.1016/0092-8674(90)90274-i. PMID: 1975517.*
- *Geisterfer-Lowrance AA, Kass S, Tanigawa G, Vosberg HP, McKenna W, Seidman CE, Seidman JG. A molecular basis for familial hypertrophic cardiomyopathy: a beta cardiac myosin heavy chain gene missense mutation. Cell. 1990 Sep 7;62(5):999-1006. doi: 10.1016/0092-8674(90)90274-i. PMID: 1975517.*
- *Gerull B, Gramlich M, Atherton J, McNabb M, Trombitás K, Sasse-Klaassen S, Seidman JG, Seidman C, Granzier H, Labeit S, Frenneaux M, Thierfelder L. Mutations of TTN, encoding the giant muscle filament titin, cause familial dilated cardiomyopathy. Nat Genet. 2002 Feb;30(2):201-4. doi: 10.1038/ng815. Epub 2002 Jan 14. PMID: 11788824.*
- *Gilbert R, Cohen JA, Pardo S, Basu A, Fischman DA. Identification of the A-band localization domain of myosin binding proteins C and H (MyBP-C, MyBP-H) in skeletal*

muscle. J Cell Sci. 1999 Jan;112 (Pt 1):69-79. doi: 10.1242/jcs.112.1.69. PMID: 9841905.

- *Girolami F, Passantino S, Verrillo F, Palinkas ED, Limongelli G, Favilli S, Olivotto I. The Influence of Genotype on the Phenotype, Clinical Course, and Risk of Adverse Events in Children with Hypertrophic Cardiomyopathy. Heart Fail Clin. 2022 Jan;18(1):1-8. doi: 10.1016/j.hfc.2021.07.013. Epub 2021 Oct 22. PMID: 34776071.*
- *Govada L, Carpenter L, da Fonseca PC, Helliwell JR, Rizkallah P, Flashman E, Chayen NE, Redwood C, Squire JM. Crystal structure of the C1 domain of cardiac myosin binding protein-C: implications for hypertrophic cardiomyopathy. J Mol Biol. 2008 Apr 25;378(2):387-97. doi: 10.1016/j.jmb.2008.02.044. Epub 2008 Mar 4. PMID: 18374358.*
- *Gruen M, Gautel M. Mutations in beta-myosin S2 that cause familial hypertrophic cardiomyopathy (FHC) abolish the interaction with the regulatory domain of myosin-binding protein-C. J Mol Biol. 1999 Feb 26;286(3):933-49. doi: 10.1006/jmbi.1998.2522. PMID: 10024460.*
- *Haghighi K, Kolokathis F, Gramolini AO, Waggoner JR, Pater L, Lynch RA, Fan GC, Tsiapras D, Parekh RR, Dorn GW 2nd, MacLennan DH, Kremastinos DT, Kranias EG. A mutation in the human phospholamban gene, deleting arginine 14, results in lethal, hereditary cardiomyopathy. Proc Natl Acad Sci U S A. 2006 Jan 31;103(5):1388-93. doi: 10.1073/pnas.0510519103. Epub 2006 Jan 23. PMID: 16432188; PMCID: PMC1360586.*
- *Halas M, Langa P, Warren CM, Goldspink PH, Wolska BM, Solaro RJ. Effects of Sarcomere Activators and Inhibitors Targeting Myosin Cross-Bridges on Ca^{2+}-Activation of Mature and Immature Mouse Cardiac Myofilaments. Mol Pharmacol. 2022 May;101(5):286-299. doi: 10.1124/molpharm.121.000420. Epub 2022 Mar 2. PMID: 35236770; PMCID: PMC9092471.*
- *Hariharan N, Zhai P, Sadoshima J. Oxidative stress stimulates autophagic flux during ischemia/reperfusion. Antioxid Redox Signal. 2011 Jun;14(11):2179-90. doi: 10.1089/ars.2010.3488. Epub 2011 Jan 27. PMID: 20812860; PMCID: PMC3085947.*
- *Hartzell HC, Glass DB. Phosphorylation of purified cardiac muscle C-protein by purified cAMP-dependent and endogenous Ca2+-calmodulin-dependent protein kinases. J Biol Chem. 1984 Dec 25;259(24):15587-96. PMID: 6549009.*

- *Hensley N, Dietrich J, Nyhan D, Mitter N, Yee MS, Brady M. Hypertrophic cardiomyopathy: a review. Anesth Analg. 2015 Mar;120(3):554-569. doi: 10.1213/ANE.0000000000000538. PMID: 25695573.*
- *Hershberger RE, Hedges DJ, Morales A. Dilated cardiomyopathy: the complexity of a diverse genetic architecture. Nat Rev Cardiol. 2013 Sep;10(9):531-47. doi: 10.1038/nrcardio.2013.105. Epub 2013 Jul 30. PMID: 23900355.*
- *Hinson JT, Chopra A, Nafissi N, Polacheck WJ, Benson CC, Swist S, Gorham J, Yang L, Schafer S, Sheng CC, Haghighi A, Homsy J, Hubner N, Church G, Cook SA, Linke WA, Chen CS, Seidman JG, Seidman CE. HEART DISEASE. Titin mutations in iPS cells define sarcomere insufficiency as a cause of dilated cardiomyopathy. Science. 2015 Aug 28;349(6251):982-6. doi: 10.1126/science.aaa5458. PMID: 26315439; PMCID: PMC4618316.*
- *Hopf FW, Turner PR, Denetclaw WF Jr, Reddy P, Steinhardt RA. A critical evaluation of resting intracellular free calcium regulation in dystrophic mdx muscle. Am J Physiol. 1996 Oct;271(4 Pt 1):C1325-39. doi: 10.1152/ajpcell.1996.271.4.C1325. PMID: 8897840.*
- *Huke S, Knollmann BC. Increased myofilament Ca2+-sensitivity and arrhythmia susceptibility. J Mol Cell Cardiol. 2010 May;48(5):824-33. doi: 10.1016/j.yjmcc.2010.01.011. Epub 2010 Jan 22. PMID: 20097204; PMCID: PMC2854218.*
- *Ivashchenko CY, Pipes GC, Lozinskaya IM, Lin Z, Xiaoping X, Needle S, Grygielko ET, Hu E, Toomey JR, Lepore JJ, Willette RN. Human-induced pluripotent stem cell-derived cardiomyocytes exhibit temporal changes in phenotype. Am J Physiol Heart Circ Physiol. 2013 Sep 15;305(6):H913-22. doi: 10.1152/ajpheart.00819.2012. Epub 2013 Jul 5. PMID: 23832699.*
- *Karbassi E, Fenix A, Marchiano S, Muraoka N, Nakamura K, Yang X, Murry CE. Cardiomyocyte maturation: advances in knowledge and implications for regenerative medicine. Nat Rev Cardiol. 2020 Jun;17(6):341-359. doi: 10.1038/s41569-019-0331-x. Epub 2020 Feb 3. PMID: 32015528; PMCID: PMC7239749.*
- *Knollmann BC, Kirchhof P, Sirenko SG, Degen H, Greene AE, Schober T, Mackow JC, Fabritz L, Potter JD, Morad M. Familial hypertrophic cardiomyopathy-linked mutant troponin T causes stress-induced ventricular tachycardia and Ca2+-dependent action*

potential remodeling. Circ Res. 2003 Mar 7;92(4):428-36. doi: 10.1161/01.RES.0000059562.91384.1A. Epub 2003 Feb 6. PMID: 12600890.

- *Konagaya M, Takayanagi T. Regularity in the change of serum creatine kinase level in Duchenne muscular dystrophy. A study with long-term follow-up cases. Jpn J Med. 1986 Feb;25(1):2-8. doi: 10.2169/internalmedicine1962.25.2. PMID: 3712859.*
- *Konieczny P, Swiderski K, Chamberlain JS. Gene and cell-mediated therapies for muscular dystrophy. Muscle Nerve. 2013 May;47(5):649-63. doi: 10.1002/mus.23738. Epub 2013 Mar 29. PMID: 23553671; PMCID: PMC4077844.*
- *Koretz JF. Effects of C-protein on synthetic myosin filament structure. Biophys J. 1979 Sep;27(3):433-46. doi: 10.1016/S0006-3495(79)85227-3. PMID: 263692; PMCID: PMC1328598.*
- *Krylova OO, Pohl P. Ionophoric activity of pluronic block copolymers. Biochemistry. 2004 Mar 30;43(12):3696-703. doi: 10.1021/bi035768l. PMID: 15035640.*
- *Laflamme MA, Chen KY, Naumova AV, Muskheli V, Fugate JA, Dupras SK, Reinecke H, Xu C, Hassanipour M, Police S, O'Sullivan C, Collins L, Chen Y, Minami E, Gill EA, Ueno S, Yuan C, Gold J, Murry CE. Cardiomyocytes derived from human embryonic stem cells in pro-survival factors enhance function of infarcted rat hearts. Nat Biotechnol. 2007 Sep;25(9):1015-24. doi: 10.1038/nbt1327. Epub 2007 Aug 26. PMID: 17721512.*
- *Lakdawala NK, Winterfield JR, Funke BH. Dilated cardiomyopathy. Circ Arrhythm Electrophysiol. 2013 Feb;6(1):228-37. doi: 10.1161/CIRCEP.111.962050. Epub 2012 Sep 28. PMID: 23022708; PMCID: PMC3603701.*
- *Lewis JF, Webber JD, Sutton LL, Chesoni S, Curry CL. Discordance in degree of right and left ventricular dilation in patients with dilated cardiomyopathy: recognition and clinical implications. J Am Coll Cardiol. 1993 Mar 1;21(3):649-54. doi: 10.1016/0735-1097(93)90097-k. PMID: 8436746.*
- *Lieu DK, Fu JD, Chiamvimonvat N, Tung KC, McNerney GP, Huser T, Keller G, Kong CW, Li RA. Mechanism-based facilitated maturation of human pluripotent stem cell-derived cardiomyocytes. Circ Arrhythm Electrophysiol. 2013 Feb;6(1):191-201. doi: 10.1161/CIRCEP.111.973420. Epub 2013 Feb 7. PMID: 23392582; PMCID: PMC3757253.*
- *Lipshultz SE, Cochran TR, Briston DA, Brown SR, Sambatakos PJ, Miller TL, Carrillo AA, Corcia L, Sanchez JE, Diamond MB, Freundlich M, Harake D, Gayle T, Harmon*

WG, Rusconi PG, Sandhu SK, Wilkinson JD. Pediatric cardiomyopathies: causes, epidemiology, clinical course, preventive strategies and therapies. Future Cardiol. 2013 Nov;9(6):817-48. doi: 10.2217/fca.13.66. PMID: 24180540; PMCID: PMC3903430.

- *Loh YH, Agarwal S, Park IH, Urbach A, Huo H, Heffner GC, Kim K, Miller JD, Ng K, Daley GQ. Generation of induced pluripotent stem cells from human blood. Blood. 2009 May 28;113(22):5476-9. doi: 10.1182/blood-2009-02-204800. Epub 2009 Mar 18. PMID: 19299331; PMCID: PMC2689048.*
- *Lundy SD, Zhu WZ, Regnier M, Laflamme MA. Structural and functional maturation of cardiomyocytes derived from human pluripotent stem cells. Stem Cells Dev. 2013 Jul 15;22(14):1991-2002. doi: 10.1089/scd.2012.0490. Epub 2013 Apr 5. PMID: 23461462; PMCID: PMC3699903.*
- *Lundy SD, Zhu WZ, Regnier M, Laflamme MA. Structural and functional maturation of cardiomyocytes derived from human pluripotent stem cells. Stem Cells Dev. 2013 Jul 15;22(14):1991-2002. doi: 10.1089/scd.2012.0490. Epub 2013 Apr 5. PMID: 23461462; PMCID: PMC3699903.*
- *Malik V, Rodino-Klapac LR, Mendell JR. Emerging drugs for Duchenne muscular dystrophy. Expert Opin Emerg Drugs. 2012 Jun;17(2):261-77. doi: 10.1517/14728214.2012.691965. PMID: 22632414; PMCID: PMC3486431.*
- *Mannhardt I, Breckwoldt K, Letuffe-Brenière D, Schaaf S, Schulz H, Neuber C, Benzin A, Werner T, Eder A, Schulze T, Klampe B, Christ T, Hirt MN, Huebner N, Moretti A, Eschenhagen T, Hansen A. Human Engineered Heart Tissue: Analysis of Contractile Force. Stem Cell Reports. 2016 Jul 12;7(1):29-42. doi: 10.1016/j.stemcr.2016.04.011. Epub 2016 May 19. PMID: 27211213; PMCID: PMC4944531.*
- *Marian AJ, Braunwald E. Hypertrophic Cardiomyopathy: Genetics, Pathogenesis, Clinical Manifestations, Diagnosis, and Therapy. Circ Res. 2017 Sep 15;121(7):749-770. doi: 10.1161/CIRCRESAHA.117.311059. PMID: 28912181; PMCID: PMC5654557.*
- *Maron BJ, Desai MY, Nishimura RA, Spirito P, Rakowski H, Towbin JA, Dearani JA, Rowin EJ, Maron MS, Sherrid MV. Management of Hypertrophic Cardiomyopathy: JACC State-of-the-Art Review. J Am Coll Cardiol. 2022 Feb 1;79(4):390-414. doi: 10.1016/j.jacc.2021.11.021. PMID: 35086661.*

- *Maron BJ, Maron MS, Semsarian C. Genetics of hypertrophic cardiomyopathy after 20 years: clinical perspectives. J Am Coll Cardiol. 2012 Aug 21;60(8):705-15. doi: 10.1016/j.jacc.2012.02.068. Epub 2012 Jul 11. PMID: 22796258.*
- *Maron BJ, Rastegar H, Udelson JE, Dearani JA, Maron MS. Contemporary surgical management of hypertrophic cardiomyopathy, the need for more myectomy surgeons and disease-specific centers, and the Tufts initiative. Am J Cardiol. 2013 Nov 1;112(9):1512-5. doi: 10.1016/j.amjcard.2013.06.040. Epub 2013 Sep 5. PMID: 24012037.*
- *Maron BJ, Towbin JA, Thiene G, Antzelevitch C, Corrado D, Arnett D, Moss AJ, Seidman CE, Young JB; American Heart Association; Council on Clinical Cardiology, Heart Failure and Transplantation Committee; Quality of Care and Outcomes Research and Functional Genomics and Translational Biology Interdisciplinary Working Groups; Council on Epidemiology and Prevention. Contemporary definitions and classification of the cardiomyopathies: an American Heart Association Scientific Statement from the Council on Clinical Cardiology, Heart Failure and Transplantation Committee; Quality of Care and Outcomes Research and Functional Genomics and Translational Biology Interdisciplinary Working Groups; and Council on Epidemiology and Prevention. Circulation. 2006 Apr 11;113(14):1807-16. doi: 10.1161/CIRCULATIONAHA.106.174287. Epub 2006 Mar 27. PMID: 16567565.*
- *Maron BJ. A phenocopy of sarcomeric hypertrophic cardiomyopathy: LAMP2 cardiomyopathy (Danon disease) from China. Eur Heart J. 2012 Mar;33(5):570-2. doi: 10.1093/eurheartj/ehr438. Epub 2011 Dec 20. PMID: 22187509.*
- *Maron BJ. Hypertrophic cardiomyopathy: a systematic review. JAMA. 2002 Mar 13;287(10):1308-20. doi: 10.1001/jama.287.10.1308. PMID: 11886323.*
- *Maron MS. The current and emerging role of cardiovascular magnetic resonance imaging in hypertrophic cardiomyopathy. J Cardiovasc Transl Res. 2009 Dec;2(4):415-25. doi: 10.1007/s12265-009-9136-3. Epub 2009 Nov 7. PMID: 20560000.*
- *Maroto M, Reshef R, Münsterberg AE, Koester S, Goulding M, Lassar AB. Ectopic Pax-3 activates MyoD and Myf-5 expression in embryonic mesoderm and neural tissue. Cell. 1997 Apr 4;89(1):139-48. doi: 10.1016/s0092-8674(00)80190-7. PMID: 9094722.*
- *Marston S, Copeland O, Jacques A, Livesey K, Tsang V, McKenna WJ, Jalilzadeh S, Carballo S, Redwood C, Watkins H. Evidence from human myectomy samples that*

MYBPC3 mutations cause hypertrophic cardiomyopathy through haploinsufficiency. Circ Res. 2009 Jul 31;105(3):219-22. doi: 10.1161/CIRCRESAHA.109.202440. Epub 2009 Jul 2. PMID: 19574547.

- *Mathur A, Loskill P, Shao K, Huebsch N, Hong S, Marcus SG, Marks N, Mandegar M, Conklin BR, Lee LP, Healy KE. Human iPSC-based cardiac microphysiological system for drug screening applications. Sci Rep. 2015 Mar 9;5:8883. doi: 10.1038/srep08883. PMID: 25748532; PMCID: PMC4352848.*
- *McMurray JJV, Solomon SD, Inzucchi SE, Køber L, Kosiborod MN, Martinez FA, Ponikowski P, Sabatine MS, Anand IS, Bělohlávek J, Böhm M, Chiang CE, Chopra VK, de Boer RA, Desai AS, Diez M, Drozdz J, Dukát A, Ge J, Howlett JG, Katova T, Kitakaze M, Ljungman CEA, Merkely B, Nicolau JC, O'Meara E, Petrie MC, Vinh PN, Schou M, Tereshchenko S, Verma S, Held C, DeMets DL, Docherty KF, Jhund PS, Bengtsson O, Sjöstrand M, Langkilde AM; DAPA-HF Trial Committees and Investigators. Dapagliflozin in Patients with Heart Failure and Reduced Ejection Fraction. N Engl J Med. 2019 Nov 21;381(21):1995-2008. doi: 10.1056/NEJMoa1911303. Epub 2019 Sep 19. PMID: 31535829.*
- *Menke A, Jockusch H. Extent of shock-induced membrane leakage in human and mouse myotubes depends on dystrophin. J Cell Sci. 1995 Feb;108 (Pt 2):727-33. doi: 10.1242/jcs.108.2.727. PMID: 7769014.*
- *Merovci A, Mari A, Solis-Herrera C, Xiong J, Daniele G, Chavez-Velazquez A, Tripathy D, Urban McCarthy S, Abdul-Ghani M, DeFronzo RA. Dapagliflozin lowers plasma glucose concentration and improves β-cell function. J Clin Endocrinol Metab. 2015 May;100(5):1927-32. doi: 10.1210/jc.2014-3472. Epub 2015 Feb 24. Erratum in: J Clin Endocrinol Metab. 2017 Dec 1;102(12):4662. PMID: 25710563; PMCID: PMC4422889.*
- *Nistri S, Olivotto I, Betocchi S, Losi MA, Valsecchi G, Pinamonti B, Conte MR, Casazza F, Galderisi M, Maron BJ, Cecchi F. Prognostic significance of left atrial size in patients with hypertrophic cardiomyopathy (from the Italian Registry for Hypertrophic Cardiomyopathy). Am J Cardiol. 2006 Oct 1;98(7):960-5. doi: 10.1016/j.amjcard.2006.05.013. Epub 2006 Aug 14. PMID: 16996883.*
- *Ogura I, Abe S, Negishi T, Saito H. [Development of a simple measurement system for routine management of X-ray equipment]. Nihon Hoshasen Gijutsu Gakkai Zasshi.*

2014 Dec;70(12):1403-12. Japanese. doi: 10.6009/jjrt.2014_JSRT_70.12.1403. PMID: 25672445.

- *Olivotto I, Cecchi F, Yacoub MH. Myocardial bridging and sudden death in hypertrophic cardiomyopathy: Salome drops another veil. Eur Heart J. 2009 Jul;30(13):1549-50. doi: 10.1093/eurheartj/ehp216. Epub 2009 Jun 1. PMID: 19491131.*
- *Olivotto I, Cecchi F. The epidemiologic evolution and present perception of hypertrophic cardiomyopathy. Ital Heart J. 2003 Sep;4(9):596-601. PMID: 14635376.*
- *Olivotto I, Oreziak A, Barriales-Villa R, Abraham TP, Masri A, Garcia-Pavia P, Saberi S, Lakdawala NK, Wheeler MT, Owens A, Kubanek M, Wojakowski W, Jensen MK, Gimeno-Blanes J, Afshar K, Myers J, Hegde SM, Solomon SD, Sehnert AJ, Zhang D, Li W, Bhattacharya M, Edelberg JM, Waldman CB, Lester SJ, Wang A, Ho CY, Jacoby D; EXPLORER-HCM study investigators. Mavacamten for treatment of symptomatic obstructive hypertrophic cardiomyopathy (EXPLORER-HCM): a randomised, double-blind, placebo-controlled, phase 3 trial. Lancet. 2020 Sep 12;396(10253):759-769. doi: 10.1016/S0140-6736(20)31792-X. Epub 2020 Aug 29. Erratum in: Lancet. 2020 Sep 12;396(10253):758. PMID: 32871100.*
- *Ommen SR, Mital S, Burke MA, Day SM, Deswal A, Elliott P, Evanovich LL, Hung J, Joglar JA, Kantor P, Kimmelstiel C, Kittleson M, Link MS, Maron MS, Martinez MW, Miyake CY, Schaff HV, Semsarian C, Sorajja P. 2020 AHA/ACC Guideline for the Diagnosis and Treatment of Patients With Hypertrophic Cardiomyopathy: Executive Summary: A Report of the American College of Cardiology/American Heart Association Joint Committee on Clinical Practice Guidelines. Circulation. 2020 Dec 22;142(25):e533-e557. doi: 10.1161/CIR.0000000000000938. Epub 2020 Nov 20. PMID: 33215938.*
- *Palpant NJ, Hofsteen P, Pabon L, Reinecke H, Murry CE. Cardiac development in zebrafish and human embryonic stem cells is inhibited by exposure to tobacco cigarettes and e-cigarettes. PLoS One. 2015 May 15;10(5):e0126259. doi: 10.1371/journal.pone.0126259. PMID: 25978043; PMCID: PMC4433280.*
- *Pesl M, Acimovic I, Pribyl J, Hezova R, Vilotic A, Fauconnier J, Vrbsky J, Kruzliak P, Skladal P, Kara T, Rotrekl V, Lacampagne A, Dvorak P, Meli AC. Forced aggregation and defined factors allow highly uniform-sized embryoid bodies and functional cardiomyocytes from human embryonic and induced pluripotent stem cells. Heart*

Vessels. 2014 Nov;29(6):834-46. doi: 10.1007/s00380-013-0436-9. Epub 2013 Nov 21. PMID: 24258387.

- *Petrof BJ, Shrager JB, Stedman HH, Kelly AM, Sweeney HL. Dystrophin protects the sarcolemma from stresses developed during muscle contraction. Proc Natl Acad Sci U S A. 1993 Apr 15;90(8):3710-4. doi: 10.1073/pnas.90.8.3710. PMID: 8475120; PMCID: PMC46371.*
- *Pioner JM, Guan X, Klaiman JM, Racca AW, Pabon L, Muskheli V, Macadangdang J, Ferrantini C, Hoopmann MR, Moritz RL, Kim DH, Tesi C, Poggesi C, Murry CE, Childers MK, Mack DL, Regnier M. Absence of full-length dystrophin impairs normal maturation and contraction of cardiomyocytes derived from human-induced pluripotent stem cells. Cardiovasc Res. 2020 Feb 1;116(2):368-382. doi: 10.1093/cvr/cvz109. PMID: 31049579; PMCID: PMC8053310.*
- *Pioner JM, Santini L, Palandri C, Langione M, Grandinetti B, Querceto S, Martella D, Mazzantini C, Scellini B, Giammarino L, Lupi F, Mazzarotto F, Gowran A, Rovina D, Santoro R, Pompilio G, Tesi C, Parmeggiani C, Regnier M, Cerbai E, Mack DL, Poggesi C, Ferrantini C, Coppini R. Calcium handling maturation and adaptation to increased substrate stiffness in human iPSC-derived cardiomyocytes: The impact of full-length dystrophin deficiency. Front Physiol. 2022 Nov 7;13:1030920. doi: 10.3389/fphys.2022.1030920. Erratum in: Front Physiol. 2023 Jun 13;14:1222400. PMID: 36419836; PMCID: PMC9676373.*
- *Pioner JM, Santini L, Palandri C, Langione M, Grandinetti B, Querceto S, Martella D, Mazzantini C, Scellini B, Giammarino L, Lupi F, Mazzarotto F, Gowran A, Rovina D, Santoro R, Pompilio G, Tesi C, Parmeggiani C, Regnier M, Cerbai E, Mack DL, Poggesi C, Ferrantini C, Coppini R. Calcium handling maturation and adaptation to increased substrate stiffness in human iPSC-derived cardiomyocytes: The impact of full-length dystrophin deficiency. Front Physiol. 2022 Nov 7;13:1030920. doi: 10.3389/fphys.2022.1030920. Erratum in: Front Physiol. 2023 Jun 13;14:1222400. PMID: 36419836; PMCID: PMC9676373.*
- *Pioner JM, Santini L, Palandri C, Martella D, Lupi F, Langione M, Querceto S, Grandinetti B, Balducci V, Benzoni P, Landi S, Barbuti A, Ferrarese Lupi F, Boarino L, Sartiani L, Tesi C, Mack DL, Regnier M, Cerbai E, Parmeggiani C, Poggesi C, Ferrantini C, Coppini R. Optical Investigation of Action Potential and Calcium Handling Maturation of hiPSC-Cardiomyocytes on Biomimetic Substrates. Int J Mol*

Sci. 2019 Aug 3;20(15):3799. doi: 10.3390/ijms20153799. PMID: 31382622; PMCID: PMC6695920.

- *Pioner JM, Vitale G, Steczina S, Langione M, Margara F, Santini L, Giardini F, Lazzeri E, Piroddi N, Scellini B, Palandri C, Schuldt M, Spinelli V, Girolami F, Mazzarotto F, van der Velden J, Cerbai E, Tesi C, Olivotto I, Bueno-Orovio A, Sacconi L, Coppini R, Ferrantini C, Regnier M, Poggesi C. Slower Calcium Handling Balances Faster Cross-Bridge Cycling in Human MYBPC3 HCM. Circ Res. 2023 Mar 3;132(5):628-644. doi: 10.1161/CIRCRESAHA.122.321956. Epub 2023 Feb 6. PMID: 36744470; PMCID: PMC9977265.*
- *Querceto S, Santoro R, Gowran A, Grandinetti B, Pompilio G, Regnier M, Tesi C, Poggesi C, Ferrantini C, Pioner JM. The harder the climb the better the view: The impact of substrate stiffness on cardiomyocyte fate. J Mol Cell Cardiol. 2022 May;166:36-49. doi: 10.1016/j.yjmcc.2022.02.001. Epub 2022 Feb 6. PMID: 35139328.*
- *Raab S, Klingenstein M, Liebau S, Linta L. A Comparative View on Human Somatic Cell Sources for iPSC Generation. Stem Cells Int. 2014;2014:768391. doi: 10.1155/2014/768391. Epub 2014 Nov 6. PMID: 25431601; PMCID: PMC4241335.*
- *Rahimov F, Kunkel LM. The cell biology of disease: cellular and molecular mechanisms underlying muscular dystrophy. J Cell Biol. 2013 May 13;201(4):499-510. doi: 10.1083/jcb.201212142. PMID: 23671309; PMCID: PMC3653356.*
- *Rayment I, Holden HM, Sellers JR, Fananapazir L, Epstein ND. Structural interpretation of the mutations in the beta-cardiac myosin that have been implicated in familial hypertrophic cardiomyopathy. Proc Natl Acad Sci U S A. 1995 Apr 25;92(9):3864-8. doi: 10.1073/pnas.92.9.3864. PMID: 7731997; PMCID: PMC42062.*
- *Reichart D, Magnussen C, Zeller T, Blankenberg S. Dilated cardiomyopathy: from epidemiologic to genetic phenotypes: A translational review of current literature. J Intern Med. 2019 Oct;286(4):362-372. doi: 10.1111/joim.12944. Epub 2019 Jul 29. PMID: 31132311.*
- *Richardson P, McKenna W, Bristow M, Maisch B, Mautner B, O'Connell J, Olsen E, Thiene G, Goodwin J, Gyarfas I, Martin I, Nordet P. Report of the 1995 World Health Organization/International Society and Federation of Cardiology Task Force on the Definition and Classification of cardiomyopathies. Circulation. 1996 Mar 1;93(5):841-2. doi: 10.1161/01.cir.93.5.841. PMID: 8598070.*

- *Ronaldson-Bouchard K, Ma SP, Yeager K, Chen T, Song L, Sirabella D, Morikawa K, Teles D, Yazawa M, Vunjak-Novakovic G. Advanced maturation of human cardiac tissue grown from pluripotent stem cells. Nature. 2018 Apr;556(7700):239-243. doi: 10.1038/s41586-018-0016-3. Epub 2018 Apr 4. Erratum in: Nature. 2019 Aug;572(7769):E16-E17. PMID: 29618819; PMCID: PMC5895513.*
- *Sacchetto C, Vitiello L, de Windt LJ, Rampazzo A, Calore M. Modeling Cardiovascular Diseases with hiPSC-Derived Cardiomyocytes in 2D and 3D Cultures. Int J Mol Sci. 2020 May 11;21(9):3404. doi: 10.3390/ijms21093404. PMID: 32403456; PMCID: PMC7246991.*
- *Salvatore T, Galiero R, Caturano A, Rinaldi L, Di Martino A, Albanese G, Di Salvo J, Epifani R, Marfella R, Docimo G, Lettieri M, Sardu C, Sasso FC. An Overview of the Cardiorenal Protective Mechanisms of SGLT2 Inhibitors. Int J Mol Sci. 2022 Mar 26;23(7):3651. doi: 10.3390/ijms23073651. PMID: 35409011; PMCID: PMC8998569.*
- *Sarkar SS, Trivedi DV, Morck MM, Adhikari AS, Pasha SN, Ruppel KM, Spudich JA. The hypertrophic cardiomyopathy mutations R403Q and R663H increase the number of myosin heads available to interact with actin. Sci Adv. 2020 Apr 3;6(14):eaax0069. doi: 10.1126/sciadv.aax0069. PMID: 32284968; PMCID: PMC7124958.*
- *Sarkar SS, Trivedi DV, Morck MM, Adhikari AS, Pasha SN, Ruppel KM, Spudich JA. The hypertrophic cardiomyopathy mutations R403Q and R663H increase the number of myosin heads available to interact with actin. Sci Adv. 2020 Apr 3;6(14):eaax0069. doi: 10.1126/sciadv.aax0069. PMID: 32284968; PMCID: PMC7124958.*
- *Schaaf S, Shibamiya A, Mewe M, Eder A, Stöhr A, Hirt MN, Rau T, Zimmermann WH, Conradi L, Eschenhagen T, Hansen A. Human engineered heart tissue as a versatile tool in basic research and preclinical toxicology. PLoS One. 2011;6(10):e26397. doi: 10.1371/journal.pone.0026397. Epub 2011 Oct 20. PMID: 22028871; PMCID: PMC3197640.*
- *Schlossarek S, Mearini G, Carrier L. Cardiac myosin-binding protein C in hypertrophic cardiomyopathy: mechanisms and therapeutic opportunities. J Mol Cell Cardiol. 2011 Apr;50(4):613-20. doi: 10.1016/j.yjmcc.2011.01.014. Epub 2011 Feb 1. PMID: 21291890.*
- *Scuderi GJ, Butcher J. Naturally Engineered Maturation of Cardiomyocytes. Front Cell Dev Biol. 2017 May 5;5:50. doi: 10.3389/fcell.2017.00050. PMID: 28529939; PMCID: PMC5418234.*

- *Seeger T, Shrestha R, Lam CK, Chen C, McKeithan WL, Lau E, Wnorowski A, McMullen G, Greenhaw M, Lee J, Oikonomopoulos A, Lee S, Yang H, Mercola M, Wheeler M, Ashley EA, Yang F, Karakikes I, Wu JC. A Premature Termination Codon Mutation in MYBPC3 Causes Hypertrophic Cardiomyopathy via Chronic Activation of Nonsense-Mediated Decay. Circulation. 2019 Feb 5;139(6):799-811. doi: 10.1161/CIRCULATIONAHA.118.034624. PMID: 30586709; PMCID: PMC6443405.*
- *Semsarian C, Hamilton RM. Key role of the molecular autopsy in sudden unexpected death. Heart Rhythm. 2012 Jan;9(1):145-50. doi: 10.1016/j.hrthm.2011.07.034. Epub 2011 Aug 2. PMID: 21816129.*
- *Sewanan LR, Shen S, Campbell SG. Mavacamten preserves length-dependent contractility and improves diastolic function in human engineered heart tissue. Am J Physiol Heart Circ Physiol. 2021 Mar 1;320(3):H1112-H1123. doi: 10.1152/ajpheart.00325.2020. Epub 2021 Jan 15. PMID: 33449850; PMCID: PMC7988756.*
- *Spindler M, Saupe KW, Ingwall JS. MR spectroscopy of transgenic mice. MAGMA. 1998 Sep;6(2-3):109-10. doi: 10.1007/BF02660924. PMID: 9803376.*
- *Staerk J, Dawlaty MM, Gao Q, Maetzel D, Hanna J, Sommer CA, Mostoslavsky G, Jaenisch R. Reprogramming of human peripheral blood cells to induced pluripotent stem cells. Cell Stem Cell. 2010 Jul 2;7(1):20-4. doi: 10.1016/j.stem.2010.06.002. PMID: 20621045; PMCID: PMC2917234.*
- *Streckfuss-Bömeke K, Tiburcy M, Fomin A, Luo X, Li W, Fischer C, Özcelik C, Perrot A, Sossalla S, Haas J, Vidal RO, Rebs S, Khadjeh S, Meder B, Bonn S, Linke WA, Zimmermann WH, Hasenfuss G, Guan K. Severe DCM phenotype of patient harboring RBM20 mutation S635A can be modeled by patient-specific induced pluripotent stem cell-derived cardiomyocytes. J Mol Cell Cardiol. 2017 Dec;113:9-21. doi: 10.1016/j.yjmcc.2017.09.008. Epub 2017 Sep 21. PMID: 28941705.*
- *Takahashi K, Tanabe K, Ohnuki M, Narita M, Ichisaka T, Tomoda K, Yamanaka S. Induction of pluripotent stem cells from adult human fibroblasts by defined factors. Cell. 2007 Nov 30;131(5):861-72. doi: 10.1016/j.cell.2007.11.019. PMID: 18035408.*
- *Takahashi K, Yamanaka S. Induction of pluripotent stem cells from mouse embryonic and adult fibroblast cultures by defined factors. Cell. 2006 Aug 25;126(4):663-76. doi: 10.1016/j.cell.2006.07.024. Epub 2006 Aug 10. PMID: 16904174.*

- *Tan Y, Ooi S, Wang L. Immunogenicity and tumorigenicity of pluripotent stem cells and their derivatives: genetic and epigenetic perspectives. Curr Stem Cell Res Ther. 2014 Jan;9(1):63-72. doi: 10.2174/1574888x113086660068. PMID: 24160683; PMCID: PMC3873036.*
- *Taylor MR, Fain PR, Sinagra G, Robinson ML, Robertson AD, Carniel E, Di Lenarda A, Bohlmeyer TJ, Ferguson DA, Brodsky GL, Boucek MM, Lascor J, Moss AC, Li WL, Stetler GL, Muntoni F, Bristow MR, Mestroni L; Familial Dilated Cardiomyopathy Registry Research Group. Natural history of dilated cardiomyopathy due to lamin A/C gene mutations. J Am Coll Cardiol. 2003 Mar 5;41(5):771-80. doi: 10.1016/s0735-1097(02)02954-6. Erratum in: J Am Coll Cardiol. 2003 Aug 6;42(3):590. PMID: 12628721.*
- *Teekakirikul P, Zhu W, Huang HC, Fung E. Hypertrophic Cardiomyopathy: An Overview of Genetics and Management. Biomolecules. 2019 Dec 16;9(12):878. doi: 10.3390/biom9120878. PMID: 31888115; PMCID: PMC6995589.*
- *Thavandiran N, Hale C, Blit P, Sandberg ML, McElvain ME, Gagliardi M, Sun B, Witty A, Graham G, Do VTH, Bakooshli MA, Le H, Ostblom J, McEwen S, Chau E, Prowse A, Fernandes I, Norman A, Gilbert PM, Keller G, Tagari P, Xu H, Radisic M, Zandstra PW. Functional arrays of human pluripotent stem cell-derived cardiac microtissues. Sci Rep. 2020 Apr 24;10(1):6919. doi: 10.1038/s41598-020-62955-3. PMID: 32332814; PMCID: PMC7181791.*
- *Tiburcy M, Zimmermann WH. Modeling myocardial growth and hypertrophy in engineered heart muscle. Trends Cardiovasc Med. 2014 Jan;24(1):7-13. doi: 10.1016/j.tcm.2013.05.003. Epub 2013 Aug 15. PMID: 23953977.*
- *Toepfer CN, Garfinkel AC, Venturini G, Wakimoto H, Repetti G, Alamo L, Sharma A, Agarwal R, Ewoldt JK, Cloonan P, Letendre J, Lun M, Olivotto I, Colan S, Ashley E, Jacoby D, Michels M, Redwood CS, Watkins HC, Day SM, Staples JF, Padrón R, Chopra A, Ho CY, Chen CS, Pereira AC, Seidman JG, Seidman CE. Myosin Sequestration Regulates Sarcomere Function, Cardiomyocyte Energetics, and Metabolism, Informing the Pathogenesis of Hypertrophic Cardiomyopathy. Circulation. 2020 Mar 10;141(10):828-842. doi: 10.1161/CIRCULATIONAHA.119.042339. Epub 2020 Jan 27. Erratum in: Circulation. 2020 Mar 10;141(10):e645. PMID: 31983222; PMCID: PMC7077965.*

- *Toepfer CN, Sikkel MB, Caorsi V, Vydyanath A, Torre I, Copeland O, Lyon AR, Marston SB, Luther PK, Macleod KT, West TG, Ferenczi MA. A post-MI power struggle: adaptations in cardiac power occur at the sarcomere level alongside MyBP-C and RLC phosphorylation. Am J Physiol Heart Circ Physiol. 2016 Aug 1;311(2):H465-75. doi: 10.1152/ajpheart.00899.2015. Epub 2016 May 27. PMID: 27233767; PMCID: PMC5005282.*
- *Towbin JA. Cardiomyopathy and heart transplantation in children. Curr Opin Cardiol. 2002 May;17(3):274-9. doi: 10.1097/00001573-200205000-00011. PMID: 12015478.*
- *Veerman CC, Mengarelli I, Lodder EM, Kosmidis G, Bellin M, Zhang M, Dittmann S, Guan K, Wilde AAM, Schulze-Bahr E, Greber B, Bezzina CR, Verkerk AO. Switch From Fetal to Adult SCN5A Isoform in Human Induced Pluripotent Stem Cell-Derived Cardiomyocytes Unmasks the Cellular Phenotype of a Conduction Disease-Causing Mutation. J Am Heart Assoc. 2017 Jul 24;6(7):e005135. doi: 10.1161/JAHA.116.005135. PMID: 28739862; PMCID: PMC5586268.*
- *Vizzardi E, D'Aloia A, Salghetti F, Aljassim O, Raweh A, Bonadei I, Bontempi L, Curnis A. Efficacy of ranolazine in a patient with idiopathic dilated cardiomyopathy and electrical storm. Drug Discov Ther. 2013 Feb;7(1):43-5. doi: 10.5582/ddt.2013.v7.1.43. PMID: 23524943*
- *Volkmann N, Lui H, Hazelwood L, Trybus KM, Lowey S, Hanein D. The R403Q myosin mutation implicated in familial hypertrophic cardiomyopathy causes disorder at the actomyosin interface. PLoS One. 2007 Nov 7;2(11):e1123. doi: 10.1371/journal.pone.0001123. PMID: 17987111; PMCID: PMC2040505.*
- *Wang H, Zhou J, Liu Z, Wang C. Injectable cardiac tissue engineering for the treatment of myocardial infarction. J Cell Mol Med. 2010 May;14(5):1044-55. doi: 10.1111/j.1582-4934.2010.01046.x. Epub 2010 Feb 27. PMID: 20193036; PMCID: PMC3822739.*
- *Watkins H, Ashrafian H, Redwood C. Inherited cardiomyopathies. N Engl J Med. 2011 Apr 28;364(17):1643-56. doi: 10.1056/NEJMra0902923. PMID: 21524215.*
- *Weintraub RG, Semsarian C, Macdonald P. Dilated cardiomyopathy. Lancet. 2017 Jul 22;390(10092):400-414. doi: 10.1016/S0140-6736(16)31713-5. Epub 2017 Feb 10. PMID: 28190577.*

- *Weintraub RG, Semsarian C, Macdonald P. Dilated cardiomyopathy. Lancet. 2017 Jul 22;390(10092):400-414. doi: 10.1016/S0140-6736(16)31713-5. Epub 2017 Feb 10. PMID: 28190577.*
- *Wendt T, Leonard K. Structure of the insect troponin complex. J Mol Biol. 1999 Jan 29;285(4):1845-56. doi: 10.1006/jmbi.1998.2414. PMID: 9917416.*
- *Willis MS, Schisler JC, Portbury AL, Patterson C. Build it up-Tear it down: protein quality control in the cardiac sarcomere. Cardiovasc Res. 2009 Feb 15;81(3):439-48. doi: 10.1093/cvr/cvn289. Epub 2008 Oct 29. PMID: 18974044; PMCID: PMC2721652.*
- *Winegrad S. Cardiac myosin binding protein C. Circ Res. 1999 May 28;84(10):1117-26. doi: 10.1161/01.res.84.10.1117. PMID: 10347086.*
- *Wu P, Xi X, Li R, Sun G. Engineering Polysaccharides for Tissue Repair and Regeneration. Macromol Biosci. 2021 Sep;21(9):e2100141. doi: 10.1002/mabi.202100141. Epub 2021 Jul 4. PMID: 34219388.*
- *Yamamoto K. [Structure of myosin subfragment-1]. Seikagaku. 1983;55(3):176-80. Japanese. PMID: 6350501.*
- *Yan AT, Bradley TD, Liu PP. The role of continuous positive airway pressure in the treatment of congestive heart failure. Chest. 2001 Nov;120(5):1675-85. doi: 10.1378/chest.120.5.1675. PMID: 11713153.*
- *Zhou Tf, Wang Xz, Zhang Gr. [All-ceramic resin bonded fixed partial denture made of IPS hot-pressed casting porcelain restore anterior missing teeth: a three years clinical observation]. Beijing Da Xue Xue Bao Yi Xue Ban. 2011 Feb 18;43(1):77-80. Chinese. PMID: 21321625.*
- *Zimmermann WH, Fink C, Kralisch D, Remmers U, Weil J, Eschenhagen T. Three-dimensional engineered heart tissue from neonatal rat cardiac myocytes. Biotechnol Bioeng. 2000 Apr 5;68(1):106-14. PMID: 10699878.*
- *Zoghbi GJ, Dorfman TA, Iskandrian AE. The effects of medications on myocardial perfusion. J Am Coll Cardiol. 2008 Aug 5;52(6):401-16. doi: 10.1016/j.jacc.2008.04.035. PMID: 18672159*